The Photophysics and Photochemistry of a series of Phthalocyanines as Potential Photosensitisers in Photodynamic Therapy

Magda van Leeuwen

A thesis submitted in part fulfilment of the requirements for the degree of Doctor of Philosophy of the University of East Anglia, Department of Chemistry, Norwich, England.

January 2013

Abstract

The photophysical and photochemical measurements have been made on 3 series of novel alpha octa(alkyl-substituted) phthalocyanines. Each series is defined by the distinct non-metal or metal ion centre, silicon hydroxide, zinc(II) and palladium(II). It is well documented that the phthalocyanine molecule possesses several distinct properties, including absorption in the red, low fluorescence and high triplet quantum yields that make it an ideal candidate as a potential photosensitiser in photodynamic therapy. Photodynamic therapy is an alternative treatment to cancer using a photosensitiser, which is preferentially absorbed by malignant cells and remains dormant until activated by red light. This results in the formation of singlet delta oxygen via the excited state of the photosensitiser. The generation of singlet oxygen leads to cell death.

Fluorescence quantum yields and lifetimes, triplet quantum yields, lifetimes and energies and singlet delta oxygen quantum yields were measured in 1% v/v pyridine in toluene. The effects of alkyl substitution, with increasing chain length, variation of metal ion centre and the core modification of the phthalocyanine unit are investigated and compared relative to the unsubstituted parent molecules, SiPc, ZnPc and PdPc.

All substituted phthalocyanines exhibited a typical phthalocyanine absorption spectrum with significant red-shift of the Q-band maxima. Q-band maxima for all compounds ranged between 660 – 712 nm and extinction coefficients of the Q-band between 10^{-4} – 10^{-5} M^{-1} cm^{-1}. All compounds also exhibited triplet quantum yields in the range 0.52 –

0.96 and singlet delta oxygen quantum yields of 0.49 – 0.94, illustrating promising photophysical and photochemical properties for photodynamic therapy.

Acknowledgements

To my family

Contents

3. Singlet Delta Oxygen, $O_2(^1\Delta_g)$

4. Silicon Phthalocyanine Derivatives

5. Zinc Phthalocyanine Derivatives

6. Palladium Phthalocyanine Derivatives

7. Discussion and Conclusion

List of Figures

1. Introduction

3. Singlet Delta Oxygen, $O_2(^1\Delta_g)$

4. Silicon Phthalocyanine Derivatives

5. Zinc Phthalocyanine Derivatives

6. Palladium Phthalocyanine Derivatives

7. Discussion and Conclusion

List of Tables

3. Singlet Delta Oxygen, $O_2(^1\Delta_g)$

4. Silicon Phthalocyanine Derivatives

5. Zinc Phthalocyanine Derivatives

6. Palladium Phthalocyanine Derivatives

7. Discussion and Conclusion

1. Introduction

1.1 Cancer

According to statistics published by Cancer Research UK, every two minutes someone is diagnosed with cancer. Cancer, medically termed malignant neoplasm, is the rapid and uncontrolled division of cells, which form malignant tumours that have the potential to spread further a field from the site of origin, via the bloodstream and lymphatic system, to infect other organs.[1] The word cancer is derived from the Greek *carcinos* referring to the crab like appearance of a solid malignant tumour.[2-4] While there is a vast range to the degree and severity of the disease Cancer Research UK showed that 1 in 3 people will get cancer in their lifetime.[5] With this in mind, research is ongoing to identify the key causes of cancer in order to prevent the disease, whether through medically advanced gene therapy or, more simply, through changes in diet and lifestyle. Nevertheless, the high instance of cancer diagnosis suggests that developing efficient and successful treatments is also a major priority.

Depending on the source, severity and spread of the disease there are three main approaches used to reduce and remove a tumour. Surgery is often the primary option when the tumour is on tissue, organs or nodes that can be removed with little disruption to vital organs within the body. This treatment comes with all of the risks and side-effects of standard surgery, including a risk of death, paralysis and infection.[1]

If the tumour is too large to remove and needs to be reduced first then chemotherapy may be the route of choice. Chemotherapy is a

chemical approach to the treatment of cancer and is often the combination of two or more drugs from a catalogue of 50 clinically tested compounds.[6] The treatment affects both cancerous and normal cells, though healthy cells have the ability to repair the damage caused by chemotherapy whereas malignant cells cannot. As a consequence, many of the side-effects are related to areas that have a high cell turnover, such as the mouth, bone marrow and the digestive system. Common side effects include increased risk of infection, anaemia, bleeding and bruising, hair loss, nausea and vomiting, diarrhoea and constipation, change of taste and an increased risk of secondary cancers.

Radiotherapy is the third option often used to cure cancer or reduce the chances of cancer returning.[1] This technique uses a radioactive source, either internally or externally, to destroy cancer cells within the affected area. However, as with chemotherapy, it is a non-discriminatory treatment and so normal cells are susceptible to damage, though, it is thought they have the mechanism to self-repair. The common side-effects include fatigue, nausea, loss of appetite, sore skin, sensitivity to the sun, hair loss and more long-term effects such as infertility and a risk of secondary cancers.

With the severe side-effects associated with these treatments and a combined vulnerability of the patients involved, research is moving forward to find alternative non-invasive therapies with reduced side-effects. With this in mind there has been the emergence of hormonal therapies, biological therapies and investigations into phototherapy.

A promising alternative to chemotherapy and radiotherapy is the use of chemical agents in combination with light; this is known as photodynamic therapy (PDT). However, unlike chemotherapy, the chemicals administered are preferentially absorbed by cancerous cells where they remain dormant until activated with targeted light of specified wavelength. These chemicals are called photosensitisers. Once the photosensitiser is activated it forms excited states that interact with the molecular oxygen present in the cells to generate singlet delta oxygen, the cytotoxic agent responsible for cell death.

There are many benefits to PDT over standard techniques including efficiency, ease of use and low costs.[7, 8] However, the key advantage in terms of patient care is the minimisation of harmful side-effects. The very nature of the technique with preferential absorption of a dormant photosensitiser coupled with targeted light delivery produces a highly selective and non-invasive treatment thereby limiting the damage to surrounding healthy tissue. This means PDT does not yield the same threat of secondary cancers as demonstrated with other techniques. The only significant side-effect appears to be a heightened sensitivity to light post-treatment, which remains until the photosensitiser has cleared the system. With current photosensitisers this may take up to 10 weeks.[9]

1.2 Light Therapies from Ancient Civilizations to the Modern World

Light as a form of therapy is repeatedly referred to throughout history and across the globe. It has been most widely used in the treatment of a variety of commonly occurring ailments. The Ancient Greeks are documented as employing whole-body sun exposure to treat a variety

of ailments. In fact, the famous Greek physician, Herodotus, is recorded as emphasising the importance of sunlight for health and coining the term heliotherapy. There was particular emphasis placed on the importance of light in restoring the entire body to health.[10]

In eighteenth and nineteenth century France, sunlight was commonly used in the treatment of a number of conditions including, tuberculosis, rickets, scurvy, rheumatism, paralysis and oedema.[11] In 1815, Carvin documented the curing effects of sunlight on rheumatism, scurvy, paralysis and muscle weakness.[12] In 1822, Sniadecki, a Polish physician, wrote of the importance of sun exposure for the prevention of rickets.[13]

In 1903, Danish scientist Niels Ryberg Finsen was awarded one of the first Nobel Prizes in Medicine for his work on the treatment of facial sores of patients suffering from tuberculosis. His research demonstrated the impact of ultraviolet light, using carbon arc phototherapy, in treating these lesions and brought to the attention of the modern world the potential of light in medicine. For this he is often referred to as the father of modern light therapy.[14]

In today's world we are increasingly aware of the dangers of over exposure to sunlight and, in particular, ultraviolet radiation. However, it is important to recognize two biological processes in which light plays a significant role. The first process is one alluded to throughout history, which is the treatment of rickets.[9] Rickets is a bone deformation as a result of insufficient calcium uptake. This in turn is due to insufficient production of vitamin D within the body. During the reign of the British Empire it was noticed that there were huge

differences in the number of people suffering from rickets in Victorian Britain, where it was a common ailment, compared with those in India, where it was virtually unheard of. It is now understood that this is due to the different degrees of exposure to sunlight in the two locations.[9] It was shown that Vitamin D is synthesised within the body through biological processes that are stimulated by the absorption of ultraviolet light.[15, 16]

The second significant case of light therapy was discovered in the 1950s by Dr. Richard Cremer and the acute observations of his neonatal nurse Sister J Ward.[17] This is the treatment of neonatal hypobilirubinaemia, otherwise known as jaundice. The discovery that light had some involvement in the treatment of this condition came about due to the combination of two key observations. Sister Ward was a strong believer in the benefits of fresh air and sunshine in improving the health of premature infants and would often walk the cots through the hospitals courtyard. On one occasion she observed significant changes in the skin tone of jaundiced infants with the bleaching of skin exposed to the sun compared to that which was still covered. This observation was further corroborated when a sample of blood taken from an infant with severe jaundice was tested for plasma bilirubin and found to have far lower levels than expected. Upon investigation it was found that the sample had been accidentally left on a windowsill for some time before being tested. Upon repeating the tests bilirubin levels were found to continue to fall upon additional exposure to sunlight. The combination of these observations prompted Richard Cremer to introduce phototherapy as a treatment for jaundice in newborn babies.[18]

The treatment is based on the fact that babies are born without the enzymes to breakdown an excess of the fat-soluble chemical bilirubin into water-soluble components that can be excreted in urine and stools, which a foetus has no requirement to do. For premature infants the development of this enzyme may take much longer and the fat-soluble bilirubin builds up and is stored in the skin, hence the yellow appearance of jaundice babies. It is now widely believed that with the influence of light the bilirubin molecule undergoes a photochemical cis-trans transformation that results in a product that can be excreted.[9]

1.3 The Discovery of Photodynamic Therapy

The development of modern light therapy is primarily concerned with the combination of light and an administered chemical, the photosensitiser. There is evidence to suggest that such methods were practised in a range of civilizations over the last 3000 years.[12] The relationship between light and health in combination with pastes and ointments is well established through history and has been indicated in texts dating as far back as 1550 BC.[12] In Ancient India, from evidence in the holy book Atharva Veda, and in Ancient Egypt, from the Ebers Papyrus, it appears that it was common practice to treat skin complaints such as psoriasis and vitiligo with light. Plant-derived psoralens, a furocoumarin, were applied to the affected area in the form of pastes and ointments and treated in combination with sunlight. In fact the furocoumarins contained in plants have been shown to make the skin photosensitive, stimulating the production of the pigment melanin in the skin.[19]

The discovery of photodynamic therapy is attributed to Professor Herman von Tappeiner. However, it was the work carried out by his

medical student Oscar Raab that proved to be the initial discovery and foundation of the technique. During the winter of 1897-8 Raab was conducting research on the effects of dyes and light on paramecia.[20, 21] An experiment conducted on Insuforia showed unusual results: application of an acridine solution and light had a lethal effect. The anomalous result was due to a large thunderstorm that Raab noted had provided unusually high light levels during the experiment. He hypothesised that the death of the paramecium had occurred either due to the acridine solution imparting toxic properties to light or that the light had somehow transformed the acridine dye into a toxic agent. An experiment passing light through an acridine solution before illuminating paramecia in an undyed solution proved that light had not been changed into toxic radiation. Raab went on to prove that the fluorescing properties of acridine had the potential to convert energy from absorbed light into an active chemical energy, which was responsible for the death of paramecia. It was this active energy that formed the foundations of photodynamic therapy.

In 1900 the French neurologist Prime reported the effect of the dye eosin as a photosensitiser in humans.[22] In a study for the oral treatment of epilepsy with eosin it was discovered that exposure of the skin to sunlight following drug administration induced dermatitis. Between 1903 and 1905, based on the discoveries of Raab, von Tappeiner and Jesionek made some of the first photodynamic therapy attempts to treat tumours and other skin diseases.[23] A variety of experiments were conducted investigating the potential of dyes, including eosin, fluorescein, sodium dichloroanthracene disulfonate and ‘Gruber’s Magdalene red’ in treatments. Furthermore, in 1905, von Tappeiner published the results of the first photodynamic treatment of six

patients with facial basal cell carcinoma. The treatment was performed using a 1% eosin solution and a long-term exposure either to sunlight or to an arc-lamp, with four out of the six showing total tumour resolution. With Jodlbauer, von Tappeiner identified and demonstrated the necessity to have oxygen as the third and final component in photosensitisation reactions and in 1907 coined the term 'photodynamic action'.[24]

1.4 Photodynamic Therapy – Importance of Light

The first light sources used in photodynamic therapy were standard lamps for which filters had to be used to define an output wavelength. The key drawbacks to this method include the significant thermal component and an inability to accurately calculate the light dosimetry. The development of lasers in the 1960s provided a light that was monochromatic and directional in nature, had a well defined output wavelength, and light dosimetry that was easy to measure and calculate. It also provided a source of light that can be passed down an optical fibre affording the highly localized treatment of affected sites. Portable and compact light sources, such as LEDs, are now available that can be optimized according to the desired wavelength[25, 26]

1.5 Early Photosensitisers

The discovery of modern, clinically approved photosensitisers can be attributed to the initial observations of the tumour-localizing properties of porphyrins, revealed by Policard.[27] In 1924, Policard observed the characteristic red fluorescence of hematoporphyrin when experimental rat sarcoma was exposed to UV light. Hematoporphyrin was first produced by Scherer in 1841 during experiments investigating the nature of blood.[28] Dried blood was treated with

concentrated sulphuric acid and the precipitate was washed free of iron before being treated with alcohol. However, it was not until 1867 that the fluorescent properties were described and only in 1871 that the compound was named as hematoporphyrin.[11] In 1911, Hausmann performed the first biological studies using HpD and reported the effects of light on paramecium and red blood cells, specifically noting skin reactions in mice when exposed to light after hematoporphyrin administration.[29] Lastly, in 1913 the first report of human photosensitisation by pophyrins was made by Friedrich Meyer-Betz.[30] In order to determine whether previously observed reactions in mice could be induced in humans he injected himself with 200 mg of hematoporphyrin and subsequently notice prolonged pain and swelling in light exposed areas. Following several publications regarding the tumour-localising properties of hematoporphyrin no further developments come to light until 1942 when Auler and Banzer investigated the localisation and fluorescence of hematoporphyrin in malignant tumors.[31] In 1948, Figge, Weiland and Manganiello demonstrated the potential role of hematoporphyrins as a diagnostic tool in oncology due to their preferential absorption by malignant cells and characteristic red fluorescence upon illumination.[32]

In 1955, Schwartz *et al.* demonstrated that the hematoporphyrin used in earlier studies was actually not a single compound, but a complex mixture of porphyrins.[33] By partial purification Schwartz was able to show that the pure isolated hematoporphyrin localized very poorly in tumours, yet the residue had a far greater affinity for tumour tissue. In his investigations Schwartz treated crude hematoporphyrin with acids, in particular acetic and sulphuric, before filtering and further treating with sodium acetate to neutralise. Redissolving the precipitate in

saline produced a substance which became known as hematoporphyrin derivative (HpD). Previous studies, had alluded to the fact that HpD may have use in the detection as well as the potential for treatment of human tumors.[34]

In 1972 Diamond *et al.* suggested the concept that the combination of tumour-localising and phototoxic properties of porphyrins could be exploited to produce an effective treatment for cancer.[35] They went on to test whether HpD may serve as a selective photosensitising agent in order to destroy tumour cells through exposure to light. In 1975 Dougherty *et al.* reported the first successful complete tumour cure following administration of HpD.[36] However, the clinical approval of an HpD based photosensitiser did not occur until 1993, when Photofrin® was approved in Canada for the treatment of bladder cancer.[37] Photofrin® is prepared by removing monomer fractions of HpD and, as the first clinically approved photosensitiser, is the reference compound by which all new photosensitisers are compared.[38]

1.6 Designing new photosensitisers

One of the main complications arising from the design and development of an optimised photosensitiser is a distinct lack of knowledge concerning the biological mechanisms involved in photodynamic therapy. It is currently accepted that an administered photosensitiser is preferentially absorbed by malignant cells where it remains dormant until excited with light. Upon absorption of light the photosensitiser forms excited states that react with molecular oxygen to generate singlet excited states of oxygen, which leads to cell death.

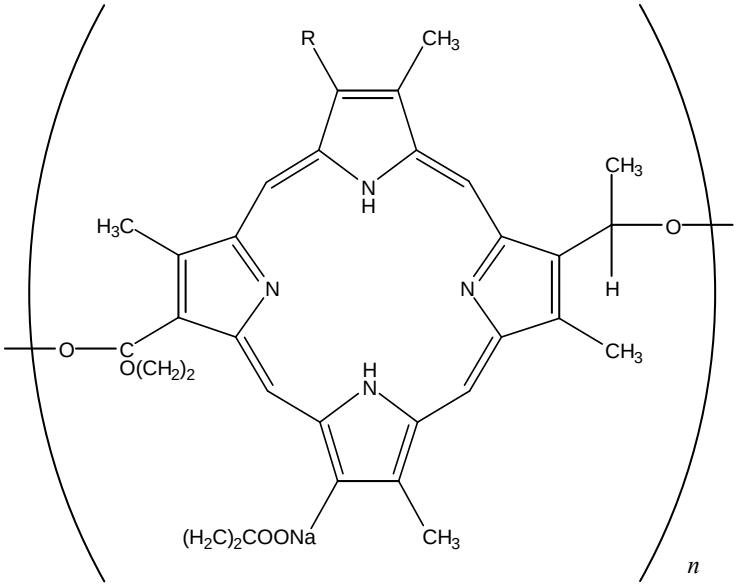

Figure 1. 1 Structure of Photofrin®, the first clinically approved photosensitiser.

The target and mechanism by which this cell death occurs has yet to be fully identified. Research targeted at identifying the mode of action of Photofrin® suggests that mitochondrial sites may be the targets for optimal photodynamic action.[8] However, evidence suggests that vascular shutdown occurs as a reaction of singlet delta oxygen with the unsaturated lipids and proteins of biological membranes.[39] The reaction step from sensitizer to molecular oxygen with subsequent cell death and a combination of lack of a defined biological target makes photosensitiser optimisation using potential structure activity relationships a difficult task.[40] Consequently, the research to date has centred on the development and enhancement of HpD, Photofrin® and compounds related in structure to porphyrins.

Following the approval of Photofrin® as a photosensitiser in photodynamic therapy of bladder cancer, the natural course of action has been to identify the photodynamically active component.

Photofrin® comprises a complex mixture of porphyrin isomers and oligomers, of which a sole active component has yet to be identified, Figure 1.1.[41] It may in fact be the case that the inherent success of the drug is the relationship between the mixture of molecules. Other shortfalls of Photofrin® include a weak absorption at the therapeutic wavelength, ε_s = 3 x 10^3 M^{-1} cm^{-1} at 630 nm, poor tumour selectivity and only moderate singlet oxygen quantum yields, typically $\Phi_\Delta \sim 0.2$.[42-44] It follows that in the design of an optimised photosensitiser a number of conditions can be optimised,[8, 10, 43, 45-47] these are as follows:

1.6.1 A Single Substance

The complications associated with Photofrin® are largely centred on its complex composition of isomers and oligomers and the problems in the identification of an active component. Hence, there is great benefit in synthesising an efficient photosensitiser that consists of one compound, whereby it is hoped that the biological targets can be identified.

1.6.2 Tumour Selectivity

Photodynamic therapy is built on early research following the localisation of HpD in malignant cells. Tumour selectivity provides a huge advantage in the treatment of cancer as it means that healthy cells remain undisturbed and so minimises the risks of recurring illness and secondary cancers as can be experienced by patients being treated with chemotherapy and radiotherapy.

1.6.3 Stability and Toxicity

It is of great importance that any potential photosensitiser does not cause further damage or new illnesses to the patient. The benefit of

Photofrin® is that it is a product of dried blood and therefore a naturally occurring biological molecule with a well established metabolic pathway. The dangers associated with any alien compound introduce to the body are not only what the compound itself can do, but also the risks associated with any by-products of metabolism. It is important, therefore, that the molecule is relatively stable, but also clears rapidly from the body post-treatment.

1.6.4 Amphiphilicity

Amphiphilicity is important as the drug is usually administered in an aqueous environment but to get into a cell has to cross fat based cell membranes. It takes into account the aqueous and fatty environments encountered both inside and outside the cell.

1.6.5 Red Absorption

Light penetration through tissue and tumours is limited by optical scattering within the tissue, the absorption of light by biological chromophores and the physiochemical features of the photosensitiser. Typically, the region where biological chromophores, such as haemoglobin and oxyhaemoglobin, have minimum absorption is at wavelengths greater than 600 nm. Water is another key component of cells, absorbing light at wavelengths greater than 1200 nm. The minimum energy required to generate singlet oxygen is 94 kJ mol^{-1} which corresponds to a wavelength of 1270 nm. Thus the triplet state of the photosensitiser must exceed this energy. It has been well documented that the photophysical sequence is affected by thermal losses such that the upper limit for a photosensitiser to efficiently produce singlet delta oxygen is 140 kJ mol^{-1}, which corresponds to a wavelength of 850 nm.[48] Hence, to maximise the

effectiveness of the technique it is important to develop photosensitisers with high molar extinction coefficients in the optical window of 600 – 850 nm in order to increase the penetration depth of the treatment.

1.6.6 Fluorescence

It is broadly accepted that an efficient photosensitiser should have minimal fluorescence.[49] Hence the absorbed energy is not lost through emission, but rather, transferred to the triplet state of the molecule via spin-forbidden intersystem crossing. However, there may be some argument for the benefits of a small amount of fluorescence in order to identify whether there is photosensitiser localisation and therefore the maximum thresholds for absorption of the photosensitiser by malignant cells and optimum treatment windows.

1.6.7 Triplet Energies and Quantum Yields

The optical window is defined, in part, by the minimum energy required to generate singlet delta oxygen via the triplet state of the photosensitiser. Triplet energies must exceed 100 kJ mol^{-1} to allow for efficient energy transfer to ground state oxygen. High quantum yields and long triplet lifetimes increase the efficiency of singlet delta oxygen production.

1.6.8 Singlet Delta Oxygen Quantum Yields (Φ_Δ)

Singlet delta oxygen, $O_2(^1\Delta_g)$, is believed to be the component responsible for cell death so it is important to generate it as efficiently as possible. The quantum yield is the ratio of singlet delta oxygen states formed compared to the number of photons initially absorbed by the photosensitiser. Quantum yields approach unity if the triplet state

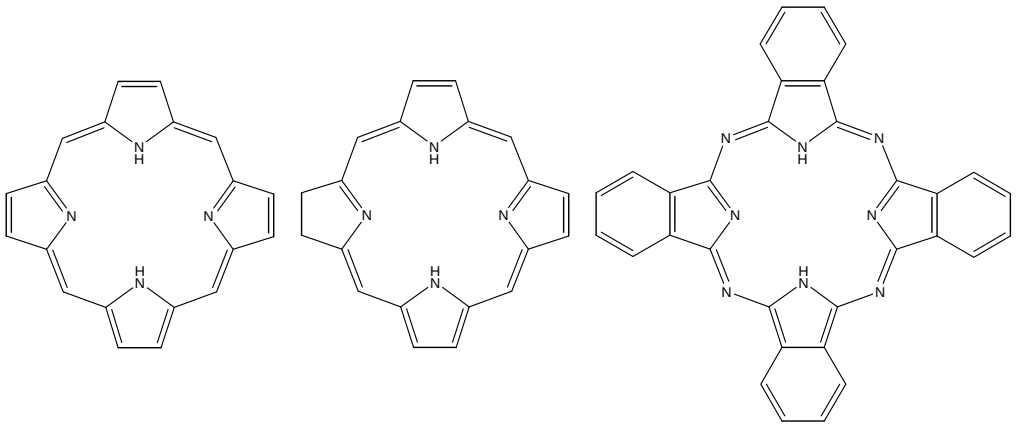

Figure 1. 2. Illustration of the core structures, form left to right, of porphyrins, chlorines and phthalocyanines.

of the photosensitiser is formed efficiently and is fully quenched by molecular oxygen.

1.7 Second-Generation Photosensitisers

In an attempt to find the optimum photosensitiser, thousands of compounds have been synthesised and the details published over the last 30 years.[50] Many claiming to be novel photosensitisers have turned out not to be optimal for oncology based photodynamic therapy, however some shining examples have appeared that have potential as photosensitisers in other medical arenas. The photosensitisers reviewed are all loosely related in structure and will be broken down into 3 core families, porphyrins, chlorins and phthalocyanine dyes, Figure 1.2.

1.7.1 Porphyrins

Investigating porphyrins is the natural approach to take in the development of photosensitisers from Photofrin®. The core structure allows for countless variations, which in turn can be used to fine-tune some of the key properties required for PDT. Research shows that porphyrins can be substituted at the reactive pseudobenzylic position

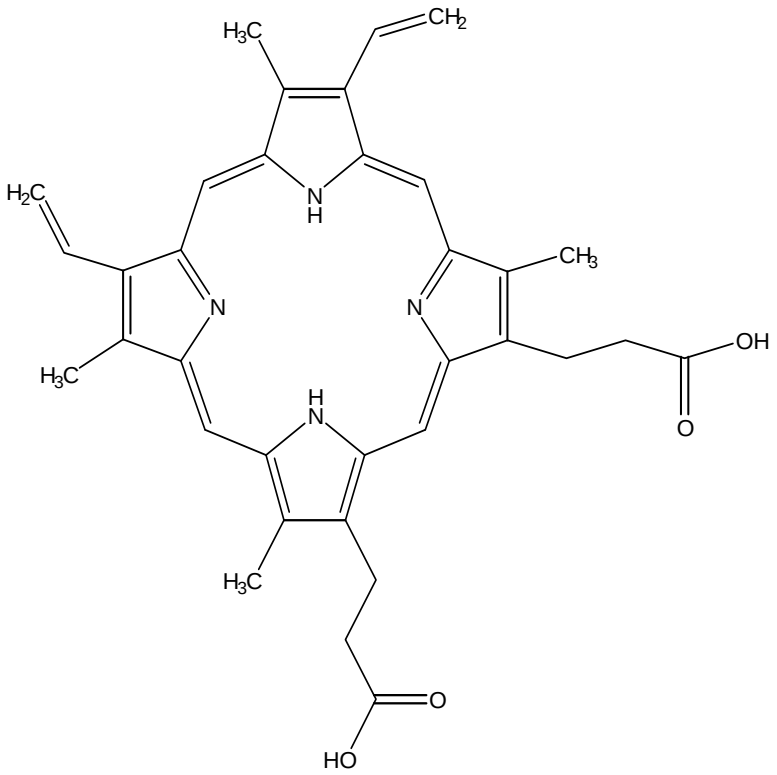

Figure 1. 3. Structure of protoporphyrin IX (PpIX) formed *in situ* when the haem biosynthetic pathway is disrupted with the application of excess ALA.

with a variety of functional groups including ethers, thioethers, esters and amines, all of which have shown to exhibit some biological activity.[51] However, efforts to enhance absorption in the red region have had only small influences on both shift and improvement of molar extinction coefficients.

One remarkable and unique discovery has been the identification and exploitation of aminolevulinic (ALA) acid induced *in vitro* photosensitisation, as discovered in 1987 by Malik and Lugaci.[52] Though ALA itself is not a porphyrin and has no intrinsic photosensitising properties, an excess of the compound in cells disrupts the haem biosynthetic pathway, of which it is a naturally-occurring intermediate and precursor of the photosensitising agent protoporphyrin IX (PpIX), Figure 1.3. The topical application of the

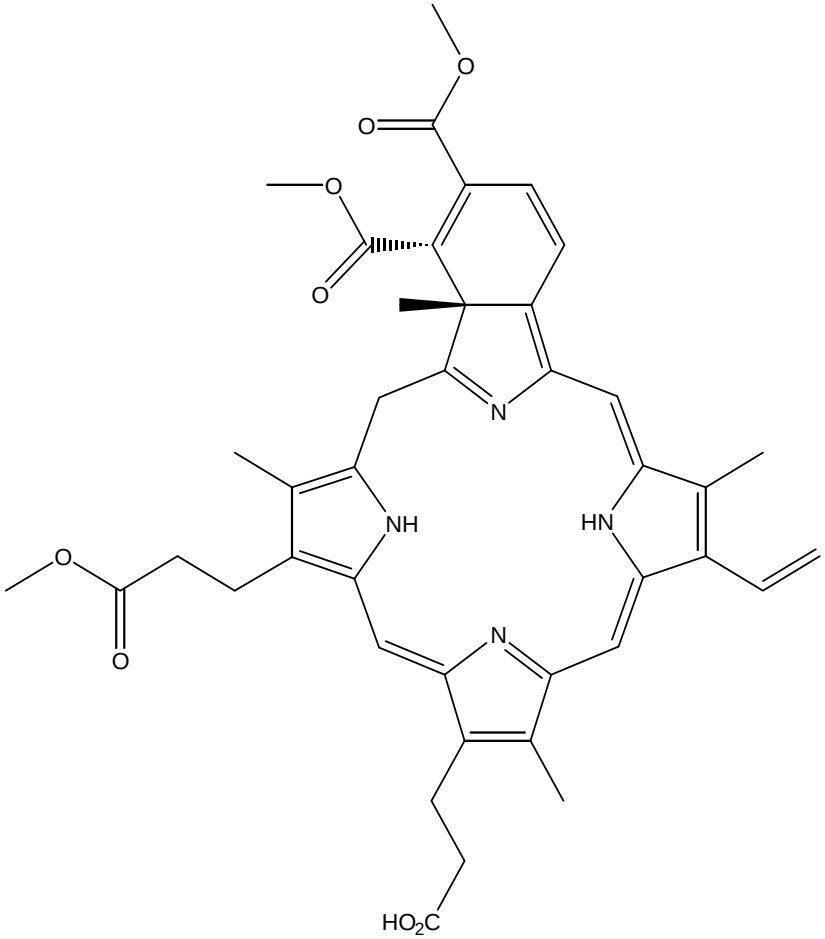

Figure 1. 4. Structure of Visudyne, a photosensitiser used in the treatment of AMD.

hydrophilic porphyrin precursor disrupts the negative feedback mechanism and stimulates the body into producing an excess of PpIX, which, when combined with light, produces a photodynamic effect. The advantages are immediately clear as the photosensitiser is synthesised *in situ*, hence eliminating issues addressed with administering the drug and transporting it to the correct location. It is also a naturally occurring compound so can be metabolised by the body and rapidly cleared post treatment without the threat of toxic by-products. The treatment uses light with wavelength of 630 – 635 nm, 3 – 6 hrs after application. The key drawback seems to be an upper limitation of 1 mm for penetration depth, so it is best used on tumours at relatively small depths.[53]

1.7.2 Chlorins

Chlorins are modified porphyrins, Chlorophyll *a* falls into this category and is already well known for its photophysical properties through its role in photosynthesis. A key development in this area has been the research into the benzoporphyrin derivative mono acid, commercially known as Visudyne and Verteporfrin, Figure 1.4.[54] This compound exhibits a significant red-shift in Band I, with absorption at 690 nm and good biological activity. The drawbacks, however, are that it clears very rapidly from biological tissue, both malignant and healthy, resulting in poor tumour selectivity. However, where this drug fails in photodynamic therapy for oncology it has enormous potential in the treatment of age-related macular eye degeneration (AMD). The wet-form of AMD is currently a leading cause of blindness in the over 50s in the western world. It involves the abnormal growth of blood vessels in the eye, which subsequently leads to loss in central vision. Prior to AMD-PDT the course of treatment followed involved thermal laser coagulation to cauterise the leaky vessels, with little effect. However, intravenous administration of Visudyne gives a 3 hr therapeutic window during which a 3 mm spot at the neovasculature can be illuminated. This results in sealing of the leaky vessel, which cannot restore lost eyesight, but does slow down and even halt further vision loss.[55]

Another example of a chlorin-based photosensitizer is m-THPC, commercially known as Foscan, Figure 1.5.[56] Foscan is of particular interest because, on paper, it fulfils many of the criteria for an optimised photosensitiser. It has comparable singlet oxygen quantum yields to other chlorins, it has red absorption at 660 nm and requires only low doses to achieve the same results as Photofrin®. The

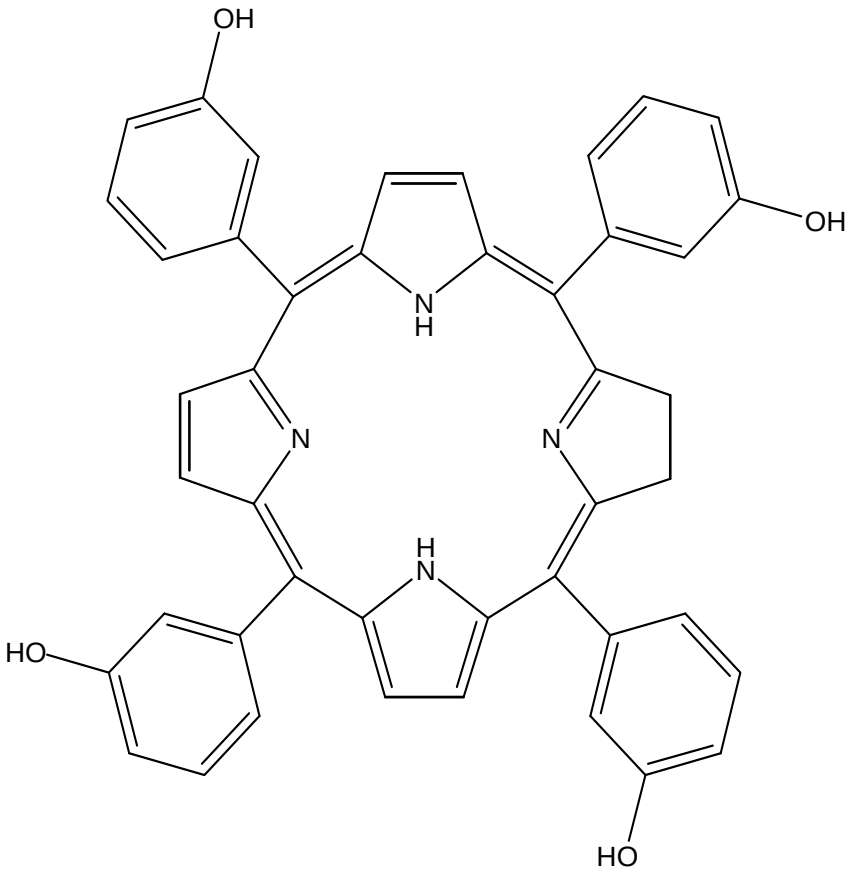

Figure 1. 5. Structure of Foscan.

problems arising from the potency of the drug and its efficient ability to convert light energy combined with the necessity for a 4 day delay between drug administration and treatment. Foscan appears to be so potent that extreme measures have to be taken in order to block any healthy tissue from reflected and scattered light prior to treatment. Patients are also susceptible to damage out of direct light so treatment needs to be administered in dark rooms. Part of the problem is that there is far greater penetration with Foscan than expected, which may be a property unique to this drug, but also may be in part due to differences in optical properties of tumours compared with healthy tissue. Even the rhythmic motion of patients breathing can be detrimental to the success of the technique as the movement can lead to either under dosage to the tumour or over dosage to healthy skin.

Current research is involved in toning down the potency by administration of green light, which has a much reduced penetration.

1.7.3 Dyes

Some researchers believe that a step backwards to the original research by Raab is an appropriate way to develop photosensitisers.[57] Raabs work was based around the properties of a number of dyes. Phthalocyanines are blue dyes that have been extensively used in the dyes and pigments industries and may have great potential in photodynamic therapy.

1.8 An Introduction to Phthalocyanines

The word phthalocyanine originates from the Greek for naphtha meaning 'rock oil' and cyanine meaning 'dark blue', a reflection of the intense blue colour of these compounds. As is so often the case in science, the discovery of phthalocyanines came about accidentally. Literature tells us that four chemists working at Scottish Dyes Ltd. observed an insoluble blue material during the routine manufacture of phthalimide from phthalic anhydride, both of which are white solids.[58] A letter written by Ron Grieg, the analytical chemist of the department working at Scottish Dyes Ltd. at the time, and reproduced by Gregory illustrates a more colourful version of events.[59] Grieg states that, in a bid to prove negligence of the foreman in the contamination of the reaction with a blue dye manufactured in the same place, analysis performed on the mystery compound actually found it to be an organo-iron compound. The structure was later elucidated as iron phthalocyanine through studies by Linstead *et al.* in 1929 and further proved by Robertson through X-ray diffraction.[60-67] In hindsight, the first recorded observation of a phthalocyanine was made in 1907 when

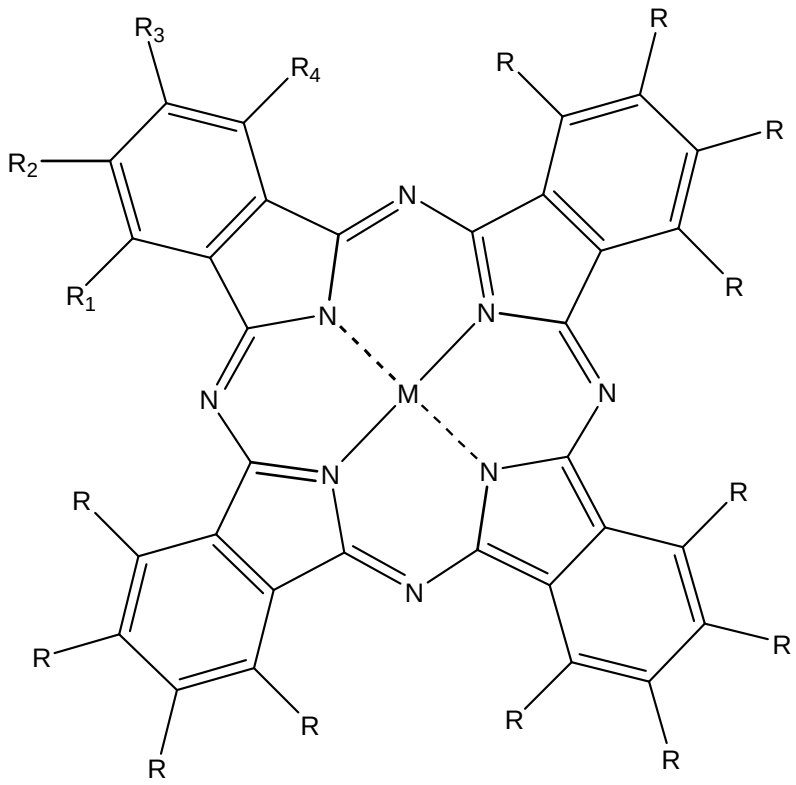

Figure 1. 6. Structure of the phthalocyanine molecule illustrating positions for alpha substitution (R = 1 and 4) and beta substitution (R = 2 and 3). Axial modification can also be applied to the central metal ion.

Braun and Tcherniac observed the production of a coloured impurity with unknown structure and origin in the reaction of phthalamide and acetic anhydride to produce *o*-cyanobenzamide.[68] Nevertheless, Scottish Dyes Ltd. went on to get the first patent in 1928 and began to exploit the visible properties of phthalocyanines through synthesis of a series of copper phthalocyanine dyes.[69]

Phthalocyanines are large macrocyclic systems containing 18-π electrons and comprising of four modified pyrrole units. These compounds are structurally similar to earlier first generation photosensitisers, specifically porphyrins and chlorins. Phthalocyanines are a particularly attractive family of compounds to study as the synthetic pathways allow for a number of systematic modifications to be made to the molecule, including metal centres, axial ligands and

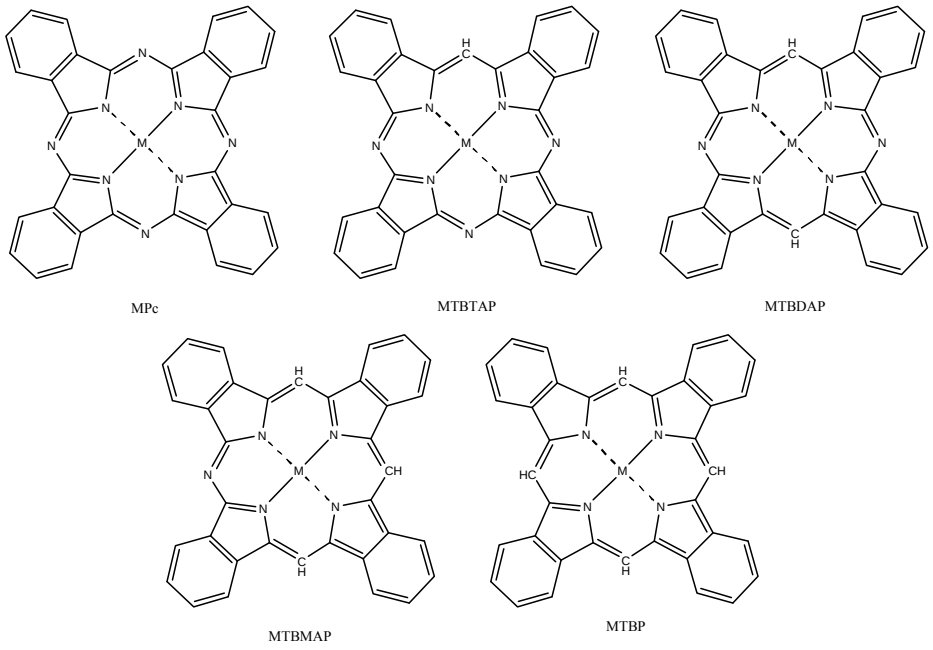

Figure 1. 7. Schematic diagram illustrating the structural modifications from phthalocyanine to tetrabenzoporphyrin.

incorporation of substituents in the alpha (1 and 4) and beta (2 and 3) position, see Figure 1.6. Such changes can be used to fine-tune key physical and photophysical properties of these compounds.

In addition to modifying phthalocyanines by the incorporation of substituents, Linstead *et al.*[70] showed it was possible to synthesise unsymmetrical phthalocyanine derivatives by the reaction of methylmagnesium halide with phthalonitrile to yield magnesium phthalocyanine structures with a modified internal cavity. In these compounds one, two, three or all of the aza links are exchanged for methine links, giving tetrabenzotriazaporphyrin (TBTAP), tetrabenzodiazaporphyrin (TBDAP) and tetrabenzomonoazaporphyrin (TBMAP) and tetrabenzoporphyrin (TBP), respectively, as illustrated in Figure 1.7. It is believed that these unsymmetrical systems may have potential in photodynamic therapy and provide higher stability

and efficiency than the generally less stable porphyrin equivalents. Due to a challenging synthesis little is known about these compounds, and how they fair against their phthalocyanine counterparts. Only recently, Cook *et al.* have reported the facile synthesis of a series of alpha octa-alkyl substituted H_2 and Mg phthalocyanines with an emphasis on the absorption spectra and crystallographic data, opening up the opportunity to study similar systems with a variety metal centres and benzenoid substituents.[71]

Since their discovery, phthalocyanines have been extensively utilised in the dyes and pigments industries due to high thermal, chemical and photochemical stabilities.[59] Unbeknownst to many, phthalocyanines are commonly encountered in everyday life in products such as the blue coating on re-writeable compact discs and cyan inks in printers. In fact extensive research over the last three decades has shown phthalocyanines to have potential application in fields as diverse as solar cells, photocopiers, catalysts and semi-conductors.[58]

The intense blue-green colour exhibited by phthalocyanines was the primary motivation prompting the investigation and subsequent exploitation of these compounds by the dyes and pigments industries. However, on closer inspection of the absorption spectrum of these compounds it is immediately evident that this property fulfils the absorption requirements of an ideal photosensitiser. Figure 1.8 shows a typical absorption spectrum of metal-free and metallated phthalocyanine. The spectrum contains five main bands labelled Q, B (or Soret), N, L and C.[72-75] The four highest energy bands (B, N, L and C) absorb in the UV region of the spectrum. The B band is typically a broad band between 320 – 370 nm and is the second most intense

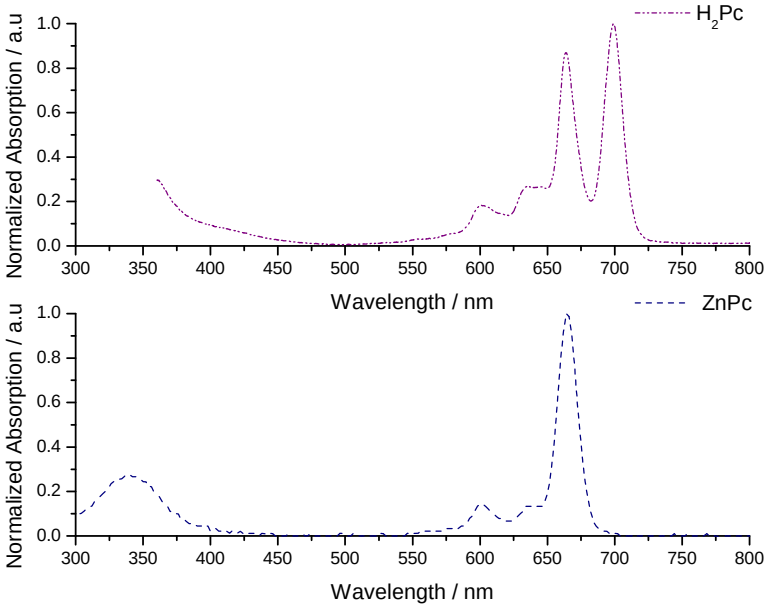

Figure 1. 8. Absorption spectrum of metal-free phthalocyanine and metallated phthalocyanine, containing zinc(II) in the central cavity, illustrating the distinct absorption in the red region of the UV-vis spectrum.

band arising from π – π* transition. The remaining three bands (N, L and C) occur at higher energy than this, typically observed between 210 – 280 nm. These bands are typically not used in the analysis of phthalocyanines and will not be discussed further. In the case of phthalocyanines, the Q-band, in the red region, is the most intense and distinctive absorption band and is responsible for the intense colour exhibited by unaggregated monomeric phthalocyanines. This band is assigned to a $\pi - \pi^*$ transition. In the example given it is obvious that there is a distinct difference in Q-band structure between the metal-free and metallated phthalocyanine. In the case of the metallated compound, a single ion placed at the centre of the phthalocyanine structure gives the molecule D_{4h} symmetry. This leads to a doubly degenerate excited state, thus the Q-band exhibits a sharp single peak. Two ions, as in the case of the metal-free compound, reduces the symmetry to D_{2h}, which results in the degeneracy being lifted and the

Q-band separating into two well-defined peaks, Q_x and Q_y, at lower and higher energy, respectively. In addition to this, the absolute position of the Q-band maxima can vary by 100 nm according to the central metal ion such that the greatest blue-shift occurs with iron(II) inserted into the central cavity and the greatest red-shift occurs with the incorporation of manganese(II).[76]

Phthalocyanines are promising candidates as photosensitisers not only due to the intense red absorption, but also due to low fluorescence quantum yields, high triplet quantum yields and long-lived triplet states. They also typically exhibit high singlet oxygen quantum yields.[77, 78]

Over the past four decades a great interest has been placed on investigating the unique and diverse properties of phthalocyanines, in particular zinc and silicon phthalocyanines and more recently palladium derivatives which have shown a great potential for application in PDT. Subsequently, research has concentrated on the ability to optimise physical and photophysical properties including solubility, Q-band absorption, triplet state properties and singlet delta oxygen quantum yields. Tuning of such properties can be achieved by the substitution of functional groups in the alpha (1, 4) and beta (2, 3) position.

Herein three series of alpha octa-alkyl phthalocyanines, as defined by the metal-ion centre, will be studied in relation to potential application of these compounds as photosensitisers in PDT. Each series will contain silicon, zinc or palladium in the central cavity and will be substituted with alkyl chains of carbon length in the range 1 – 15,

which have previously been shown to enhance solubility. In addition to this an alpha octa-alkyl zinc tetrabenzotriazaporphyrin substituted with hexyl chains will also be examined. Standard techniques will be used to determine fluorescence and triplet data. The approach to the determination of singlet delta oxygen quantum yields will be discussed and investigated and two methods will be considered for the calculation of these values. Where possible results will be compared to unsubstituted parent compounds in order to evaluate the effects of systematic modifications to the phthalocyanine molecule.

1.9 References

1. B. Dunn, *Nature*, 2012, **483**, S2
2. Hippocrate, *Prorrhétique II*, in Ouevres Complètes d'Hippocrate, E. Littré, Paris, J. B. Baillière, 1861, **9**, 32.
3. G. T. Diamandopoulus, *Antican. Res.*, 1996, **16**, 1595
4. L. Weiss, *Cancer Metastasis Rev.*, 2000, **19**, 205.
5. P. D. Sasieni, J. Shelton, N. Ormiston-Smith, C. S. Thomson and P. B. Silcocks, *Br. J. Cancer*, 2011, **105**, 460
6. J. Hirsch, *J. Am. Med. Assoc.*, 2006, **296**, 1518.
7. R. R. Allison, G. H. Downie, R. Cuenca, X. Hu, C. J. H. Childs and C. H. Sibata, *Photodiagnosis and Photodynamic Therapy*, 2004, **1**, 27
8. I. J. Macdonald and T. J. Dougherty, *J. Porph. Phthal.*, 2001, **5**, 105
9. D. Phillips, *Photochem. Photobiol.*, 2010, **9**, 1589
10. C. M. Allen, W. M. Sharman and J. E. Van Lier, *J. Porph. Phthal.*, 2001, **5**, 161.
11. R. Ackroyd, C. Kelty, N. Brown and M. Reed, *Photochem. Photobiol.*, 2001, **74**, 656
12. J. Moan and Q. Peng, *Antican. Res.*, 2003, **23**, 3591.
13. M. F. Holick, J. A. MacLaughlin, J. A. Parrish and R. R. Anderson, *The photochemistry and photobiology of vitamin D_3*, in The Science of Photomedicine, J. D. Regan and J. A. Parrish, New York, London, Plenum Press, 1982, 195
14. N. R. Finsen, *Phototherapy*, London, Edward Arnold, 1901.
15. K. Rajakumar, S. L. Greenspan, S. B. Thomas and M. F. Holick, *Am. J. Pub. Health*, 2007, **97**, 1746
16. M. F. Holick, *J. Clin. Invest.*, 2006, **116**, 2062

17. R. J. Cremer, R. W. Perryman and D. H. Richards, *Lancet*, 1958, **1**, 1094
18. R. H. Dobbs and R. J. Cremer, *Archives of Disease in Childhood*, 1975, **50**, 833.
19. T. B. Fitzpatrick and M. A. Pathak, *J. Invest. Dermatol.*, 1959, **25**, 229
20. H. von Tappeiner, *Muench. Med. Wochenschr.*, 1900, **47**, 5.
21. O. Raab, *Z. Biol.*, 1900, **39**, 524
22. J. Prime, *Les accidentes toxiques por l'eosinate de sodium*, Paris, Jouve and Boyer, 1900.
23. H. von Tappeiner and A. Jesionek, *Muench. Med. Wochenschr.*, 1903, **47**, 2042
24. H. von Tappeiner and A. Jodbauer, *Dtsch. Arch.Klin. Med.*, 1904, **80**, 427
25. Z. Huang, *Technol. Cancer. Res. Treat.*, 2005, **4**, 283
26. L. Brancaleon and H. Moseley, *Lasers Med. Sci.*, 2002, **17**, 173
27. A. Policard, *C. R. Soc. Biol.*, 1924, **91**, 1423
28. H. Scherer, *Ann. Chem. Pharm.*, 1841, **40**, 1.
29. W. Hausmann, *Biochem. Z.*, 1911, **30**, 276
30. F. Meyer-Betz, *Dtsch. Arch.Klin. Med.*, 1913, **112**, 476
31. H. Auler and G. Banzer, *Z. Krebsforsch*, 1942, **53**, 65
32. F. H. Figge, G. S. Weiland and L. O. J. Manganiello, *Proc. Soc. Exp. Biol. Med.*, 1948, **68**, 640
33. S. K. Schwartz, K. Absolon and H. Vermund, *Univ. Minn. Med. Bull.*, 1955, **27**, 7
34. R. L. Lipson, E. J. Baldes and A. M. Olsen, *J. Nat. Cancer. Inst.*, 1961, **26**, 1
35. I. Diamond, S. G. Gronelli, A. F. McDonagh, S. Nielsen, C. B. Wilson and R. Jaenicke, *Lancet*, 1972, **2**, 1175

36. T. J. Dougherty, G. B. Grinday, R. Fiel, K. R. Weishaupt and D. G. Boyle, *J. Nat. Cancer. Inst.*, 1975, **55**, 115
37. T. J. Dougherty, *J. Clin. Laser Med. Surg.*, 1996, **14**, 219
38. T. J. Dougherty, J. E. Kaufman and A. Goldfarb, *Cancer Res.*, 1978, **38**, 2628
39. T. J. Dougherty, C. J. Gomer, B. W. Henderson, G. Jori, D. Kessel, M. Korbelik, J. Moan and Q. Peng, *J. Nat. Cancer. Inst.*, 1998, **90**, 889.
40. N. L. Oleinick, R. L. Morris and I. Belichenko, *Photochem. Photobiol. Sci.*, 2002, **1**, 1
41. T. J. Dougherty, *Photochem. Photobiol.*, 1987, **46**, 569
42. J. Moan, Q. Peng, J. F. Evensen, F. Berg, A. Western and C. Rimington, *Photochem. Photobiol.*, 1987, **46**, 713
43. J. Moan, *J. Photochem.Photobiol.*, 1990, **5**, 521
44. D. V. Ash and S. B. Brown, *Eur. J. Cancer*, 1993, **29A**, 1781
45. S. Baker, M. C. Petty, G. C. Roberts and M. V. Twigg, *IEE. Proc. Part 1 Solid State Electron. Devices*, 1983, **130**, 260.
46. R. D. Gould, *Coord. Chem. Rev.*, 1996, **156**, 237.
47. R. Bonnett, *Chem. Soc. Rev.*, 1995, **24**, 19.
48. A. Juzeniene, K. P. Nielsen and J. Moan, *J. Environ. Pathol. Toxicol. Oncol.*, 2006, **25**, 7
49. K. Plaetzer, B. Krammer, J. Berlanda, F. Berr and T. Kiesslich, *Lasers Med. Sci.*, 2009, **24**, 259
50. D. Phillips, *Pure App. Chem.*, 1995, **67**, 117.
51. J. C. Kennedy and R. H. Pottier, *J. Photochem. Photobiol. B. Biol.*, 1992, **14**, 275.
52. Z. Malik and H. Lugaci, *Br. J. Cancer*, 1987, **56**, 589
53. B. C. Wilson and M. S. Patterson, *Phys. Med. Biol.*, 2008, **53**, R61

54. J. M. Houle and A. Strong, *J. Clin. Pharm.*, 2002, **42**, 547
55. N. M. Bressler and S. B. Bressler, *Invest. Ophthalmol. Vis. Sci.*, 2000, **41**, 624
56. R. Bonnett, R. D. White and U. J. Winfield, *Biochem. J*, 1989, **261**, 277
57. L. M. Moreira, F. V. dos Santos, J. P. Lyon, M. Maftoum-Costa, C. Pacheco-Soares and N. S. da Silva, *Aust. J. Chem.*, 2008, **61**, 741.
58. C. G. Claessens, U. Hahn and T. Torres, *Chem. Rec.*, 2008, **8**, 75.
59. P. Gregory, *J. Porph. Phthal.*, 2000, **4**, 432
60. R. P. Linstead and C. E. Dent, *J. Chem. Soc.*, 1934, 1027
61. R. P. Linstead, C. E. Dent and A. R. Lowe, *J. Chem. Soc.*, 1934, 1033
62. R. P. Linstead, A. R. Lowe and G. T. Byrne, *J. Chem. Soc.*, 1934, 1016
63. J. M. Robertson, *J. Chem. Soc.*, 1935, 615.
64. J. M. Robertson, *J. Chem. Soc.*, 1936, 1195.
65. J. M. Robertson, *J. Chem. Soc.*, 1936, 1736.
66. J. M. Robertson, *J. Chem. Soc.*, 1937, 219.
67. J. M. Robertson, *J. Chem. Soc.*, 1940, 36.
68. A. Braun, Tcherniac, J., *Ber. Deut. Chem. Ges*, 1907, **40**, 2709.
69. A. G. Dandridge, H. A. E. Drescher and J. Thomas, in *British Patent*, 1927, 169.
70. R. P. Linstead, Robertson, J.M, *J. Chem. Soc.*, 1936.
71. A. N. Cammidge, I. Chambrier, M. J. Cook, D. L. Hughes, M. Rahman and L. Sosa-Vargas, *Chem.-Eur. J.*, 2011, **17**, 3136.
72. L. Edwards and M. Gouterman, *J. Mol. Struct.*, 1970, **33**, 292.

73. A. M. Schaffer and M. Gouterman, *Theoret. Chim. Acta*, 1972, **25**, 62.
74. A. M. Schaffer, M. Gouterman and E. R. Davidson, *Theoret. Chim. Acta*, 1973, **30**, 9.
75. K. Jerwin and F. Wasgestian, *Spectrochim. Acta*, 1984, **40A**, 159.
76. M. J. Cook, A. J. Dunn, S. D. Howe, A. J. Thomson and K. J. Harrison, *J. Chem. Soc. Perkin Trans. 1*, 1988, 2453.
77. T. Nyokong, *Coord. Chem. Rev.*, 2007, **251**, 1707.
78. J. D. Spikes, *Photochem. Photobiol.*, 1986, **43**, 691.

2. Experimental Methods

2.1 Materials and Synthesis

All experiments were carried out in 1% v/v pyridine in toluene unless otherwise stated. The phthalocyanine derivatives under investigation were synthesised by another group in our department who describe the synthesis in detail elsewhere.[1] Substituted zinc, silicon and palladium phthalocyanines were investigated here. Each compound has a different length alkyl substituent in the alpha position. The compounds are referred to as *n*MPc, whereby *n* represents the number of carbons on the alkyl chain and M refers to the metal centre for example 6ZnPc is zinc phthalocyanine substituted in the alpha position with hexyl groups. The standards used in this work were zinc phthalocyanine, ZnPc (97 %), perinaphthenone, PPN (97 %), and zinc tetraphenylpyridine, ZnTPP, which were obtained from Aldrich and used without further purification. HPLC grade toluene (99.99 %) and pyridine (≥99.5 %) were obtained from Aldrich.

2.2 Spectroscopic Studies

UV-visible spectra were recorded on a Hitachi U-3000 spectrophotometer using 1 cm matched quartz cuvettes. The molar absorptivity was calculated from a least squares fit of absorbance against concentration. Steady-state fluorescence spectra were acquired on a Horiba Jobin Yvon Fluoromax-2 with 2 nm slit width for both excitation and emission monochromators.

2.3 Photophysics

2.3.1 Fluorescence Quantum Yields

Fluorescence quantum yields, Φ_F, were determined using the comparative method described in detail elsewhere.[2] The fluorescence quantum yield is related to that of a standard by:

$$\Phi_F = \Phi_{F,std} \frac{A_{std}}{F_{std} n_{std}^2} \frac{F n^2}{A} \qquad \text{(eq. 2.1)}$$

Where F and F_{std} are the areas under the fluorescence emission curves of the samples (**a-h**) and the standard, respectively. A and A_{std} are the respective absorbances of the samples and standard at the excitation wavelength, respectively, and n and n_{std} are the refractive indexes of solvents ($n_{toluene}$ = 1.4961 (at 20 °C and 589 nm); $n_{ethanol}$ = 1.3611 (at 20 °C and 589 nm); $n_{pyridine}$ = 1.5095 (at 20 °C and 589 nm); $n_{tol/py}$ taken to be 1.50.[3] Unsubstituted ZnPc (in EtOH) (Φ_f = 0.28)[4] was employed as the standard. The absorbance of the solutions at the excitation wavelength ranged between 0.02 and 0.1.

2.3.2 Fluorescence Lifetimes

The technique of time correlated single photon counting (TCSPC) was used to record fluorescence lifetimes of the samples. All solutions under study were prepared with a concentration so as to give a maximum absorbance at the Q-band of no greater than 0.05, in order to eliminate the effects of re-absorption. The excitation source consisted of a pulsed 635 nm diode laser (IBH NanoLED Model-02) providing output pulses of <200 ps at a repetition rate of 1 MHz. The fluorescence emission was collected at 90° to the excitation source, and the emission at λ = 716 nm recorded using a cooled, red sensitive

photomultiplier tube (IBH Model TBX-04) linked to a time-to-amplitude converter (Ortec 567) and multichannel analyzer (E.G & G. Trump Card and Maestro for Windows V.5.10). The instrument response function (IRF) of the apparatus was measured using a dilute suspension of milk powder in water as a scattering medium giving an IRF with a duration of 450 ps full width at half maximum (FWHM). The time per channel was typically ~25 ps giving a full range of ~50 ns over the 2048 point data set. All fluorescence decays were recorded to a minimum of 10,000 counts in the peak channel of the pulse height analyzer. The data were transferred to a computer and analysed by using the standard method of iterative reconvolution and non-linear least squares fitting in a Microsoft Excel spreadsheet. The quality of calculated fits was judged using statistical parameters including the Durbin-Watson parameter, reduced χ^2, random residuals and autocorrelated residuals.

2.3.3 Triplet Quantum Yields and Lifetimes

Triplet-triplet absorption spectra, triplet extinction coefficients, lifetimes and quantum yields were measured using a standard method, described in detail elsewhere.[5] Briefly, the data were recorded on a laser flash photolysis system. The excitation pulses were provided by the third-harmonic of a Q-switched Nd:YAG laser (JK 2000). Pulse energies were between 0.1 – 1 mJ and the excitation beam was directed through the sample without focussing. The analyzing source was a tungsten-halogen lamp imaged into the sample cuvette at right angles to the excitation beam. The analyzing source was subsequently relay imaged onto the entrance slits of a 50 cm monochromator and detected with a photomultiplier tube (EMI 9529B). Transient absorption spectra were collected by measuring two time gates, from 0

– 25 μs and 30 – 80 μs. These were simultaneously recorded onto computer from the two-channel digital real-time oscilloscope (LeCroy Waverunner LT262). Transient decay signals were averaged for 1024 pulses using the oscilloscope and written directly to disk. All the sample solutions were degassed, using the freeze-pump-thaw technique and irradiated in a 10 mm path-length quartz cell.

2.3.4 Steady-state Luminescence

The phosphorescence spectrum for palladium phthalocyanine derivatives was measured on a home-built system. The sample was excited at 633nm with a HeNe laser (5 mW), the luminescence collected at 90 degrees and focused onto the entrance slit of monochromator (Bentham TM-300) equipped with a NIR optimised grating (600 grooves/mm, 1 micron blaze). The selected wavelength was focussed onto a Hamamatsu NIR photomultiplier tube (H10330B-45) operating at -800V in photon counting mode. The photon count rate was measured using a digital i-o card (National Instruments PCI-6601) as a function of the selected wavelength allowing the emission spectrum to be recorded. The spectrometer was controlled by a home-written program (LabVIEW).

2.4 Singlet Delta Oxygen Quantum Yield Determination

2.4.1 Time-Resolved Singlet Oxygen Phosphorescence Detection (TRPD)

The singlet delta oxygen quantum yield, Φ_{Δ}, was determined using a similar method to those described in previous work.[6, 7] Samples dissolved in 1% v/v toluene/pyridine, to minimize aggregation, and allowed to equilibrate with air were excited using the third harmonic of a Q-switched Nd:YAG laser (355 nm). A $CoSO_4$ filter was used

upstream of the solution to remove residual 1064 nm radiation. Typical pulse energies used were in the range 0.1-1 mJ per pulse. A North Coast E0-817P Ge photodiode/amplifier combination detected the singlet oxygen phosphorescence at right angles to the incident laser beam. The sample was placed in a fluorescence cuvette with a 10 mm path length close to the detector. The singlet oxygen luminescence was selected with a 1270 nm silicon interference filter (bandpass, 30 nm) placed close to the detector.

2.4.2 Time-Resolved Thermal Lensing

The TRTL signal was collected using a similar method to those described in previous work.[8] Samples were excited using the third harmonic of a Q-switched Nd:YAG laser (355 nm) focused onto the front of the cuvette using a lens of 100 mm focal length. Typical pulse energies were in the range 0.1 – 1 mJ per pulse at a frequency of 10 Hz. A cw HeNe laser (633 nm) with energy of 2 mW was used to probe the samples by focusing into the cuvette using a lens of focal length $f = 50$ mm. A silicon photodiode combined with a trans-impedance amplifier or a photon multiplier tube used to detect the probe beam. The sample was placed in a fluorescence cuvette with a 10 mm path length. The probe beam was selected with a monochromator set to 633 nm placed close to the detector.

2.5 References

1. M. J. Cook, I. Chambrier, S. J. Cracknell, D. A. Mayes and D. A. Russell, *Photochem. Photobiol.*, 1995, **62**, 542.
2. A. T. R. Williams, S. A. Winfield and J. N. Miller, *Analyst*, 1983, **108**, 1067.
3. *Handbook of Chemistry and Physics*, CRC Press, Roca Baton, Florida, 60th edn., 1979.
4. M. N. Sibata, A. C. Tedesco and J. M. Marchetti, *Eur. J. Pharm. Sci.*, 2004, **23**, 131.
5. I. Carmichael and G. L. Hug, *J. Phys. Chem. Ref. Data*, 1986, **15**, 1.
6. R. Schmidt, K. Seikel and H. D. Brauer, *J. Phys. Chem.*, 1989, **93**, 4507.
7. S. Nonell, Braslavsky, S.E., *Singlet Oxygen, UV-A and Ozone,Methods in Enzymology*, 2000, **319**.
8. G. Rossbroich, N. A. Garcia and S. E. Braslavsky, *J. Photochem.*, 1985, **31**, 35.

3. Singlet Delta Oxygen, $O_2(^1\Delta_g)$

3.1 Introduction

The science and chemistry of ground state molecular oxygen (O_2) has been widely studied for centuries. Despite the apparent simplicity of the oxygen molecule it exhibits a variety of unusual properties with respect to magnetic behaviour, spectroscopy, energy-transfer and chemical reactivity.[1] Furthermore, molecular oxygen is essential to animal respiration and life. Oxygen also plays a significant role in photodynamic therapy as one of the three controlling factors; the other two factors are light and the chemical photosensitiser.[2] The key process in PDT appears to be the death of cells by the formation of cytotoxic oxygen, though the precise biological mechanism in this step is not yet fully understood and may in fact vary on a case by case basis.[3]

The cytotoxic oxygen referred to throughout literature is more accurately ascribed to a low-lying excited state of molecular oxygen. In 1928, Mulliken applied the molecular orbital theory to the oxygen molecule and predicted the existence of two low-lying excited singlet states.[4] The well known Fraunhofer line observed at 157 kJ mol^{-1} corresponds to the transition from the ground state to one of these singlet states and is due to the absorption spectrum of oxygen in the Earth's atmosphere.[5] Mulliken went on to claim that another singlet level existed with lower energy, predicting that the other singlet state would lie at approximately 79 kJ mol^{-1} above the ground state. It is now commonly accepted that the two electronically excited states

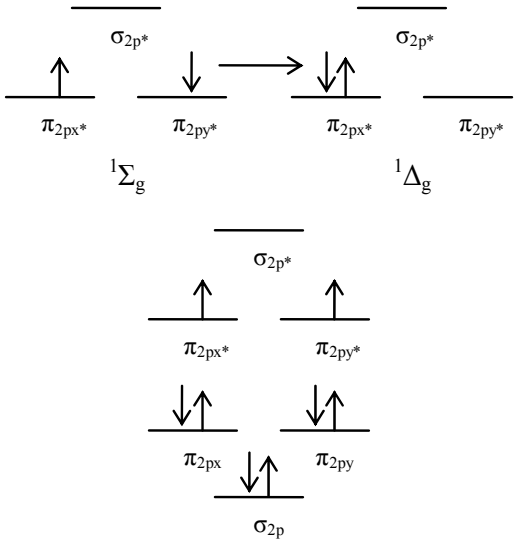

Figure 3. 1. A molecular orbital diagram illustrating the spin pairings of the electrons in the ground state and simplified diagrams of both excited states.

arise from the same configuration, but have different spin pairings of the two electrons. This leads to a $^1\Sigma_g^+$ state at 157 kJ mol^{-1} and a $^1\Delta_g$ at 94 kJ mol^{-1} above the $^3\Sigma_g$ ground state, as illustrated in Figure 3.1.[6] Though the electronic transitions are highly spin forbidden both are observed in the absorption and emission spectra in the upper atmosphere, with zero-zero transitions at 1269 nm ($^1\Delta_g \leftarrow {}^3\Sigma_g$) and 762 nm ($^1\Sigma_g^+ \leftarrow {}^3\Sigma_g$) and estimated radiative lifetimes of 64 minutes and 10 seconds, respectively.[7] The measured lifetimes in gas and solution phase are significantly shorter and, in condensed media, the lifetime of $O_2(^1\Sigma_g^+)$ is so short lived that little is known about the properties of the state, thus the term singlet oxygen refers primarily to the $^1\Delta_g$ state.

As early as 1931, Kautsky proposed that singlet oxygen was a possible intermediate in dye-sensitised photoreactions formed via the fluorescent and metastable states of dyes.[8] Furthermore, this theory was proved by performing an experiment in which photosensitised oxygenation of substrate molecules was observed when the substrate and photosensitiser molecules were absorbed on different silica gel grains. The experiment showed that the intermediate responsible for photo-oxygenation was gaseous oxygen. However, these ideas were considered too radical for their time.[9] It was not until 1963 that Khan

and Kasha interpreted the chemiluminescence of the hypochlorite-peroxide reaction as caused by liberated singlet oxygen.[10] Then, in 1964, the original ideas proposed by Kautsky were revisited in publications by Foote and Wexler and Corey and Taylor.[11] Furthermore, in 1972 Adams and Wilkinson developed a method for measuring the lifetime of singlet oxygen in solution, which paved the way for direct time measurements of singlet oxygen with a reactive substrate.[12] In 1976, Krasnovsky used a mechanical phosphorescence to detect the weak luminescence of $O_2(^1\Delta_g)$ at 1269 nm,[13] revealing kinetic information about singlet oxygen on the millisecond timescale.[14, 15] Following the development of sensitive germanium photodiodes in the 1980s, phosphorescence studies of $O_2(^1\Delta_g)$ on a microsecond timescale became routinely possible.

Between 1933 and 1935 Jabłonski reported an energy-level diagram in which it is illustrated that dye molecules possess two states, a short-lived fluorescence state and a long-lived metastable state.[5] In 1943, Terenin assigned the fluorescence state of these dyes as singlet and the metastable state as triplet, notations that are still in use today. As has previously been discussed, rather unusually, the opposite is true for the assignment of the ground and excited states of molecular oxygen.

It is now understood that $O_2(^1\Delta_g)$ can arise as a result of several mechanisms involving the excited states of dyes. The two core categories of photosensitised singlet oxygen formation are classified as Type I and Type II mechanism.[16, 17] In a Type I mechanism it is the formation of radicals by hydrogen-abstraction or electron transfer between an excited sensitiser and substrate that proceeds to react with molecular oxygen to form the superoxide radical anion. In a Type II

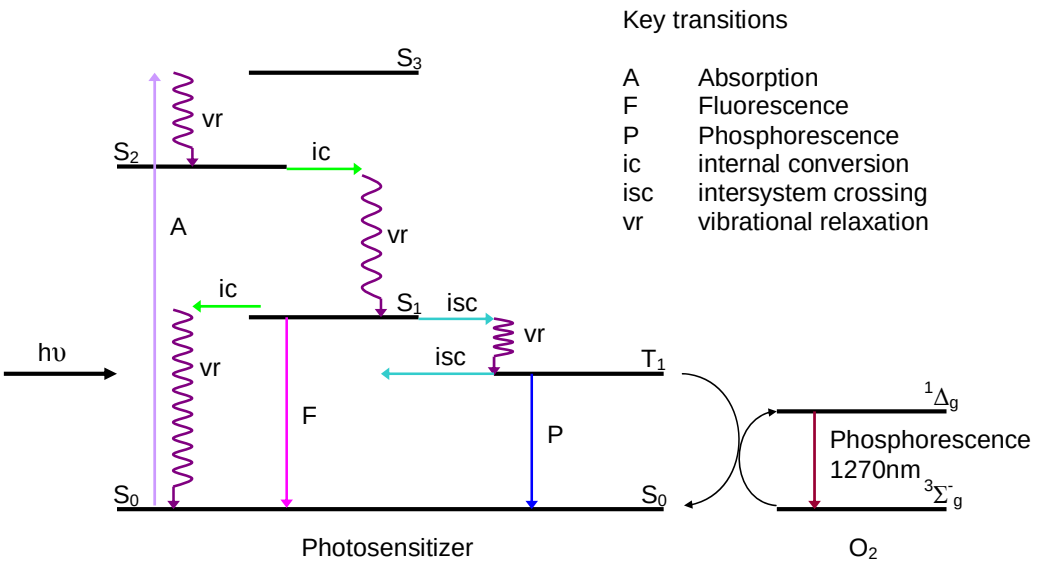

Figure 3. 2. Jablonski diagram illustrating the energtic pathways in the formation of singlet delta oxygen via the excited states of a dye photosensitizer in a Type II mechanism.

mechanism the excited sensitiser interacts directly with molecular oxygen resulting in an energy transfer and the formation of singlet delta oxygen, illustrated in the expanded Jabłonski diagram, Figure 3. 2.

The efficiency of a photosensitiser in relation to its ability to generate singlet delta oxygen is known as the singlet delta oxygen quantum yield (Φ_Δ). This is defined as the ratio of the number of absorbed photons to the number of singlet delta oxygen states that are formed.[18-20] A high quantum yield, typically defined as over 0.5, signifies that the photosensitiser will efficiently convert the absorbed energy into singlet delta oxygen. This is highly desirable as the ultimate advantage is a reduction in drug concentration or levels of radiation or, in an ideal situation, reduction of both parameters. There are a wide variety of techniques now established for the determination of Φ_Δ including, direct methods of detecting the luminescence, with time-resolved or

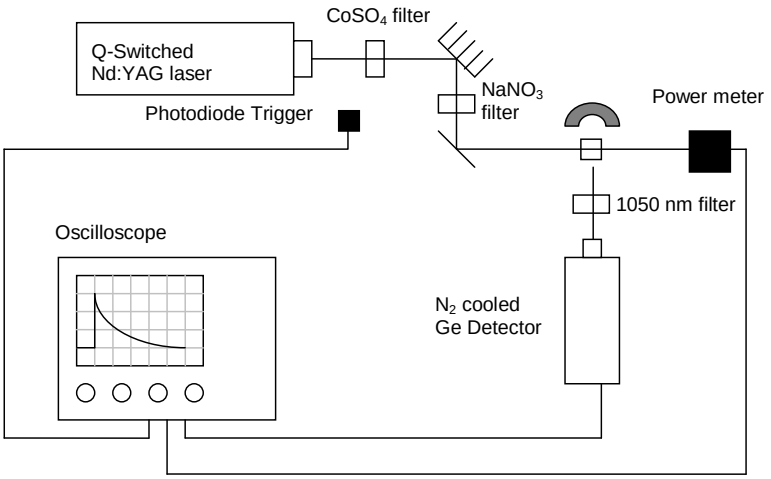

Figure 3. 3. Schematic diagram of a time-resolved singlet oxygen phosphorescence spectrometer, λ_{ex} = 355 nm

steady-state infrared luminescence, calorimetric techniques using photo acoustic calorimetry or time-resolved thermal lensing and the quantitative analysis of photooxidation reactions, monitoring either the loss of absorption or fluorescence of a quencher on oxygen uptake.

As has previously been mentioned, the advent of the germanium photodiode in the 1980s led to the development of one of the most widely used methods for the determination of Φ_{Δ}, the direct detection of the weak singlet oxygen phosphorescence in the near-infrared.[20] This technique is known as time-resolved near-infrared phosphorescence detection.[21, 22] An example of a typical experimental set-up can be seen illustrated in Figure 3.3. A potential photosensitiser, with absorption of less than 0.1 at the excitation wavelength, is excited with a pulsed laser and the singlet oxygen luminescence generated by the excitation of oxygen via the excited states of the photosensitiser is detected. From this it is possible to determine the

emission intensity of singlet delta oxygen phosphorescence, *S(0)*, when $t = 0$.

It follows that the intensity of emission of singlet oxygen phosphorescence is proportional to concentration of singlet oxygen such that:

$$S(t) = \frac{\kappa}{\eta_r^2} k_r [O_2(^1\Delta_g)](t) \qquad \text{(eq. 3. 1)}$$

where, κ is the proportionality constant, including geometrical and electronic factors of the detection system, η_r is the refractive index of the solution and k_r is the solvent-dependent $O_2(^1\Delta_g)$ radiative decay constant.[20] In order to obtain Φ_Δ the following relationship,

$$S(t) = S(0)\frac{\tau_\Delta}{\tau_T - \tau_\Delta}(e^{\frac{-t}{\tau_T}} - e^{\frac{-t}{\tau_\Delta}}) \qquad \text{(eq. 3. 2)}$$

where, τ_Δ and τ_T are $O_2(^1\Delta_g)$ and triplet lifetimes, respectively. Hence, if the triplet lifetime is much shorter than the $O_2(^1\Delta_g)$ lifetime, such as $\tau_T \ll \tau_\Delta$, and $t > 5\tau_T$ then the intensity can be described as,

$$S(t) = S(0)e^{\frac{-t}{\tau_\Delta}} \qquad \text{(eq. 3. 3)}$$

and *S(0)*, the signal intensity at $t = 0$, is given as,

$$S(0) = \frac{\kappa}{\eta_r^2} k_r \phi_\Delta \frac{E_1(1-10^{-A})}{N_A h \upsilon V} \qquad \text{(eq. 3. 4)}$$

where, E_1 is the energy of the laser pulse, A is the absorbance of the solution, N_A is Avogadro's constant, h is Planck's constant, υ is the laser frequency and V is the irradiated volume. Calculating the ratio of *S(0)* for a sensitiser and reference measured under the same geometrical conditions with the same laser energy and absorbance affords the relative value of Φ_Δ, this is illustrated in Figure 3. 4.

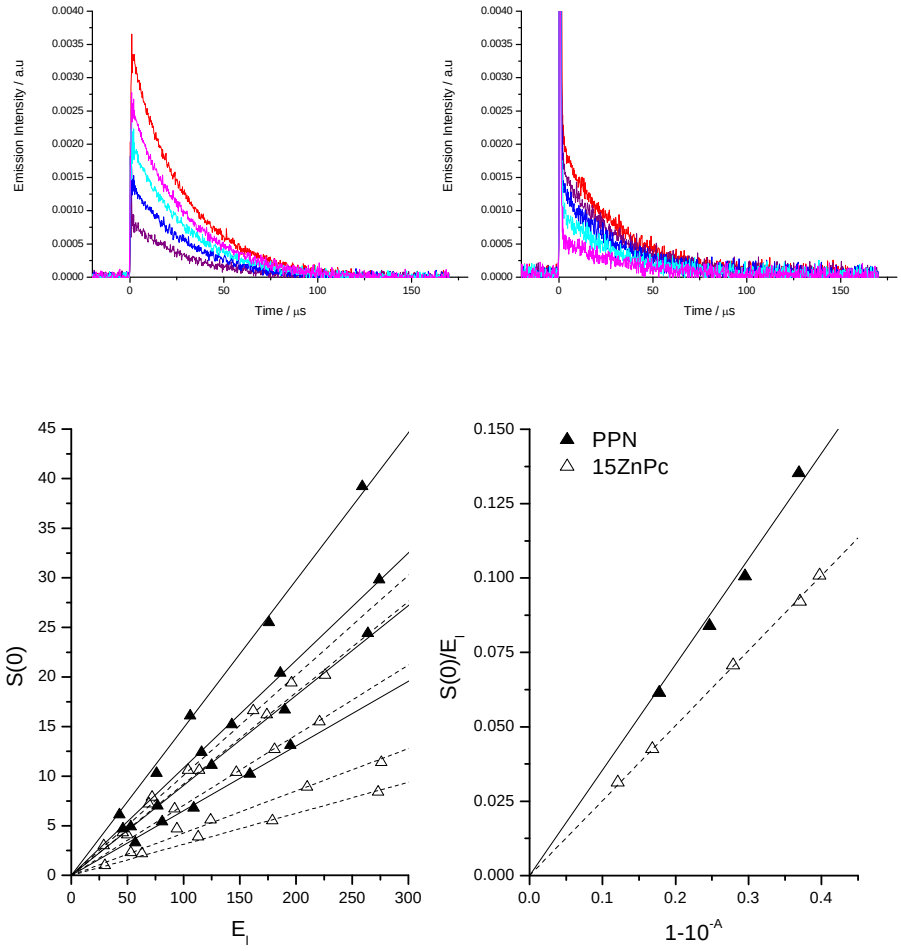

Figure 3. 4. An example of data analysis for a typical TRPD experiment. Singlet oxygen phosphorescence decay for PPN (a) and sample (b) at varying power. Slopes of the intensity relationship with power for varying power (c) followed by the relationship with concentration (d).

A key component of the success of this technique is the choice of standard, which, ideally should exhibit a similar absorption spectrum as the sample dye, can be measured in the same reaction conditions, for example, solvent system and excitation wavelength, and has Φ_Δ close to unity. The use of standards, defines the first limitation of this technique, another key disadvantage is that less than 10^{-3} of $O_2(^1\Delta_g)$ states formed decay by a radiative pathway.[23] Furthermore, any quenching species, impurities, present in the sample can significantly distort the quantum yield.[24]

In more recent years, a technique that has gained popularity is that of Φ_Δ determination by the quantitative analysis of photo-oxidation reactions. In particular, the two chemical quenchers most commonly chosen are diphenylbenzofuran, DPBF, in DMSO and bilirubin ditaurate, BDT.[25] Samples are irradiated at the Q-band, between 630 and 720 nm, and the absorption decay of the chemical quencher is monitored, in the case of DPBF this is at 417 nm. The photobleaching rate of the DPBF for the sample is measured and compared to that of a standard using the following relationship,

$$\Phi_\Delta = \Phi_{\Delta,std} \frac{I_{std}^{abs} R}{I^{abs} R_{std}} \qquad \text{(eq. 3. 5)}$$

where, subscript *std* refers to the standard, I is the intensity of absorbance and R is the rate of decay. In the case of studies performed on phthalocyanines the standard typically used is ZnPc with $\Phi_\Delta = 0.56$ in DMF and $\Phi_\Delta = 0.67$ in DMSO.[26] To date, this technique has been used to calculate quantum yields with an accuracy of 10-15%.[27]

Both singlet delta oxygen luminescence and photo-oxidation quenching techniques have been proven to provide singlet oxygen quantum yields that are comparable with one another once geometrical and experimental variations are eliminated owing to the process of comparison. Such techniques are indeed widely understood and used successfully within their field with typical uncertainties in the region of 5 - 10%.[24] However, the main objective in determining Φ_Δ in this study is in the context of photodynamic therapy where the excitation source is required to coincide with the optical window, in the range of 600 – 850 nm. It is evident that current techniques do not adequately reproduce *in vivo* conditions, which is in part due to the nature of the techniques, but also largely due to the dependence upon

standards which add a number of external constraints to the measurements. This is further hindered by a dependence upon aging techniques and vintage instruments, thus, with the development and subsequent availability of more efficient detection and laser systems, there is some argument for the modernisation of singlet oxygen quantum yield determination.[28]

With this in mind there has been a move to update Φ_Δ techniques to reflect the rate at which technology has developed over the last 50 years and determine a means of elucidating absolute Φ_Δ, and in doing so eliminate the dependence upon standards. Such methods focus predominantly on the energy lost through non-radiative pathways that is detected as localised changes in heat or pressure, brought about by a change of temperature within the excited area of the sample. Examples of such techniques include light-induced optoacoustic calorimetry, a pressure based technique, and photothermal blooming, which is heat based.[29] These techniques are considered to be more sensitive than traditional comparison techniques as the loss of energy from the singlet delta oxygen state is favoured by non-radiative pathways over the radiative.[24]

3.2 Time-Resolved Thermal Lensing

Time-resolved thermal lensing, TRTL, is a familiar technique in the field of absolute fluorescence quantum yield determination.[30-36] The thermal lens was initially discovered by Gordon *et al.* in 1965. During efforts to increase the intensity of laser Raman scattering it was noted that the laser light had been subjected to divergent effects of a lens upon insertion of a benzene sample within the resonator of the HeNe laser. It was concluded that the laser, upon reaching a steady-state, had

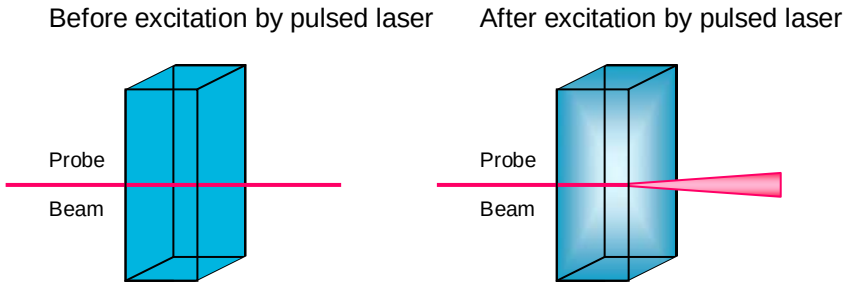

Figure 3. 5. A simplified diagram illustrating the formation of the thermal lens and subsequent divergence of the probe beam after pulsed excitation.

heated the sample and so formed a 'thermal lens'. Since then it has been widely used in a variety of measurements, including kinetics and reaction dynamics.[37, 38] In 1973, Hu and Whinnery were able to demonstrate the detection of lens formation outside the laser cavity.[39] This opened the door to Swofford *et al.* who in 1976 employed a second laser to investigate the effect itself.[40] Initially the thermal lensing effect was studied with a view to eliminate it due to interference observed in laser measurements.[41] However, with the advent of affordable and increasingly efficient laser systems, the technique has been adapted for singlet delta oxygen measurements and the study of triplet states of photosensitising dyes.[42, 43]

TRTL works on the principle of a sample, in solution or gas-phase, being excited by a focused pulsed laser of Gaussian profile, exhibiting the highest intensity in the centre compared to the wings. This non-uniform excitation subsequently results in a temperature gradient due to the release of heat, a reflection of the energy absorbed by the sample, and so a temporal refractive index gradient is generated.[23, 44] The generation and decay of the temporary lens is monitored on a millisecond and microsecond timescale using a continuous wave laser,

as illustrated in Figure 3. 5. The transparency of the ground state and excited states of the sample species to the probe beam is key in the success of this technique, as any further absorption by transients can add to the thermal lensing effect in what is known as a population lens.[45]

Throughout this work, TRPD is chosen technique by which Φ_Δ are determined, using both PPN with $\Phi_\Delta = 0.95$[46] and ZnPc with $\Phi_\Delta = 0.61$[25] as the standards and 355 nm as the excitation wavelength. This was primarily due to the long accepted history and reliability of the technique. However, it was also hoped that construction of a TRTL spectrometer would yield a technique that would afford greater degrees of freedom in terms of experimental conditions and remove the dependence upon standards in the determination of Φ_Δ values. With a view to this, a system was built that was rigorously tested using the same standards as TRPD before expanding to explore the experimental parameters available.

3.3 Experimental Set-up – Construction of a Thermal Lensing Spectrometer

A thorough search through literature revealed that the common core components of a TRTL spectrometer are:

- A sample,
- A focused pulsed 'pump' beam to excite sample,
- A focused continuous wave 'probe' beam to monitor changes in sample,
- Lenses to focus probe and pump beams,
- Beamsplitter to make pump and probe beam collinear,
- A filter before the detector to remove the pump beam,

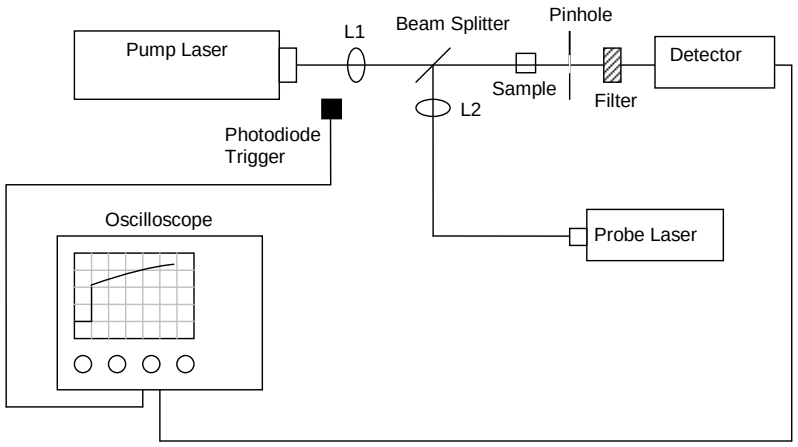

Figure 3. 6. Schematic of a dual beam mode-mismatched thermal lens spectrometer illustrating the key components

- Pinhole to select central area of the probe beam,
- A detector and data collection system.

A typical experimental set-up containing each of these components can be seen in Figure 3. 6. Traditionally the TRTL spectrometer has been constructed to include a Nd:YAG laser as the pulsed excitation source, and a HeNe laser as the cw probe.[47] The pump beam and probe beam are aligned collinearly through the sample such that the probe beam can monitor the transient thermal lens formed following excitation. Perinaphthenone (PPN) was the standard used in TRPD measurements, it is soluble in a variety of solvents and has Φ_{Δ} close to unity. The absorption spectrum is illustrated in Figure 3. 7 and shows the transparency of PPN to the probe beam at 632 nm. A similar spectrometer to those described in the literature was constructed in order to replicate and validate the technique using the calibration of a well-known standard. The components used will now be discussed in some detail.

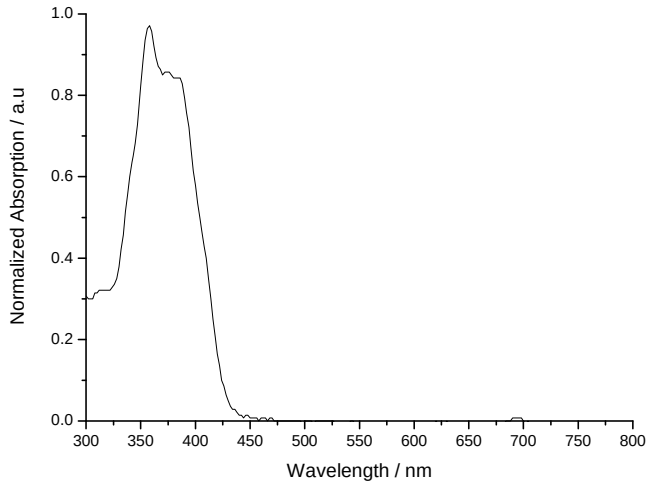

Figure 3. 7. A typical absorption spectrum of phenalenone, PPN.

3.3.1. Pump Beam

The third-harmonic of a Q-switched Nd:YAG laser, 355 nm, was used as the excitation source. This replicates previous TRTL spectrometers and also the excitation source in the TRPD experiment used in this work. A $CoSO_4$ filter was placed upstream from the sample in order to remove residual 1064 nm radiation. A 400 nm cut-off filter was placed upstream from the sample to remove residual 532 nm radiation. A repetition rate of 2 - 10 Hz was chosen to allow for full thermal relaxation of the sample between pulses. It must be noted that the Nd:YAG laser system was assembled with its associated dye-laser such that a variety of excitation wavelengths could be accessed and introduced into the set-up, if required.

3.3.2. Probe Beam

Initially a cw HeNe laser was used as the probe beam in order to replicate earlier set-ups. This was a success with PPN, however,

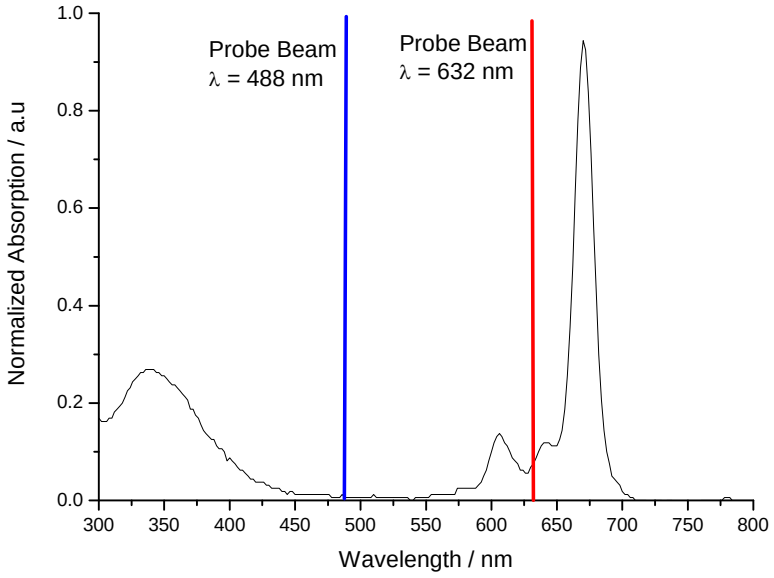

Figure 3. 8. A typical absorption spectrum of zinc phthalocyanine, ZnPc, illustrating absorption of the HeNe probe, λ = 632 nm, in the shoulder of the Q-band and transparency of the Ar ion probe, λ = 488 nm

significant modifications were required when considering the system for use with phthalocyanines. It is immediately evident that there is some significant absorption of the HeNe, at 632 nm, and a better approach would be to use an argon ion laser, 488 nm, where the phthalocyanine is transparent. Figure 3. 8 illustrates a typical absorption spectrum of a phthalocyanine and two available probe beams.

3.3.3. Beamsplitter

The fundamental element of the experiment is the relationship between the pulsed beam and probe beam relative to one another when the sample is irradiated. It is crucial that the beams are collinear through the sample. This was achieved using a series of pinholes both upstream and downstream from the sample, such that when the beams were combined at the point of the beamsplitter they were indeed collinear. The beamsplitter chosen for this spectrometer was a quartz

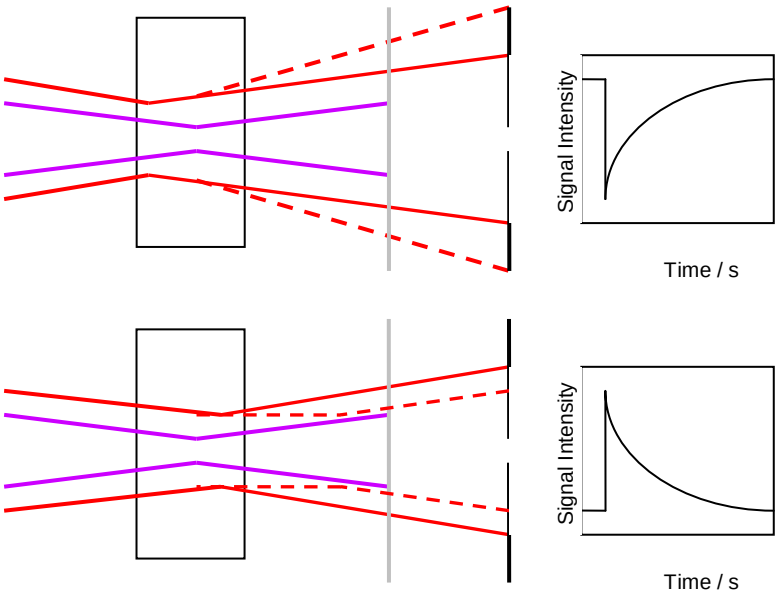

Figure 3. 9. Illustration of the dual beam mode-mismatched arrangements of pump beam relative to probe beam, with probe focussed before pump beam, top, and after pump beam, bottom, with the associated signals expected in each case. Purple lines represent pump beam. Full red line illustrates probe beam trajectory prior to lens formation, dashed red line represents probe beam trajectory following thermal lens formation.

wedge, which allowed the power of either the probe or pump, depending on the configuration, to be monitored during data collection.

3.3.4. Lenses

The arrangement of the focal points of the pump and probe beams was a fundamental point for consideration. There are two possible configurations of the focal points with respect to each other. The pump beam was focused into the centre of the cuvette and the probe beam was focused either at the front of the cuvette, leading to a large decrease in probe due to divergence of beam, or the back of the cuvette, leading to a large increase in probe due to convergence of beam, these are illustrated in Figure 3. 9.[48] It was found that, using a lens of 100 mm focal length for Nd:YAG and a lens of 50 mm for HeNe, that a mode-mismatched configuration with HeNe focused before the Nd:YAG was the most sensitive and straightforward system

possible with the space constraints presented. The same configuration was applied with success to the argon ion arrangement.

3.3.5. Detection system

The detection system comprises of a means to filter out the pump beam, a pinhole to select the very centre of the probe beam, a detector and a data collection system. Initially an iris was used to select the centre of the beam, however this was improved with the use of a pinhole with 300 μm diameter. Installation of a translation table provided the capacity to move the pinhole along the path of the probe beam into the far field in order to improve sensitivity.

A monochromator was used to select the probe beam wavelength, which resulted in alterations made in the set-up with the change of probe beam. The detector provided an interesting challenge due to the fine balance between signal magnitude and sensitivity of the detection system. Initially a large area silicon photodiode coupled to a 2mΩ trans-impedance amplifier was used. However, it was realised after several experiments that a faster means of signal acquisition was required due to significant loss of data observed in the first 10 μs of the signal. Finally a photon multiplier tube was integrated into the set-up, which gave a signal of good magnitude and reasonable S/N ratio with 200 scans. The data was recorded onto a two-channel digital real-time oscilloscope.

3.4 Data Collection

Once the construction of the TRTL spectrometer had been completed the investigation of singlet delta oxygen quantum yield determination began. An air-saturated sample of PPN was prepared in a variety of

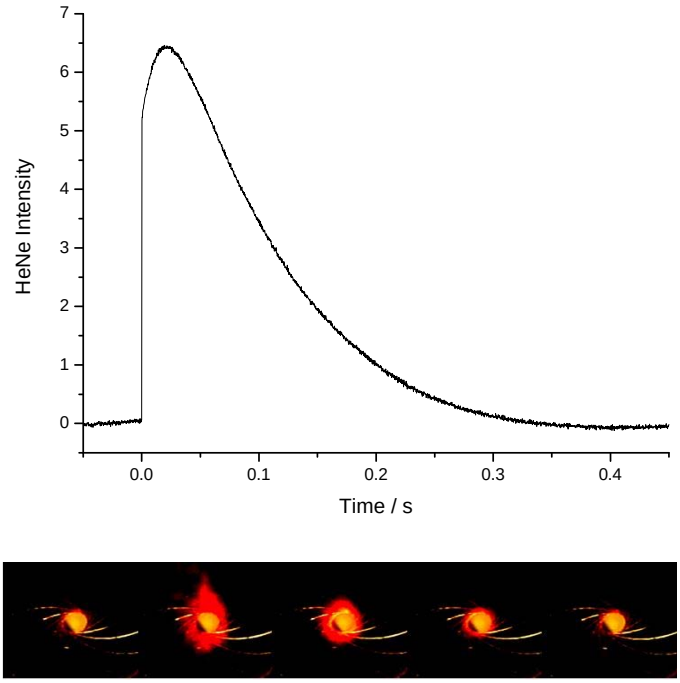

Figure 3. 10. Plot of the growth and decay of the thermal lens on a millisecond timescale and the image of the probe beam on a pinhole placed before the detector, illustrating the blooming of the signal due to divergence from the formation of a transient lens.

solvents and TRTL signal was maximized and traces collected. Initially PPN, which has Φ_Δ of unity, was used to confirm the reliability of the spectrometer. It was then necessary to explore and define the experimental conditions and protocol required for the determination of Φ_Δ for the phthalocyanines. This required investigation into the impact and effect of solvent systems, power constraints and concentration limitations, which are discussed in detail in the results and discussion.

3.5 Signal Analysis

Figure 3. 10 illustrates snapshots taken from a video clip of the signal observed on an iris directly in front the detector and the full signal that was collected over the 0.1 s timescale. It is observed that a sudden appearance of the lens is reflected in a large decrease (a decrease in light intensity results in a positive deflection of the signal) in signal

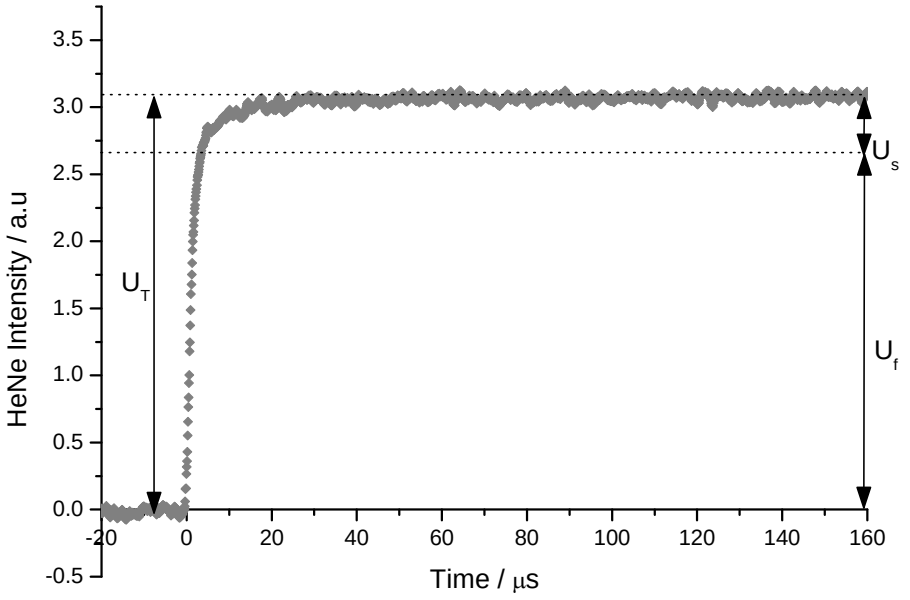

Figure 3. 11. Plot of the signal on a microsecond timescale, highlighting the fast and slow portions of the development of the lens.

intensity that relaxes by exponential decay back to the ground state as the heat dissipates through the solution. In order to acquire the desired information from the signal it is necessary to look on the microsecond timescale at the very formation of the lens to its maximum.

A typical signal is shown in Figure 3. 11. It can be separated into two distinct parts that reflect the pathways on a molecular level. The fast portion of the signal is labelled as U_f and represents the relatively fast process of energy absorbed by the photosensitiser forming the S_1 and T_1 states and the subsequent quenching of the triplet state of the dye by molecular oxygen. This typically happens on a nanosecond timescale. The much slower part of the signal is referred to as U_S and is ascribed to the decay of the excited singlet oxygen state. This can be described mathematically as,

$$U(t) = U_f + U_s\left(1 - \exp\left(\frac{-t}{\tau}\right)\right) \qquad \text{(eq. 3. 6)}$$

and can be applied as a fit to the TRTL trace in order to determine U_f and U_s. Once these parameters are known, the ratio of U_s/U_T can be used to determine Φ_Δ as follows,[49]

$$\frac{U_s}{U_T} = \frac{\phi_\Delta E_\Delta}{E_{ex} - \phi_F E_F} \qquad \text{(eq. 3. 7)}$$

Various reaction conditions have been investigated, in particular, those essential to determine the specific constraints of the reaction conditions required to obtain the most accurate values.

3.6 Results and Discussion

It was evident during construction of the thermal lensing spectrometer that absorption properties of the solute have a large role to play in defining the components to be used, in particular the pump and probe lasers. However, the degree of lensing due to singlet delta oxygen formation is exhibited through temperature changes in the solvent. It is generally accepted that the thermal lensing signal is largely dependent on the change in refractive index gradient relationship with change in temperature, *dn/dT*, as this determines the degree of lensing that will occur and subsequently the magnitude of signal due to the degree of divergence of the probe beam. Braslavsky and Heibel also suggest that the success of TRTL is highly dependent on the specific heat capacity, C_p, of the solvent and the thermal expansion coefficient, β.[24] This was put to the test by investigating the thermal lensing traces generated by PPN in a variety of solvents with a range of thermal properties. All samples had absorbance of 0.1 at λ = 355 nm and all measurements were conducted under ambient conditions. It is immediately evident that both signal size and shape are entirely solvent dependent, as illustrated in Figure 3. 12.

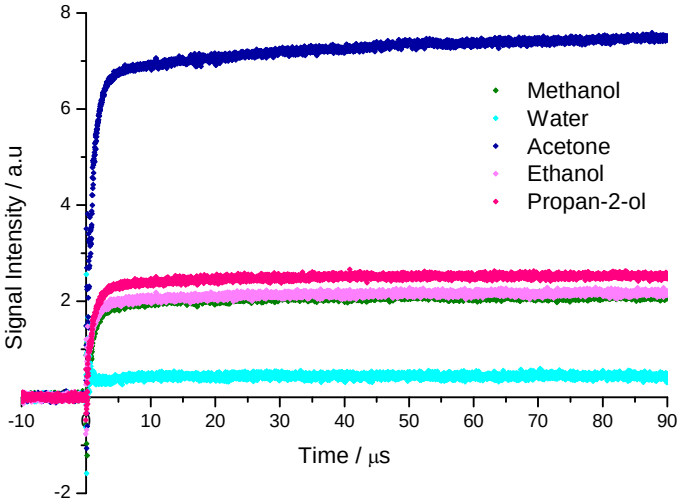

Figure 3. 12. TRTL traces illustrating the difference in magnitude of signal depending on the solvent with samples of A = 0.1 at λ = 355 nm.

Eq.3.6 was used to apply a mathematical fit to the data and identify the fast and slow portions of the signal. Analysis of the U_s portion of the TRTL trace measured for each solvent provided the non-radiative lifetime of $O_2(^1\Delta_g)$, τ_Δ. These values can be seen in Table 3. 1 and compare well with literature values.[50] Further analysis conducted on the magnitude of U_t showed that in comparison with β/C_p and $d\eta/dT$, see Figure 3. 13, these properties were key in determining whether TRTL would work successfully in a given sample or not. With this information it is obvious that water is a difficult medium to measure Φ_Δ values in, due both to the short $O_2(^1\Delta_g)$ lifetimes and relatively low

Solvent	τ_Δ[a] (μs)	τ_Δ[b] (μs)
Water	4	20 – 4
Methanol	10.7	9.6 – 12
Ethanol	12.2	9.6 – 19
Propan-2-ol	15.4	16 – 18
Acetone	30	40 – 55
Toluene	27.3	29

Table 3. 1. Radiative lifetimes of singlet delta oxygen as determined by TRTL, a, and found in literature, b.

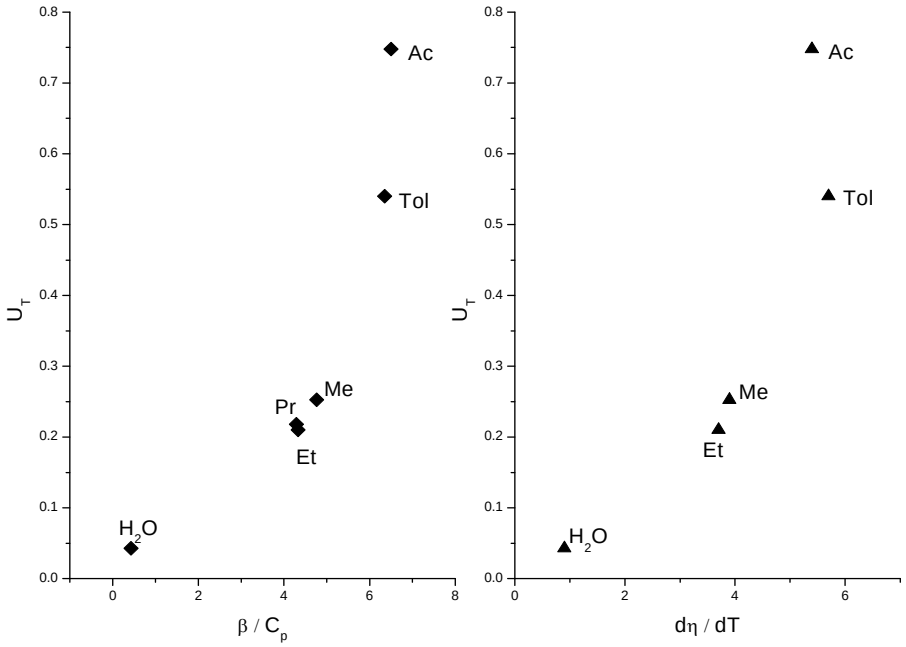

Figure 3. 13. Plots of key solvent properties with respect to magnitude of thermal lensing signal.

heat capacity and thermal expansion coefficient, when compared with other systems. It can also be predicted that the toluene/pyridine solvent system used in determining phthalocyanine results should be favourable in this sense.

A number of experiments were performed in order to determine a working protocol and set of experimental parameters, in particular those exploring the range of excitation laser power and sample concentration. The results of these preliminary tests are illustrated in Figure 3. 14 and show that the signals obey a linear relationship when absorbance at the excitation wavelength is less than 0.1 and power is less than 2 mJ.

Finally, it is hoped that the technique can be applied to the determination of triplet state properties of these molecules. This is a

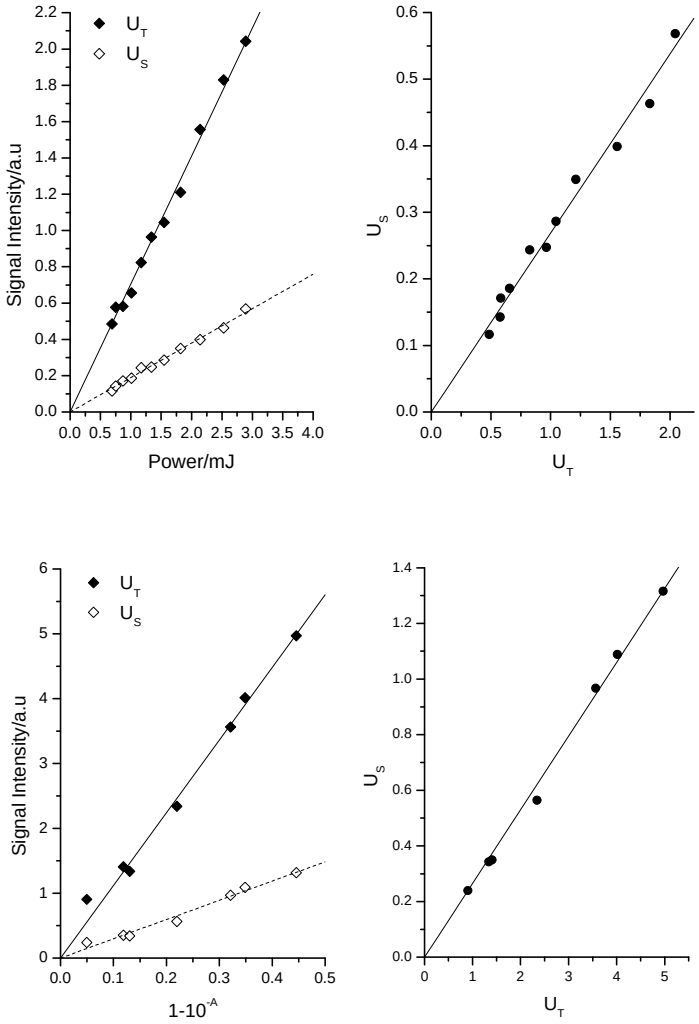

Figure 3. 14. Plots illustrating the relationship between Us and Ut and power , top, and concentration, bottom.

difficult area to measure for phthalocyanines due to the requirement of detectors that are capable of picking up weak phosphorescence signals in the near-IR range. For that reason quenching methods are often used to define triplet energies by defining a range in which the triplet state lies. In the case of TRTL, once the solutions are degassed and oxygen is no longer quenching the triplet state, the slow part of the signal, U_s, can be identified as the decay of the triplet state of the photosensitiser. Eq.3.6 can still be used to determine U_s and U_f, but now equation 7 becomes,

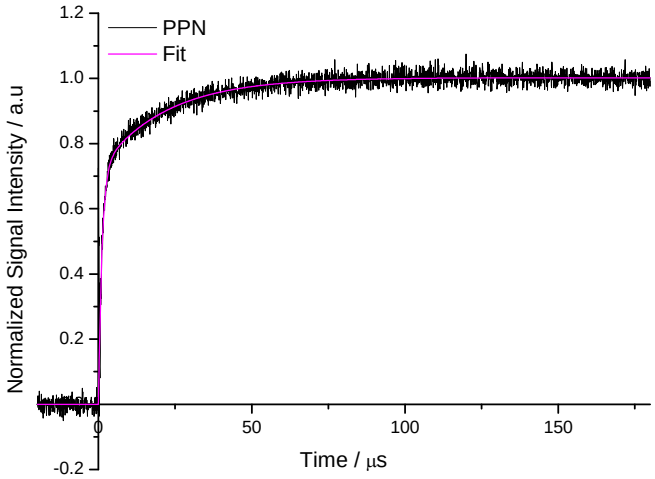

Figure 3. 15. Triplet thermal lensing signal of PPN in 1% toluene/pyridine

$$\frac{U_s}{U_T} = \frac{\varphi_T E_T}{E_{ex} - \varphi_F E_F} \qquad \text{(eq. 3. 8)}$$

Hence, if E_T is known then Φ_T can be determined and vice versa. In the case of this study the Φ_T were determined by an alternative method so an approximate value of E_T could be calculated.[45]

A degassed sample of PPN was prepared by the freeze-pump-thaw method and a TRTL trace collected, see Figure 3. 15. From the data a triplet energy of 220 kJ mol^{-1} was determined.

3.7 Conclusion

To conclude, it is believed that a viable system has been constructed for the purpose of singlet delta oxygen quantum yield determination. However, the system also has the potential to investigate phthalocyanine dyes further in terms of elucidating the necessary triplet data, which can often be difficult to do.

3.8 References

1. C. Schweitzer and R. Schmidt, *Chem. Rev.*, 2003, **103**, 1685.
2. R. Bonnett, *Chem. Soc. Rev.*, 1995, **24**, 19.
3. B. W. Henderson and T. J. Dougherty, *Photochem. Photobiol.*, 1992, **55**, 145.
4. R. S. Mulliken, *Nature*, 1928, **122**, 505.
5. A. A. Krasnovsky, *J. Photochem. Photobiol. A. Chem.*, 2008, **196**, 210.
6. M. C. DeRosa and R. J. Crutchley, *Coord. Chem. Rev.*, 2002, **233**, 351.
7. D. R. Kearns, *Chem. Rev.*, 1971, **71**, 395.
8. H. Kautsky, *Trans. Faraday. Soc.*, 1939, **35**, 216.
9. H. Kautsky, *Trans. Faraday. Soc.*, 1939, **35**, 224.
10. A. U. Khan and M. Kasha, *J. Chem. Phys.*, 1963, **39**, 2105.
11. C. S. Foote and S. Wexler, *J. Am. Chem. Soc.*, 1964, **86**, 3879.
12. D. R. Adams and F. Wilkinson, *J. Chem. Soc. Faraday Trans. 2*, 1972, **68**, 386
13. A. A. J. Krasnovsky, *Photochem. Photobiol.*, 1979, **29**, 29.
14. R. D. Scurlock and P. R. Ogilby, *J. Phys. Chem.*, 1987, **91**, 4599.
15. R. Schmidt and H. D. Brauer, *J. Am. Chem. Soc.*, 1987, **109**, 6976.
16. C. S. Foote, *Photochem. Photobiol.*, 1991, **54**, 659.
17. K. Gollnick, *Adv. Photochem.*, 1968, **6**, 1
18. F. Wilkinson, W. P. Helman and A. B. Ross, *J. Phys. Chem. Ref. Data*, 1993, **22**, 113.
19. A. A. Abdel-Shafi, D. R. Worrall and F. Wilkinson, *J. Photochem. Photobiol. A. Chem.*, 2001, **142**, 133.

20. S. Nonell, Braslavsky, S.E., *Singlet Oxygen, UV-A and Ozone,Methods in Enzymology*, 2000, **319**.
21. C. Marti, O. Jurgens, O. Cuenca, M. Casals and S. Nonell, *J. Photochem. Photobiol. A. Chem.*, 1996, **97**, 11.
22. E. Oliveros, S. H. Bossmann, S. Nonell, C. Marti, G. Heit, G. Troscher, A. Neuner, C. Martinez and A. M. Braun, *New J. Chem.*, 1999, **23**, 85.
23. R. W. Redmond and S. E. Braslavsky, *Chem. Phys. Lett.*, 1988, **148**, 523.
24. S. E. Braslavsky and G. E. Heibel, *Chem. Rev.*, 1992, **92**, 1381.
25. A. Ogunsipe, J. Y. Chen and T. Nyokong, *New J. Chem.*, 2004, **28**, 822.
26. A. Ogunsipe and T. Nyokong, *J. Photochem. Photobiol. A. Chem.*, 2005, **173**, 211.
27. P. Matlaba and T. Nyokong, *Polyhedron*, 2002, **21**, 2463.
28. Y. Harada, T. Suzuki, T. Ichimura and Y.-Z. Xu, *J. Phys. Chem. B*, 2007, **111**, 5518
29. T. Gensch and C. Viappiani, *Photochem. Photobiol. Sci.*, 2003, **2**, 699.
30. J. H. Brannon and D. Magde, *J. Phys. Chem.*, 1978, **82**, 705
31. R. D. Snook and R. D. Lowe, *Analyst*, 1995, **120**, 2051.
32. M. Fischer and J. Georges, *Analyt. Chim. Acta*, 1996, **322**, 117.
33. M. Fischer and J. Georges, *Chem. Phys. Lett.*, 1996, **260**, 115.
34. J. Georges, *Talanta*, 1999, **48**, 501.
35. C. V. Bindhu and S. S. Harilal, *Analyt. Sci.*, 2001, **17**, 141.
36. J. Hung, A. Marcano, J. Castillo, J. Gonzalez, V. Piscitelli, A. Reyes and A. Fernandez, *Chem. Phys. Lett.*, 2004, **386**, 206.
37. J. P. Gordon, R. C. C. Leite, R. S. Moore, S. P. S. Porto and J. R. Whinnery, *J. App. Phys.*, 1965, **36**, 3.

38. M. Kopczynski, T. Lenzer, K. Oum, J. Seehusen, M. T. Seidel and V. G. Ushakov, *Phys. Chem. Chem. Phys.*, 2005, **7**, 2793.
39. C. Hu and J. R. Whinnery, *Appl. Opt.*, 1973, **12**, 72.
40. R. L. Swofford, M. E. Long and A. C. Albrecht, *Science*, 1976, **191**, 183.
41. D. S. Kliger, *Acc. Chem. Res.*, 1980, **13**, 129.
42. K. Fuke, M. Ueda and M. Itoh, *J. Am. Chem. Soc.*, 1983, **105**, 1091.
43. F. Tanaka, T. Furuta, M. Okamoto and S. Hirayama, *Phys. Chem. Chem. Phys.*, 2004, **6**, 1219.
44. G. Rossbroich, N. A. Garcia and S. E. Braslavsky, *J. Photochem.*, 1985, **31**, 35.
45. X. Allonas, C. Ley, C. Bibaut, P. Jacques and J. P. Fouassier, *Chem. Phys. Lett.*, 2000, **322**, 483.
46. R. Schmidt and M. Bodesheim, *J. Phys. Chem.*, 1994, **98**, 2874.
47. *J. Photochem.*, 1985, **31**, 37.
48. N. J. Dovichi and J. M. Harris, *Analyt. Chem.*, 1980, **52**, 2338.
49. M. Terazima, N. Hirota, H. Shinohara and Y. Saito, *J. Phys. Chem.*, 1991, **95**, 9080.
50. F. Wilkinson, W. P. Helman and A. B. Ross, *J. Phys. Chem. Ref. Data*, 1995, **22**.

4. Silicon Phthalocyanine Derivatives

4.1 Introduction

The past three decades have played witness to an explosion of interest in the research of silicon phthalocyanine derivatives.[1-4] These compounds have proved hugely successful in both *in vitro* and *in vivo* studies as sensitizers for phototherapies in dermatological conditions,[5] fungal infections,[6] oncology[7] and HIV.[8] One of the most successful silicon phthalocyanine compounds to progress to clinical trials is Pc 4, a silicon-based hydrophobic phthalocyanine containing an axial aminosiloxy ligand, Figure 4.1 structure f.[5, 10-12] Pc 4 has a number of advantageous properties including high molar extinction coefficient, 2×10^{-5} M cm^{-1}, maximum Q-band absorption at 675 nm and singlet delta oxygen quantum yields of 0.43.[3] The defining modification in this molecule is the axial substitution, which is considered to significantly enhance the solubility of the compound. Nevertheless, a key disadvantage associated with the Pc 4 molecule is the tedious and lengthy synthesis, which hampers chemical modifications and subsequent investigations into the structure-activity relationship.[7, 13]

Previous research has predominantly focused on the influence of axial modification, Figure 4.1, with a view to synthesizing amphiphilic phthalocyanines with a high cellular uptake.[14, 15] These compounds have proven to have enhanced photodynamic activity in *in vivo* studies compared to analogous compounds with limited solubility in aqueous and lipid environments.[16] However, such research also indicates that there is limited impact upon photophysical and photochemical properties using axial modifications, with triplet and singlet oxygen

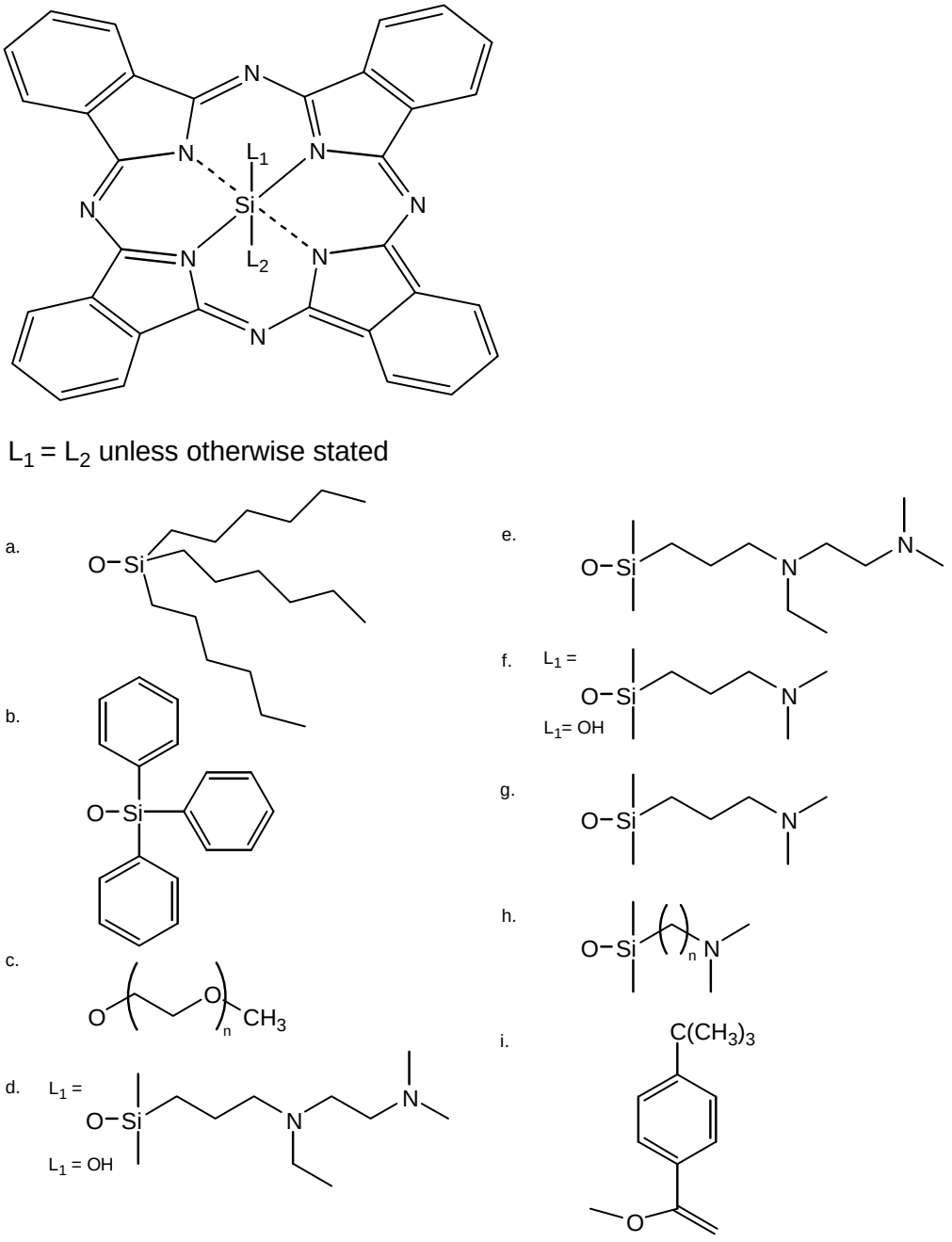

Figure 4. 1. Schematic diagram of a variety of axial modifications applied to silicon phthalocyanine.

Compound	Φ_Δ	τ_T / μs	Solvent	Ref.
Cl_2SiPc	0.37		$CHCl_3$	1
$(OH)_2SiPc$	0.28		DMSO	2
a		243	THF	1
	0.32		$CHCl_3$	1
b		213	THF	1
	0.35		$CHCl_3$	1
c	0.20		DMF	4
d	0.50	139	Acetonitrile	3
e	0.20	188	Acetonitrile	3
f	0.43	113	CH_3CN	3
g	0.32	160	CH_3CN	3
h (n = 1)	0.392			9
h (n = 2)	0.35		MeOH	9
h (n = 3)	0.37		MeOH	9
h (n = 4)	0.371		MeOH	9
h (n = 5)	0.375		MeOH	9
h (n = 6)	0.384		MeOH	9

Table 4. 1. Summary of axially modified silicon phthalocyanine compounds with triplet lifetimes, τ_T, and singlet delta oxygen quantum yields, Φ_Δ.

quantum yields remaining low, as illustrated in Table 4.1. The limited research performed on substitution of the benzenoid rings in either the alpha or beta position has indicated that there is opportunity for significant tuning of desired singlet and triplet state properties in similar ways that have been achieved for other phthalocyanines.[17, 18] The research herein is centred on the influence of octa-alpha substitution of alkyl chains on the benzenoid rings in order to enhance both solubility and the required properties for photodynamic therapy.

4.2 Results and Discussion

4.2.1 Spectroscopic data

The absorption spectra of silicon phthalocyanine hydroxide, 6SiPc and 8SiPc can be seen in Figure 4.2. All absorption spectra fall well within the desired optical window of 650 – 800 nm and exhibit the typical shape of phthalocyanines.[19] The sharp Q-band at 710 nm is an indication that there is no aggregation occurring in solution. This is due to hydroxide substitution in the axial position, which prevents aggregation that is commonly accepted to be brought about by π-π stacking.[20] Upon substitution of alkyl groups in the alpha position, the absorption spectra of the substituted silicon phthalocyanine

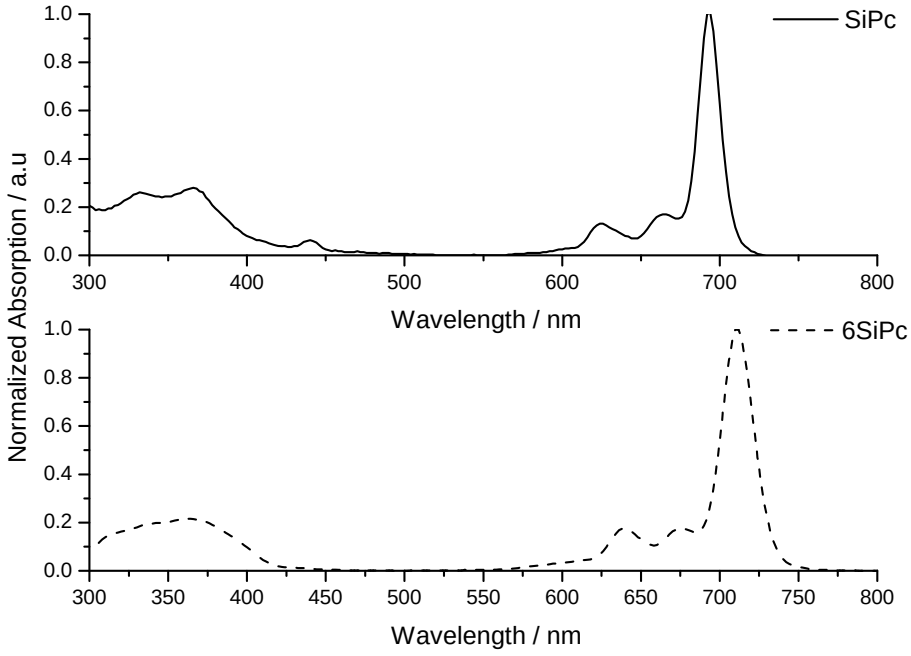

Figure 4. 2. Absorption spectra for silicon phthalocyanine derivatives.

compounds exhibit a broadening of the Q-band, which is suggestive of a minor change in structure. This is an expected outcome due to steric hinderance brought about by the nature and position of the long alkyl chains on the benzenoid ring. A bathochromic shift of 18 nm is also observed for both compounds relative to the parent compound, which exhibits a Q-band maximum at 692 nm, and is attributed to the electron-donating nature of the alkyl groups, which causes a reduction of the HOMO – LUMO gap. This has been previously observed in other phthalocyanines that bear different metal centres.[21-23] Substitution of the alkyl groups also affords this set of compounds improved solubility in a number of solvents including water and ethanol compared to the parent compound, which exhibits no solubility in either solvent. This is a significant development in the pursuit of new photosensitizers in photodynamic therapy. In silicon phthalocyanine systems improved solubility is typically associated

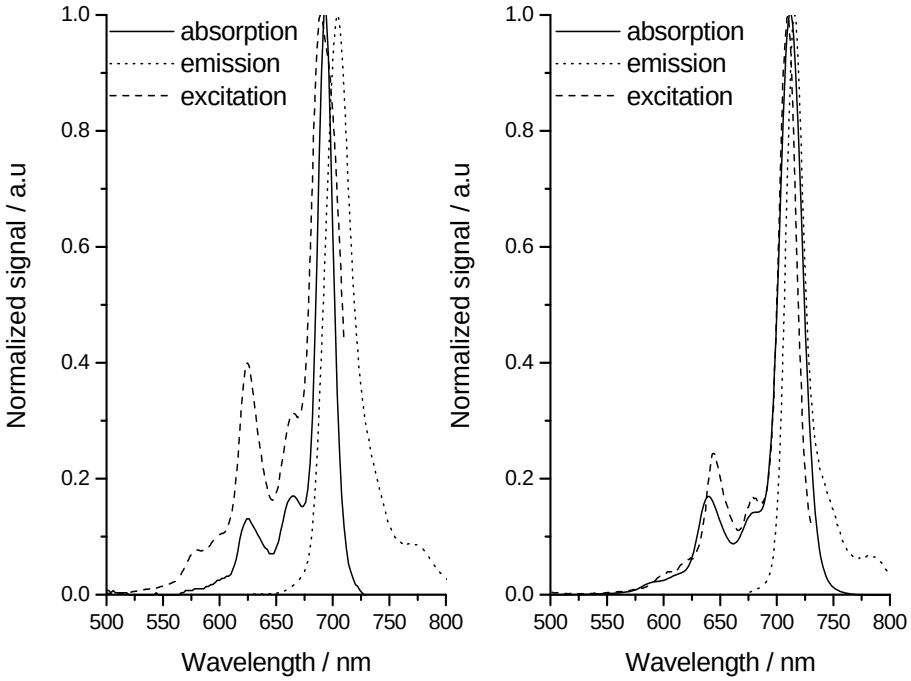

Figure 4. 3. Emission and excitation data of SiPc (left) and 6SiPc (right).

with axial modification, due to a reduction in the propensity towards aggregation. However, it is widely recognized in other metallophthalocyanine systems that octa-substitution of long chains enhances solubility in both organic and aqueous environments, which is the case in this example as both substituted compound and parent compound contain identical axial substituents.[24]

Emission and excitation spectra for the substituted silicon phthalocyanine compounds are similar, Figure 4.3, with maximum emission at 716 nm for the substituted compounds compared to 704 nm for the parent. Unlike the parent compound, where some broadening of the emission is observed, the emission is the mirror image of the absorption. This is a strong indication that the structure does not undergo major distortion upon excitation.

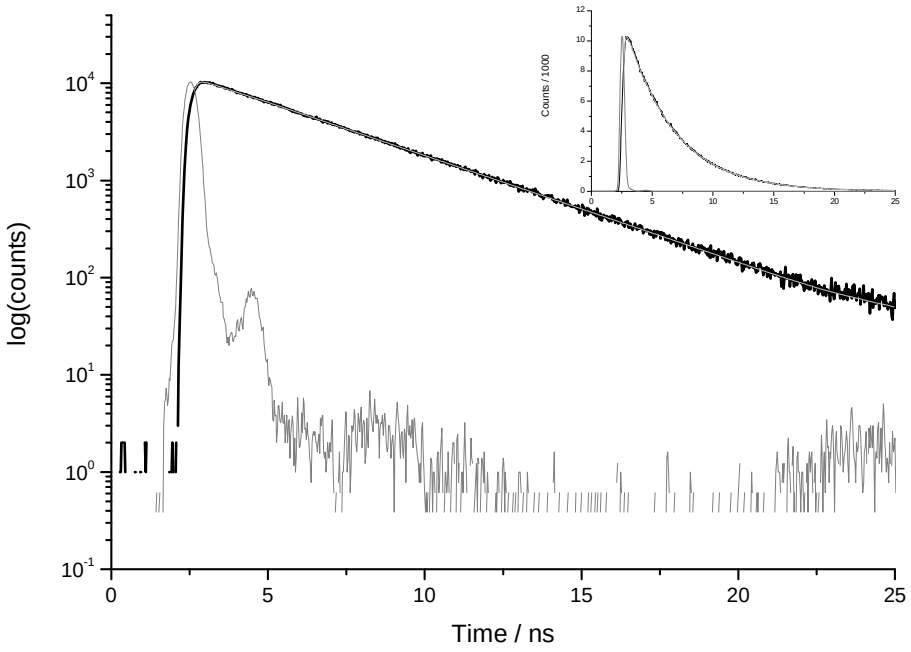

Figure 4. 4. Typical fluorescence signal decay with fit measured at 720 nm. The lighter line indicates the instrument response function. The decay is shown on a linear scale in the inset.

4.2.2 Photophysics

Fluorescence lifetimes determined using time-correlated single photon counting are 3.8 ns for both 6SiPc and 8SiPc, which are in the expected range for these compounds. An example of a typical decay is given in Figure 4.4. Fluorescence quantum yields were determined to be 0.27, compared to 0.18 of the parent compound, and are also well within the range expected for silicon phthalocyanine compounds.

The transient absorption spectra of the parent compound and substituted compounds are similar and typical examples can be seen in Figure 4.5. The spectra show a broad band between 400 – 600 nm with a peak at 552 nm. Triplet decays were determined by fitting an exponential to the decay of transient absorption at 530 nm and 552 nm for SiPc and *n*SiPc respectively to give lifetimes of 103 μs and 160 μs

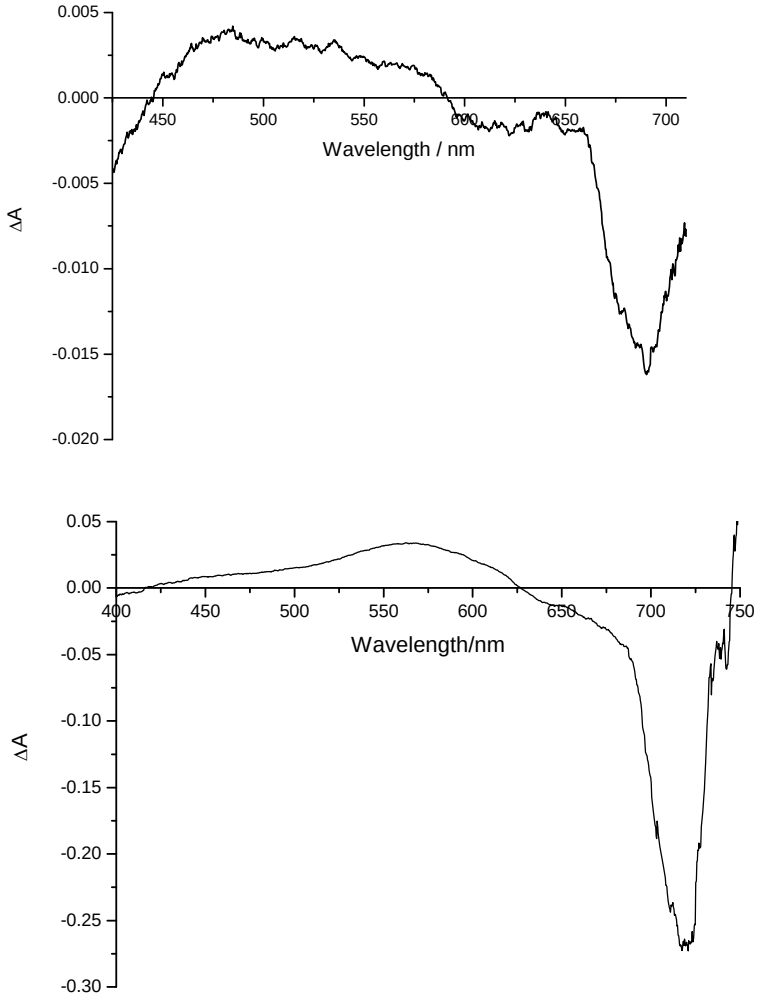

Figure 4. 5 Transient triplet-triplet absorption spectrum of SiPc (top) and 6SiPc (bottom) in 1% v/v pyridine/toluene at 1 x 10^{-5} M, λ_{ex} = 355 nm. The broad absorption with peak observed between 400 – 600 nm is due to T-T* absorption.

respectively. It can be seen that the effect of alkyl substitution is a longer triplet lifetime, a highly desired property for photodynamic therapy. Triplet quantum yields were found to be 0.53 and 0.55 for 6SiPc and 8SiPc respectively. These are substantially larger than those typically found for silicon phthalocyanine compounds and suggests that alpha-substitution of an electron-donating group promotes spin-forbidden intersystem crossing from the excited singlet state to the triplet state.

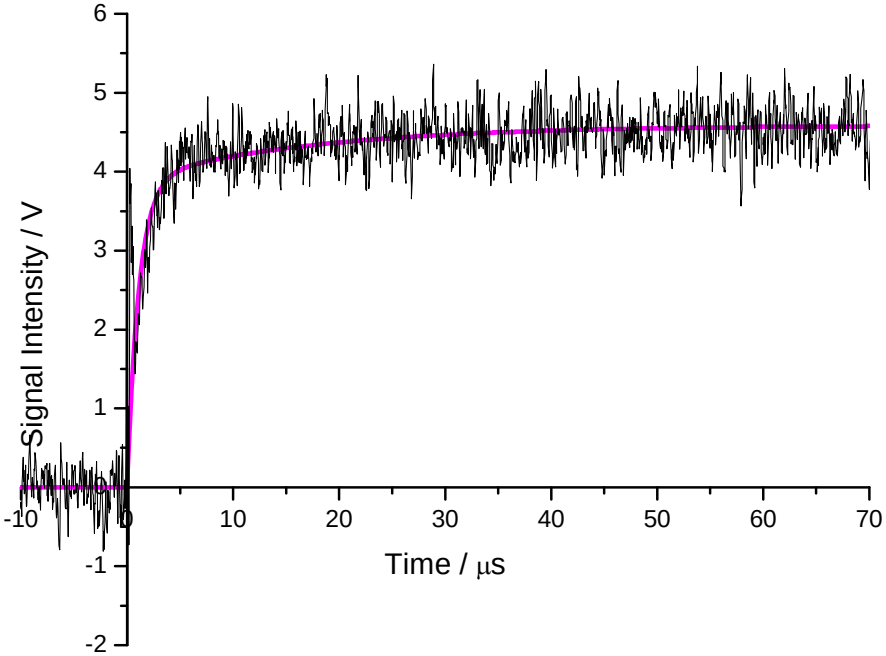

Figure 4. 6 Time-resolved thermal lensing signal of 8SiPc in 1% v/v pyridine/toluene

4.2.3 Photochemistry

The final parameter to be quantified is the singlet delta oxygen quantum yield. Literature values of SiPc in DMSO present $\Phi_\Delta = 0.28$. Through time-resolved singlet oxygen phosphorescence detection this work has determined that 6SiPc and 8SiPc both have Φ_Δ values of 0.49 in 1% v/v pyridine/toluene. Furthermore, due to the solubility of these compounds in aqueous media it was considered viable to measure the same parameter in ethanol and water. As has previously been discussed, it is notoriously difficult to determine Φ_Δ in water due to the fast non-radiative lifetimes, which are typically in the region of 3 – 5 μs. However, provisional signals using the time-resolved thermal lensing technique has afforded results for ethanol show Φ_Δ for 8SiPc to be 0.48, Figure 4.6. This is a promising results as previous solvent studies conducted by Nyokong *et al.* on substituted zinc

phthalocyanine compounds have often indicated that observed Φ_Δ values in protic solvents such as water and methanol are typically determined to be lower due to the deactivation of singlet oxygen by these solvents.[25] It has also been observed that the substituted silicon phthalocyanine compounds have high S_Δ values of 0.94 and 0.95 for 6SiPc and 8SiPc, respectively. This means that of the triplet states produced a large proportion is successfully quenched by molecular oxygen to generate singlet delta oxygen, the cytotoxic agent required in photodynamic therapy to induce cell death.

4.3 Conclusion

To conclude, it has been revealed that there is significant enhancement of several key properties of silicon phthalocyanine as a consequence of alpha alkyl substitution. These include the enhancement of solubility in aqueous and organic environments, fulfilling the requirements of amphiphilicity, a red-shift of the Q-band from 694 nm to 710 nm, hence deeper skin penetration, longer triplet lifetimes and improved triplet quantum yields resulting in an enhancement of the triplet state population and subsequently an improved singlet oxygen quantum yields. Though there is little to no discernable difference, within error, between the substituted compounds when comparing chain length of the alkyl substituent, both compounds have enhanced properties that make for promising candidates for *in vivo* studies and clinical trials.

4.4 References

1. J.-P. Daziano, S. Steenken, C. Chabannon, P. Mannoni, M. Chanon and M. Julliard, *Photochem. Photobiol.*, 1996, **96**, 712.
2. I. Seotsanyana-Mokhosi, N. Kuznetsova and T. Nyokong, *J. Photochem. Photobiol. A. Chem.*, 2001, **140**, 215.
3. J. He, J.-S. Li, H. E. Larkin, B. D. Rfliter, S. L. A. Zaidi, M. A. J. Rodgers, H. Mukhtar, M. E. Kenney and N. L. Oleinick, *Photochem. Photobiol.*, 1997, **65**, 581
4. T. H. Huang, K. E. Rieckhoff and E. M. Voigt, *Chem. Phys.*, 1977, **19**, 25.
5. K. Kalka, H. Merk and H. Mukhtar, *J. Am. Acad. Dermatol.*, 2000, **42**, 389.
6. P. Calzavara-Pinton, M. Venturini and R. Sala, *J. Photochem. Photobiol. B. Biol.*, 2005, **78**, 1.
7. N. L. Oleinick, A. R. Antunez, M. E. Clay, B. D. Rihter and M. E. Kenney, *Photochemistry and Photobiology*, 1993, **57**, 242.
8. E. D. Ben-Hur, J. Oetjen and B. Horowitz, *Photochem. Photobiol.*, 1997, **65**, 456.
9. A. Sholto and E. Ehrenberg, *Photochem. Photobiol. Sci.*, 2008, **7**, 344
10. C. M. Allen, W. M. Sharman and J. E. Van Lier, *J. Porph. Phthal.*, 2001, **5**, 161.
11. M. Lam, N. L. Oleinick and A. L. Nieminen, *J. Bio. Chem.*, 2001, **276**, 47379.
12. E. D. Baron, C. L. Malbasa, D. Santo-Domingo, P. Fu, J. D. Miller, K. K. Hanneman, A. H. Hsia, N. L. Oleinick, V. C. Colussi and K. D. Cooper, *Lasers Surg. Med*, 2010, **42**, 728.

13. X. J. Zhao, S. Lustigman, M. E. Kenney and E. BenHur, *Photochem. Photobiol.*, 1997, **66**, 282.
14. I. J. Macdonald and T. J. Dougherty, *J. Porph. Phthal.*, 2001, **5**, 105
15. T. Nyokong, *Coord. Chem. Rev.*, 2007, **251**, 1707.
16. C. Y. Anderson, K. Freye, K. A. Tubesing, Y. S. Li, M. E. Kenney, H. Mukhtar and C. A. Elmets, *Photochem. Photobiol.*, 1998, **67**, 332.
17. G. Winter, H. Heckmann, P. Haisch, W. Eberhardt, M. Hanack, L. Luer, H. J. Egelhaaf and D. Oelkrug, *J. Am. Chem. Soc.*, 1998, **120**, 11663.
18. N. Kobayashi, H. Ogata, N. Nonaka and E. A. Luk'yanets, *Chem.-Eur. J.*, 2003, **9**, 5123.
19. M. D. Maree, T. Nyokong, K. Suhling and D. Phillps, *J. Porph. Phthal.*, 2002, **6**, 373.
20. C. C. Leznoff, L. S. Black, A. Hiebert, P. W. Causey, D. Christendat and A. B. P. Lever, *Inorg.Chim. Acta*, 2006, **359**, 2690
21. T. B. Ogunbayo and T. Nyokong, *Polyhedron*, 2009, **28**, 2710.
22. T. B. Ogunbayo, A. Ogunsipe and T. Nyokong, *Dyes and Pigments*, 2009, **82**, 422.
23. T. B. Ogunbayo and T. Nyokong, *J. Mol. Struct.*, 2010, **973**, 96.
24. C. G. Claessens, U. Hahn and T. Torres, *Chem. Rec.*, 2008, **8**, 75.
25. A. Ogunsipe, D. Maree and T. Nyokong, *J. Mol. Struct.*, 2003, **650**, 131.

5. Zinc Phthalocyanine Derivatives

5.1 Introduction

Over the past 40 years there has been a great interest in investigating the diverse application of phthalocyanines, and in particular zinc phthalocyanines. As has previously been discussed, these compounds have real potential as photosensitisers in photodynamic therapy, PDT. However, there is also a great interest surrounding zinc phthalocyanine, ZnPc, for application in photochemical cells, optical discs, solar cells and nonlinear optical limiting devices.[1-4] Consequently, there has been much research conducted on optimising the properties of ZnPc.[5, 6] Zinc phthalocyanine has a maximum absorption of 670 nm, with extinction coefficient in the region of 3×10^{-5} M cm^{-1}, high triplet quantum yield (Φ_T = 0.6), high singlet delta oxygen quantum yield (Φ_Δ = 0.58) and is known to exhibit strong photobiological activity against tumours.[7] One of the key advantages of this compound is the opportunity afforded to fine-tuning the structure by incorporation of substituents on the benzenoid rings. Addition of substituents in the alpha (1, 4) and beta (2, 3) position can have a marked influence on the physical, photophysical and photochemical properties.[8, 9] Both the number of substituents introduced and the electronic nature of the substituent can be used to optimise the desired characteristics of the molecule. Table 5.1 provides a summary of a selection of zinc phthalocyanine based compounds studied to date containing either electron withdrawing groups or electron donating groups and includes some key photophysical and photochemical properties.

R	Position	No. of subs	λ_{max} / nm	λ_{em} / nm	Φ_f	Φ_T	Φ_Δ	Solvent	Ref.
-H		16	670	676					
			Electron-withdrawing groups						
-F	α + β	16	670						10
	α + β	16	638	688	0.21				11
-I	β	4	680		0.088	0.86	0.54	DMSO	12
-Br	β	4	676		0.17	0.76	0.41	DMSO	12
-Cl	β	4	672		0.29	0.59	0.35	DMSO	12
-Cl	β	8	683		0.02		0.34	DMSO	13
$-NO_2$	β	4	682		0.12		0.24	DMF	13
$-SO_3$	β	4	680				0.28	DMSO	13
$-SO_3H$	β	4	680						14
-COOH	β	4	680				0.48	DMF/pyridine	14
-COOH	β	4	685						10
-COOH	β	8	684				0.52	pH10	
-CN	β	8	671						10
$-SO_2Ph$	α	4	664	720	0.038				9
	β	4	676.7	686	0.397				9
$-SO_2Ph$/-tBu	α/β	4/4	668.4	678.5	0.441				9
$-NO_2$	α	4	671	683	0.23				15
$-NO_2$	α	4	669.2	678	0.488				9
	β	4	671.0	695	0.159				9
$-NO_2/-NO_2$	α/β	4/4	674	698	0.088				9
			Electron-donating groups						
-SPh/-t-Bu	α/β	4/4	709.5	727.4	0.224				9
-SPh	β	4	680	694	0.14				11
-SPh	α	4	706.7	687.5	0.276				9
	β	4	684.5	687.5	0.439				9
	β	8	707.8	721.2	0.090				9
$-S-C_6H_4CH_3$	β	8	715				0.52	DMF	16
$-S-C_4H_9$	β	8	708				0.61	DMF	16
-Sbu	α	4	708.6	718.2	0.137				9
	β	4	687.4	685	0.386				9
	α	8	779.6	781	0.036				9
	β	8	707.0	733	0.119				9
-O-Ph		8	687	687			0.60		16
$-O-Ph-CH_3$	β	8	679		0.24	0.63	0.51	DMSO	13
$-O-Ph-C(CH_3)_3$	β	4	681				0.55	DMF	12
$-O-Ph-C(CH_3)_3$	β	4	680						13
$-O-Ph-CH_2CH_2COOH$	α	4	695	708				DMF	
	β	4	679	686				DMF	

Table 5. 1. Summary of zinc phthalocyanine compounds with absorption, emission, fluorescence, triplet and singlet oxygen data, where available.

R	Position	No. of subs	λ_{max} / nm	λ_{em} / nm	Φ_f	Φ_T	Φ_Δ	Solvent	Ref.
-O-Ph-COOH	α	4	686	698				DMF	
	β	4	674	685				DMF	
-O-Ph-$COOC_4H_9$	α	4	687	696				DMF	
	β	4	675	685				DMF	
-CH_3	α	8	696						[17]
-t-Bu	β	4	675						[10]
-O^iPr	α	4	702	724	0.22				[15]
-$C(CH_3)_3$	β	4	691	712	0.11				[11]
-OCH_2CF_3		16	707	716	0.0745				
-$OCH_2CH_2CH_2CH_3$	α	8	748	-	-				[11]
-$OCH_2(CH_2)_6CH_3$	β	8	690	706	0.10				[11]
-NH_2	α	4	765	790	0.001				[15]
	β	4	725	756	0.004				[15]
-Obu	α	4	696	706	0.143				[9]
	β	4	674.5	689	0.422				[9]
	α	8	758	807.5	0.062				[9]
	β	8	674.5	681.5	0.616				[9]
-Obu	β	8	674						[10]
	α	8	739						[10]
		16	714						[10]
-OC_6H_{13}	β	8	740				0.52	DMF	[14]

Table 5. 1. (cont.) Summary of zinc phthalocyanine compounds with absorption, emission, fluorescence, triplet and singlet oxygen data, where available.

Previous reviews indicate that the addition of strongly electron donating groups result in a large red shift in absorption while addition of electron withdrawing groups has a much smaller influence on absorption shift. Other observations show that tetra or octa-substitution in the beta position aids solubilisation of phthalocyanines much more than the equivalent substitution in the alpha position.[18]

Herein we will examine a series of alpha octa-alkyl zinc phthalocyanines (n = 1, 5 – 10, 12 and 15) and ZnTBTAP (n = 6), see Figure 5.2. Originally these compounds were synthesised as part of a study into the liquid crystal properties associated with molecules with long alkyl chains.[19, 20] This proved that alkyl chains attached to the phthalocyanine nucleus at alpha sites leads to mesophase formation.[21] However, the potential as photosensitisers was soon recognised and

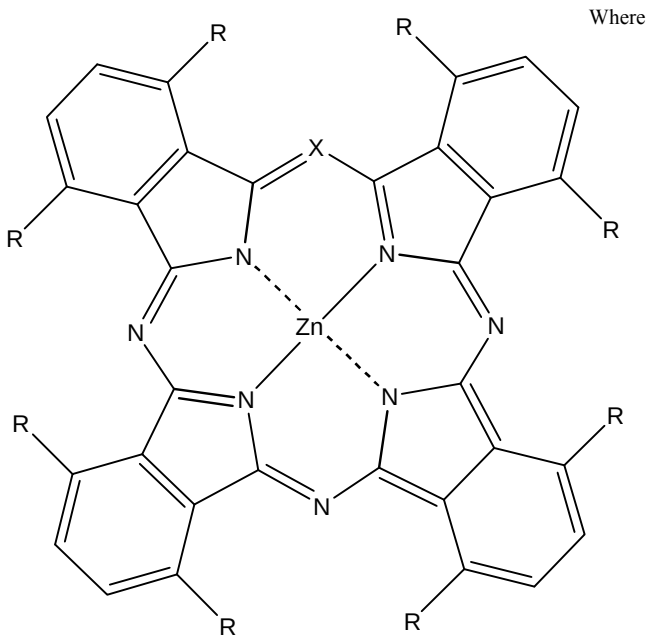

Figure 5. 1. Schematic diagram of the zinc phthalocyanine derivatives studied.

this series of compounds will be investigated with a view to determining the photophysical and photochemical parameters and comparing with other similarly related structures.

5.2 Results and Discussion

5.2.1 Spectroscopic data

The absorption spectra of the parent compound, 1ZnPc, 6ZnPc and 6ZnTBTAP can be seen in Figure 5.2. All absorption spectra are in the desired optical window of 650 – 800 nm and are typical of other phthalocyanines. It is clear to see that any substitution in the alpha position results in a red-shift of the Q-band maxima with some broadening of the band, but little influence on the shape of the absorption.[8] This is suggestive of a small disruption of the structure as a result of the addition of long alkyl chains and can be assigned to a steric factor. This has been previously observed in analogous H_2Pc structures whereby the crystal structure of octaisopentyl and octahexyl substituted H_2Pc, $5H_2Pc$ and $6H_2PC$ respectively, showed that the

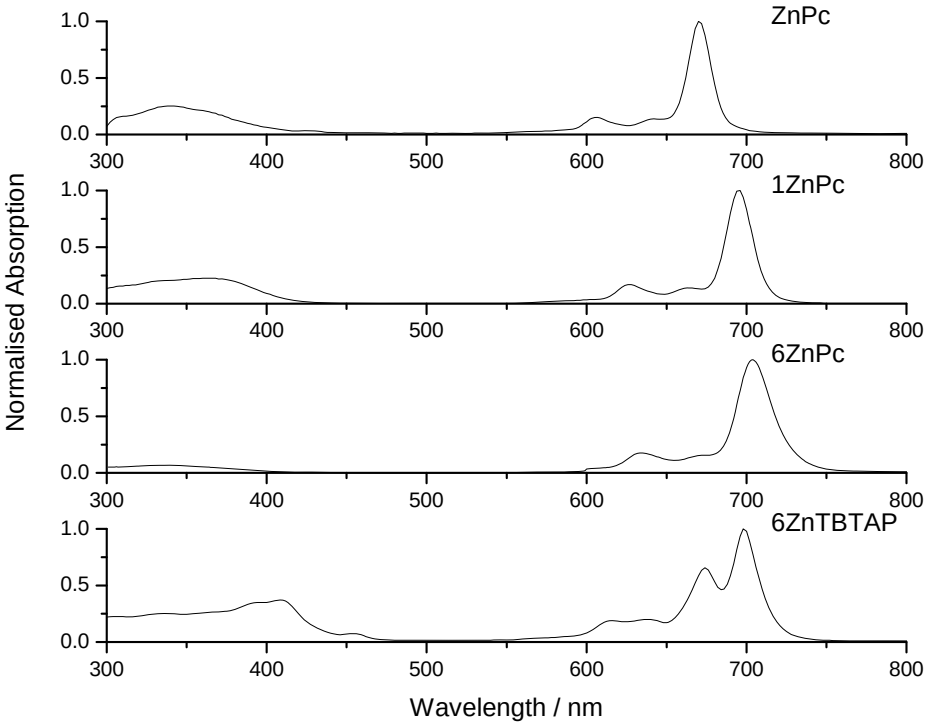

Figure 5. 2. Absorption spectra of zinc phthalocyanines (top) and derivatives, from top to bottom, 1ZnPc, 6ZnPc and 6ZnTBTAP

substitution led to some distortion from planar to a saddle shape structure.[22, 23] The red-shift of the Q-band has been attributed to the substitution of the alkyl group in the alpha position. This has previously been observed in zinc phthalocyanines with alkyl, thioalkyl and alkoxy groups in the alpha position and is ascribed to the electron-donating nature of these groups.[24] Analysis of the shift of the Q-band maxima relative to the length of the alkyl substituent indicates a positive correlation between the two components, which reaches a maximum at 3 carbons. This is similar to previously studied zinc alkoxy substituted systems, which also reach maximum shift at chain length of 3 carbons.[25]

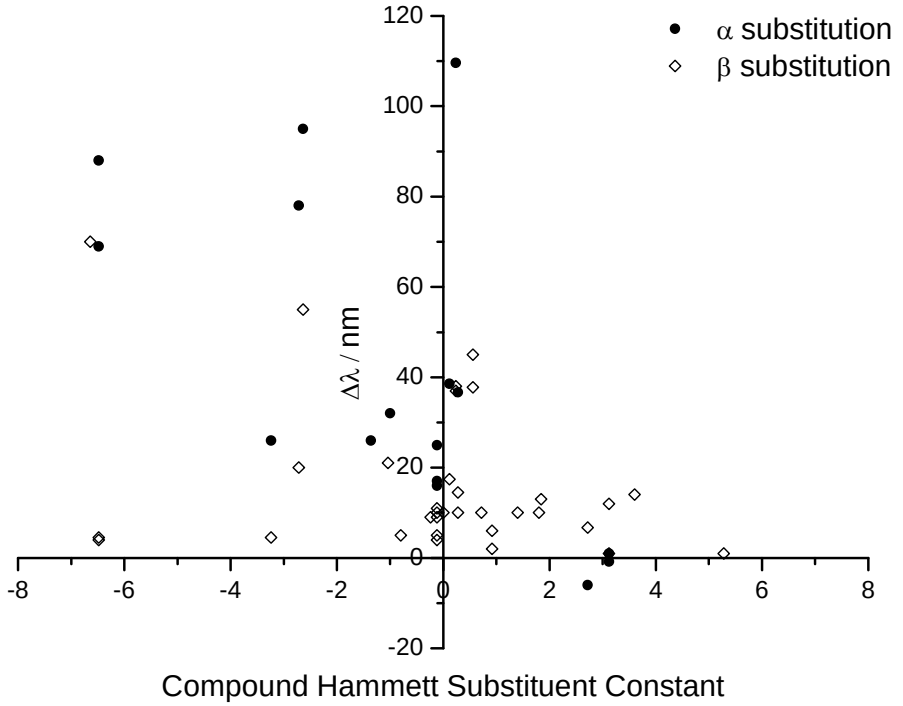

Figure 5. 3. Comparison of the compound Hammett substituent constant, σ_p, of substituent with respective shift of the Q-band relative to the position on the benzenoid ring.

Absorption maxima of the Q-band of a number of substituted compounds has been plotted relative to the Hammett substituent constant in order to determine whether there is a relationship between the magnitude and nature of the shift relative to the electronic properties of the substituent, Figure 5.3. It is clear to see that there is a more pronounced red-shift of the Q-band with electron-donating groups, which have more negative Hammett substituent constants. Previous density functional theory studies on the effect of peripheral substitution have shown that the introduction of tetra- or octa-substitution of electron-donating groups in the alpha position, where the HOMO has a large amplitude, results in an effective upward shift of the orbital and, therefore, in a diminished HOMO – LUMO gap.[26, 27] This is in contrast to substitution at the beta position where the

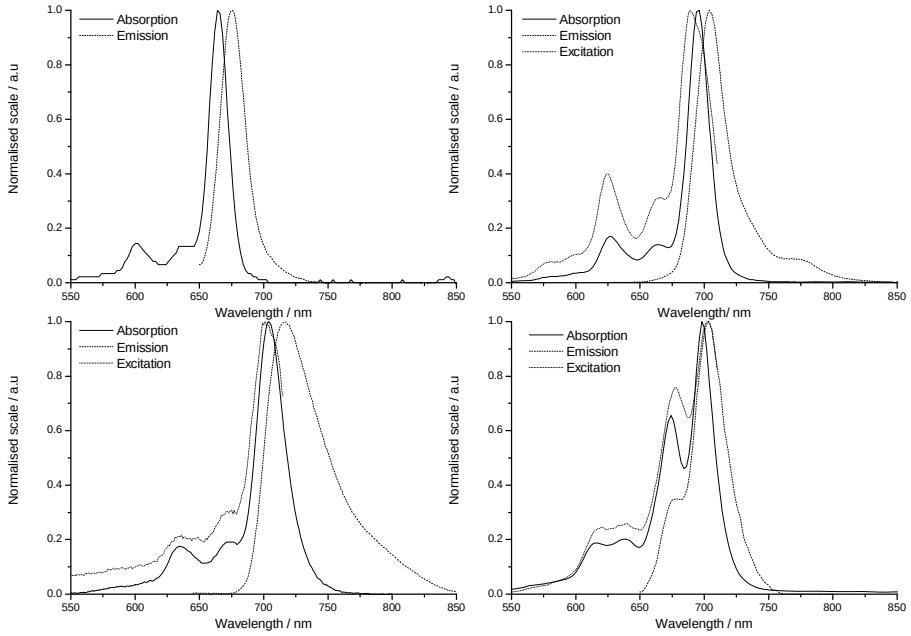

Figure 5. 4. Emission and excitation data of the zinc phthalocyanine derivatitves.

HOMO has relatively small amplitude, hence the influence of any group substituted into this position is significantly reduced with respect to the parent compound.

The absorption spectra of 6ZnTBTAP exhibits a blue-shift of the Q-band compared to 6ZnPc, Figure 5.2. As with previously published research on MgTBTAP and H_2TBTAP analogues, the doubling of the Q-band and blue shift is expected due to the change in symmetry from D_{4h} symmetry, as exhibited by the analogous phthalocyanine, to D_{2h}.[23, 28]

Emission and excitation spectra for the zinc compounds are similar, Figure 5.4, though substituted ZnPc compounds with alkyl chain length greater than 5 carbons seem to exhibit a significant broadening of the emission spectra, this may be attributed to a change in structure

Compound	λ_Q / nm	ε_s / 10^5 $M^{-1}cm^{-1}$	λ_f / nm	τ_f / ns	Φ_F	k_f / 10^7 s^{-1}
ZnPc[a]	671	2.8	676	3.1	0.34	11
1ZnPc	694	2.6 ± 0.2	704	2.5 ± 0.1	0.16 ± 0.02	6.4
2ZnPc[b]	696	-	-	-	-	-
3ZnPc[b]	702	-	-	-	-	-
4ZnPc[b]	703	-	-	-	-	-
5ZnPc	704	1.8 ± 0.2	718	1.8 ± 0.1	0.12 ± 0.02	6.67
6ZnPc	704	1.8 ± 0.2	718	1.8 ± 0.1	0.12 ± 0.02	6.67
7ZnPc	704	1.8 ± 0.2	718	1.8 ± 0.1	0.12 ± 0.02	6.67
8ZnPc	704	1.8 ± 0.2	718	1.8 ± 0.1	0.12 ± 0.02	6.67
9ZnPc	704	1.8 ± 0.2	718	1.8 ± 0.1	0.12 ± 0.02	6.67
10ZnPc	704	1.8 ± 0.2	718	1.8 ± 0.1	0.12 ± 0.02	6.67
12ZnPc	704	1.8 ± 0.2	718	1.8 ± 0.1	0.12 ± 0.02	6.67
15ZnPc	704	1.8 ± 0.2	718	1.8 ± 0.1	0.12 ± 0.02	6.67
6ZnTBTAP	698, 674	1.3 ± 0.2	703	1.6 ± 0.1	0.06 ± 0.02	3.75

Table 5. 2. Photophysical properties of the alpha substituted zinc phthalocyanines and derivatives.

of the molecule upon excitation. All exhibit a Stokes shift in the range 10 – 20 nm. 6ZnTBTAP has a modified emission spectra, with a loss of the shoulder, but no broadening is observed.

5.2.2 Photophysics

The fluorescence lifetimes have been summarised in Table 5.2. It can be seen that the lifetimes are short, 2.5 ns and 1.8 ns for 1ZnPc and *n*ZnPc, where n > 5, respectively compared to 3.1 ns for ZnPc. The fluorescence quantum yields of the compounds are also further reduced upon substitution, 0.16 and 0.12 for 1ZnPc and *n*ZnPc respectively compared with 0.34 for ZnPc in 1% v/v pyridine/toluene. This follows in the observed trend and is indicative that alkyl substitution goes some way in promoting intersystem crossing from the excited state to the triplet state. The fluorescence lifetime for 6ZnTBTAP was determined to be 1.3 ns and fluorescence quantum yield was found to be 0.06. Both values are significantly smaller than the analogous phthalocyanine, 6ZnPc. The transient absorption spectra of all compounds were similar in shape and examples can be seen in Figure 5.5. The spectra are typical of the series and all show a broad

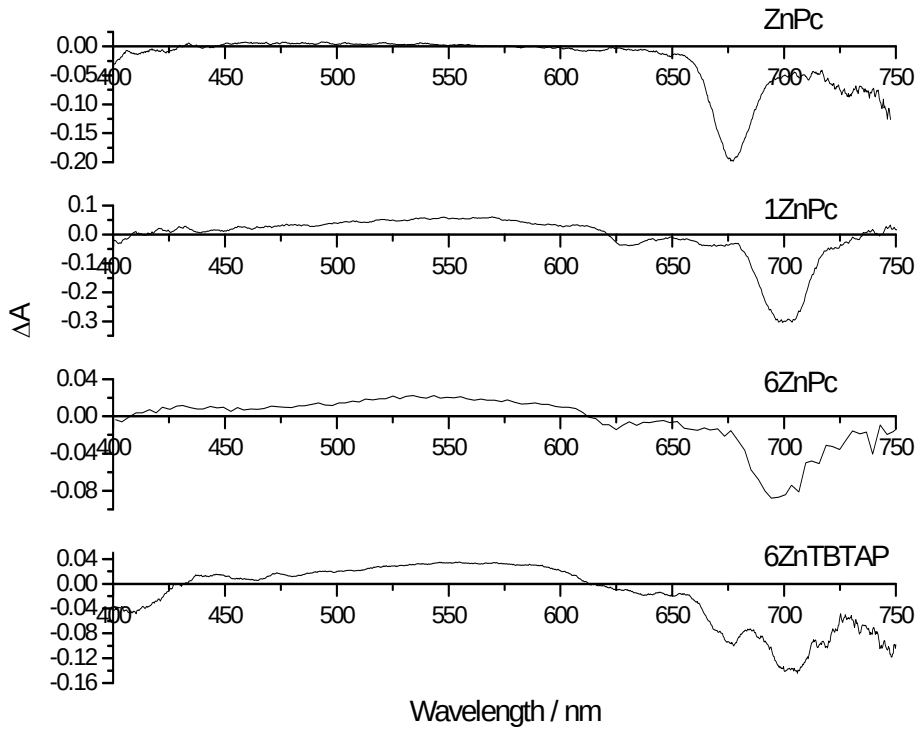

Figure 5. 5. Transient triplet-triplet absorption of ZnPc, 1ZnPc, 6ZnPc and 6ZnTBTAP in toluene-pyridine at 1 x 10^{-5} M, excitation wavelength 355 nm. The broad absorption with peak observed between 400 – 600 nm is due to T-T* absorption.

peak between 400 – 600 nm with peaks for ZnPc, 1ZnPc, and 6ZnPc at 480, 520, and 534 nm respectively. Triplet decays were determined by fitting an exponential to the decay of transient absorption measured at the respective maxima and gave values of 113 μs and 50 μs for 1ZnPc and *n*ZnPc respectively. Such triplet lifetimes are in the range expected of zinc phthalocyanines, though are significantly shorter than the parent compound, which has triplet lifetime of 300 μs. Triplet extinction coefficients were determined to be in the range 2.6 – 3.1 x 10^4 M^{-1} cm^{-1} and were used to calculate the triplet quantum yields which were are in the range 0.63 – 0.84 and are also summarized in Table 5.3. The transient absorption spectrum for 6ZnTBTAP shows a broad peak with maximum wavelength at 520 nm, and triplet lifetimes were determined to be 381 μs, with triplet absorption coefficient of

Compound	τ_T / μs	T-T_{max} / nm	$\Delta\varepsilon$ / 10^4 $M^{-1}cm^{-1}$	Φ_T	Φ_Δ	$S_\Delta = \Phi_\Delta/\Phi_T$
ZnPc	330	480	3.4	0.65	0.58	0.89
1ZnPc	113 ± 5	530 ± 10	3.1 ± 0.2	0.63 ± 0.07	0.54 ± 0.05	0.85
5ZnPc	56 ± 5	534 ± 10	3.0 ± 0.2	0.78 ± 0.07	0.71 ± 0.05	0.91
6ZnPc	51 ± 5	534 ± 10	2.8 ± 0.2	0.84 ± 0.07	0.73 ± 0.05	0.87
7ZnPc	52 ± 5	534 ± 10	3.1 ± 0.2	0.84 ± 0.07	0.72 ± 0.05	0.86
8ZnPc	50 ± 5	534 ± 10	2.6 ± 0.2	0.81 ± 0.07	0.71 ± 0.05	0.88
9ZnPc	56 ± 5	534 ± 10	2.8 ± 0.2	0.82 ± 0.07	0.67 ± 0.05	0.82
10ZnPc	58 ± 5	534 ± 10	2.6 ± 0.2	0.82 ± 0.07	0.68 ± 0.05	0.83
12ZnPc	60 ± 5	534 ± 10	2.6 ± 0.2	0.82 ± 0.07	0.67 ± 0.05	0.82
15ZnPc	58 ± 5	534 ± 10	3.1 ± 0.2	0.82 ± 0.07	0.65 ± 0.05	0.80
6ZnTBTAP	380 ± 5	520 ± 10	1.7 ± 0.2	0.78 ± 0.07		

Table 5. 3. Triplet and photochemical properties of alpha substituted zinc phthalocyanines and derivatives.

1.7×10^4 M^{-1} cm^{-1} and triplet quantum yield of 0.78, similar to the phthalocyanine counterpart.

The observed decrease in the fluorescence quantum yield in all compounds studied is complemented by an increase in the triplet quantum yield. It can be seen that the influence of alkyl alpha substitution on the orbitals of the phthalocyanine molecule has an impact on the fluorescence and triplet properties of the molecules.

In the absence of other processes the data presented above would suggest that the fluorescence transition gets progressively more intense with increasing chain length of the alkyl substituent. However, it can also be concluded that intersystem-crossing competes more effectively with fluorescence in compounds with chain length 5 – 15 compared to the parent compound and 1ZnPc as the triplet quantum yields are higher. From the quantum yields it can be seen that the fluorescence and intersystem-crossing are the dominant processes such that $\Phi_F + \Phi_T \approx 1$. Hence, we are able to express the fluorescence quantum yield as:

$$\Phi_F = \frac{k_F}{k_F + k_{ISC}}$$

Where, k_F is the radiative rate constant, which is expressed as:

$$k_F = \frac{\Phi_F}{\tau_F}$$

And k_{ISC} is the rate of intersystem crossing. Using $\Phi_F = 0.34$ and the measured value of $\tau_F = 3.1 \times 10^{-9}$ s^{-1} we obtain $k_F = 1.1 \times 10^8$ s^{-1} and $k_{ISC} = 2.3 \times 10^8$ s^{-1}. The methine substituted phthalocyanine and *n*ZnPc also have $\Phi_F + \Phi_T \approx 1$, hence, the same calculations can be carried out and the values obtained are $k_F = 6.4 \times 10^7$ s^{-1} and 6.67×10^7 s^{-1} and $k_{ISC} = 3.36 \times 10^8$ s^{-1} and 4.89×10^8 s^{-1} for 1ZnPc and *n*ZnPc respectively.

Intersystem crossing in both 1ZnPc and *n*ZnPc are 1.5 and 2.1 times as fast as in the parent compound. The only difference in these compounds is the alkyl substitution in the alpha position. This coincides with previous analysis that the difference in intersystem crossing rates may be attributed to a relative shift in energies between the S_1 and T_1 states upon alpha substitution. The maximum absorption of ZnPc is at 671 nm (14,900 cm^{-1}) and the triplet absorption has its maximum at 1092 nm (9160 cm^{-1}). The intersystem crossing rate of 1ZnPc is one and a half that of ZnPc and for *n*ZnPc is twice that of ZnPc which implies that there is a smaller energy gap between S_1 and T_1 in both cases. If it is assumed that the rate is inversely proportional to the energy difference an estimate of the phosphorescence wavelength can be calculated. The absorption wavelength of 1ZnPc is 694 nm (14409 cm^{-1}) and taking two thirds the energy difference in ZnPc the phosphorescence wavelength maximum is estimated as 945 nm (10582 cm^{-1}). The absorption wavelength of *n*ZnPc is 704 nm

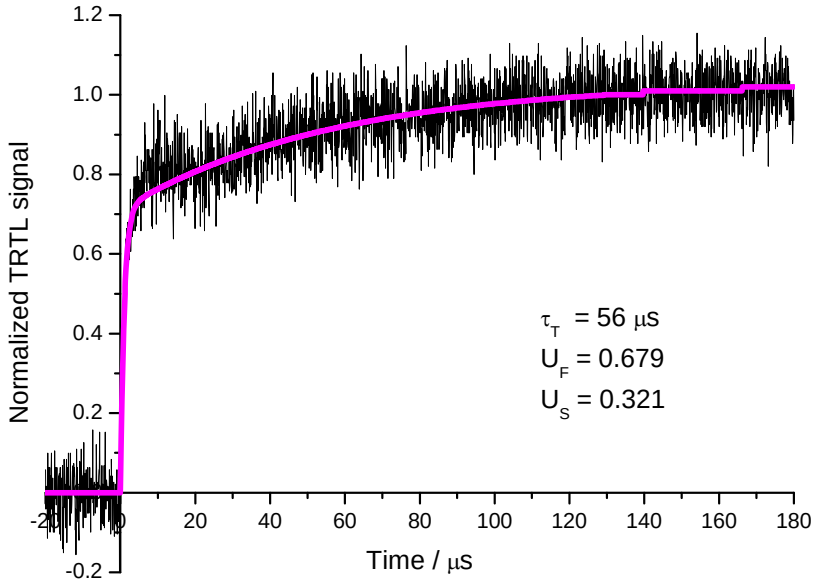

Figure 5. 6. Time-resolve thermal lensing signal of a degassed sample of 5ZnPc in 1% v/v pyridine/toluene at 1 x 10^{-5} M, excitation wavelength 355 nm.

(14205 cm^{-1}) and taking half the energy difference in ZnPc an estimate of the phosphorescence wavelength maximum is determined to be 871 nm (11472 cm^{-1}).

Using time-resolved thermal lensing techniques it was possible to determine provisional data that suggests the triplet energy of 5ZnPc to be approximately 130 kJ mol^{-1}, a typical signal including the fit is shown in Figure 5.6. This is largerr than the documented value of 110 kJ mol^{-1} for ZnPc and would agree with the data presented in this report.[29]

5.2.3 Photochemistry

A necessary requirement of photodynamic therapy is a relatively high absolute quantum yield of oxygen, specifically $\Phi_{\Delta} > 0.5$. The results are summarised in Table 5.3, where it can be seen that the values are as expected. Given previous fluorescence and triplet data determined

for each of the compounds, it can be predicted that Φ_Δ will be a reflection of the triplet state, which is indeed the case. The reduction in triplet quantum yield of 1ZnPc is mirrored in a reduced $\Phi_\Delta = 0.54$, compared to ZnPc with $\Phi_\Delta = 0.58$ and *n*ZnPc in the range $\Phi_\Delta = 0.65 – 0.73$. S_Δ values, which are a ratio of singlet oxygen quantum yields to triplet quantum yields, show all compounds behave in a similar way with values of 0.89, 0.85 and 0.80 – 0.91 for ZnPc, 1ZnPc and *n*ZnPc, respectively. Though it has not been possible to collect the singlet delta oxygen values of 6ZnTBTAP it can be predicted, given the trends observed for the analogous 6ZnPc species, that if S_Δ values fall in the range 0.80 – 0.90 then Φ_Δ will be in the range 0.62 – 0.70.

5.3 Conclusion

In conclusion, it has been shown that the series of zinc phthalocyanines and zinc triazabenzoporphyrin form a promising group of candidates as photosensitisers. The addition of alkyl chains in the alpha position of the benzenoid rings results in a red-shift of the Q-band, diminished fluorescence quantum yield and enhanced triplet quantum yield compared with the parent compound. This is a desirable property for photosensitisers as it equates to an efficient transfer of energy to the desired states. This leads to achieving the ultimate goal of high singlet delta oxygen quantum yields. In addition to modification of the alkyl substituents, the analogous 6ZnTBTAP compound also proves favourable in terms of a photosensitizing compound. Though, results are slightly lower than the analogous 6ZnPc, they are still significantly higher than the parent compound and also have the benefit of a far longer triplet state lifetime than 6ZnPc.

5.4 References

1. P. Peumans, A. Yakimov and S. R. Forrest, *J. App. Phys.*, 2003, **93**, 3693.
2. C. W. Tang and S. A. Vanslyke, *Appl. Phys. Lett.*, 1987, **51**, 913.
3. Z. Bao, A. J. Lovinger and A. Dodabalapur, *Appl. Phys. Lett.*, 1996, **69**, 3066.
4. G. de la Torre, P. Vazquez, F. Agullo-Lopez and T. Torres, *J. Mat. Chem.*, 1998, **8**, 1671.
5. T. Nyokong, *Coord. Chem. Rev.*, 2007, **251**, 1707.
6. S. Ogura, K. Tabata, K. Fukushima, T. Kamachi and I. Okura, *J. Porph. Phthal.*, 2006, **10**, 1116.
7. E. Reddi, C. Zhou, R. Biolo, E. Menegaldo and G. Jori, *Br. J. Cancer*, 1990, **61**, 407.
8. G. Winter, H. Heckmann, P. Haisch, W. Eberhardt, M. Hanack, L. Luer, H. J. Egelhaaf and D. Oelkrug, *J. Am. Chem. Soc.*, 1998, **120**, 11663.
9. N. Kobayashi, H. Ogata, N. Nonaka and E. A. Luk'yanets, *Chem.-Eur. J.*, 2003, **9**, 5123.
10. H. Shinohara, O. Tsaryova, G. Schnurpfeil and D. Wohrle, *J. Photochem. Photobiol. A. Chem.*, 2006, **184**, 50.
11. D. Wrobel and A. Boguta, *J. Photochem. Photobiol. A. Chem.*, 2002, **150**, 67.
12. X. F. Zhang and H. J. Xu, *J. Chem. Soc. Faraday. Trans.*, 1993, **89**, 3347.
13. A. Ogunsipe, J. Y. Chen and T. Nyokong, *New J. Chem.*, 2004, **28**, 822.

14. W. Spiller, H. Kliesch, D. Wohrle, S. Hackbarth, B. Roder and G. Schnurpfeil, *J. Porph. Phthal.*, 1998, **2**, 145.
15. X. F. Zhang, X. J. Li, L. H. Niu, L. Sun and L. Liu, *Journal of Fluorescence*, 2009, **19**, 947.
16. K. I. Ozoemena and T. Nyokong, *Inorg. Chem. Comm.*, 2003, **6**, 1192.
17. M. J. Cook, I. Chambrier, S. J. Cracknell, D. A. Mayes and D. A. Russell, *Photochem. Photobiol.*, 1995, **62**, 542.
18. C. G. Claessens, U. Hahn and T. Torres, *Chem. Rec.*, 2008, **8**, 75.
19. D. Masurel, C. Sirlin and J. Simon, *New J. Chem.*, 1987, **11**, 455.
20. K. Ohta, L. Jacquemin, C. Sirlin, L. Bosio and J. Simon, *New J. Chem.*, 1988, **12**, 751.
21. M. J. Cook, *Chem. Rec.*, 2002, **2**, 225.
22. I. Chambrier, M. J. Cook and P. T. Wood, *Chem. Comm.*, 2000, 2133.
23. I. Chambrier, M. J. Cook, M. Helliwell and A. K. Powell, *J. Chem. Soc. Chem. Comm.*, 1992, 444.
24. J. Mack, N. Kobayashi and M. J. Stillman, *J. Inorg. Biochem.*, **104**, 310.
25. R. W. Boyle, C. C. Leznoff and J. E. Vanlier, *Br. J. Cancer*, 1993, **67**, 1177.
26. G. Ricciardi, A. Rosa and E. J. Baerends, *J. Phys. Chem. A*, 2001, **105**, 5242.
27. G. Cheng, X. Z. Peng, G. L. Hao, V. O. Kennedy, I. N. Ivanov, K. Knappenberger, T. J. Hill, M. A. J. Rodgers and M. E. Kenney, *J. Phys. Chem. A*, 2003, **107**, 3503.

28. A. N. Cammidge, I. Chambrier, M. J. Cook, D. L. Hughes, M. Rahman and L. Sosa-Vargas, *Chem.-Eur. J.*, 2011, **17**, 3136.

29. P. S. Vincett, E. M. Voigt and Rieckhof.Ke, *J. Chem. Phys.*, 1971, **55**, 4131.

6. Palladium Phthalocyanine Derivatives

6.1 Introduction

There is a distinct lack of literature concerning metallophthalocyanines with open-shell metals such as platinum and palladium compared to diamagnetic systems such as zinc, aluminium and copper.[1-4] Table 6.1 highlights the compounds that have been synthesised and characterised to date with respect to possible application as photosensitisers in phototherapies. It can be seen that a key property of these compounds is the short triplet lifetime. Short lifetimes are fundamentally an undesirable property for any potential photosensitizer as it indicates that the electronically excited state decays preferentially by non-radiative pathways, releasing the absorbed energy as heat. This feature in itself has prompted a burst in research in the direction of photothermal therapy.[7, 8] Photothermal therapy works using similar principles to photodynamic therapy. By

R	Sol	λ_{max} / nm	Log ε	λ_{em} / nm	Φ_F	$\lambda_{T\text{-}T^*}$ / nm	Φ_T	τ_Δ / μs	Φ_Δ
-H[1]		660		664	0.0005	620		25	
$-OC_6H_5$[2]	1-CNP	668	5.11				0.51	23	0.49
$-OC_6H_4OC_6H_5$[2]	1-CNP	670	5.25	682	< 0.01		0.65	20	0.43
$-SC_5H_{13}$[5]	1-CNP	698		745	< 0.01		0.47	15	0.42
$-SC_8H_{17}$[5]	1-CNP	698		707	< 0.01		0.42	12	0.40
$-SC_{12}H_{25}$[6]	1-CNP	698		707	< 0.01		0.40	10	0.39
-OBu[9]	DMF	722	5.6	734	0.0008		0.77	3.04	

Table 6. 1. Summary of palladium phthalocyanine compounds with absorption, emission, fluorescence, triplet and singlet delta oxygen quantum yields, where available.

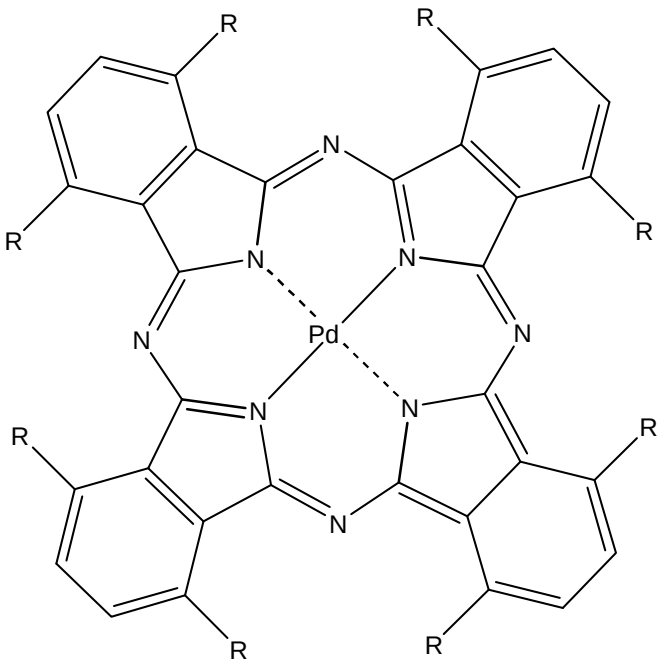

Figure 6. 1. Schematic diagram of the palladium phthalocyanine derivatives studied.

applying a combination of light and photosensitiser to treat damaged cells, rather than producing cytotoxic oxygen to induce cell death, the technique centres around the localized production of heat, which results in damage to cells and, ultimately, cell death.[10]

In 2003 Cook *et al*.[11] published the synthesis of a series of octaalkylphthalocyanines, including palladium, with respect to non-linear absorption properties for application in optical limiters. It was found that the palladium derivatives exhibited the strongest non-linear absorption of the series of compounds studied. The successful synthesis of 6PdPc and subsequently 8PdPc, see Figure 6.1, has paved the opportunity to further explore this family of heavy-metal compounds for their potential application as photosensitizers in photodynamic therapy.

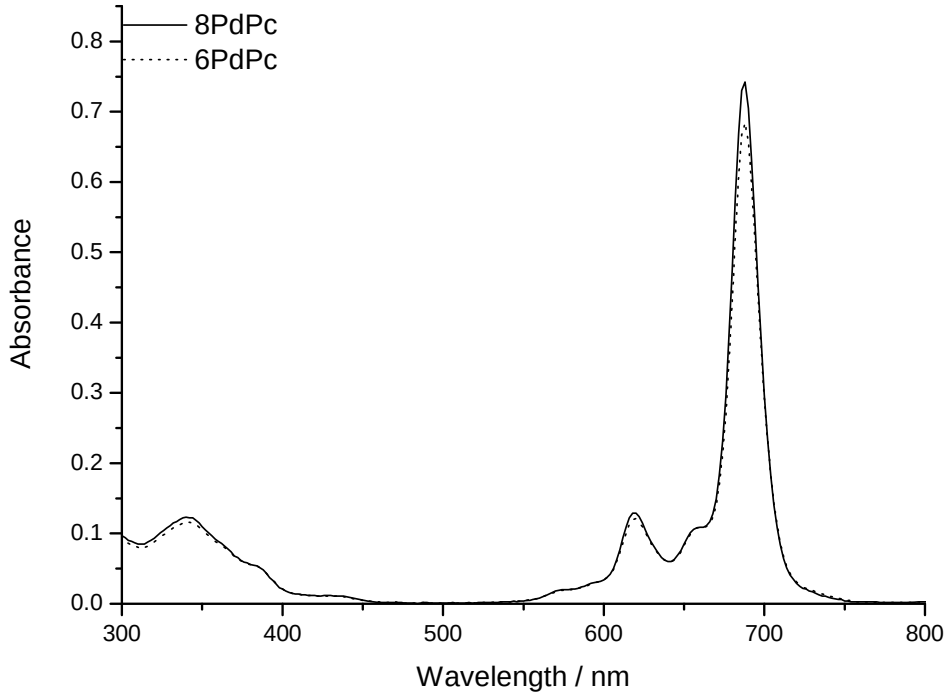

Figure 6. 2. Absorption spectra of palladium phthalocyanine derivatives.

6.2 Results and Discussion

6.2.1 Spectroscopic data

The absorption spectra of 6PdPc and 8PdPc can be seen in Figure 6.2. No absorption spectrum was available for the parent compound. However, literature values show palladium phthalocyanine to have a Q-band maxima at 664 nm compared to the substituted compounds at 690 nm, a red-shift of 26 nm into the therapeutic window, 650 – 800 nm.[1] This is attributed to the substitution of electron donating groups in the alpha position, which induces a reduction of the HOMO – LUMO distance. Both compounds exhibit the typical shape for

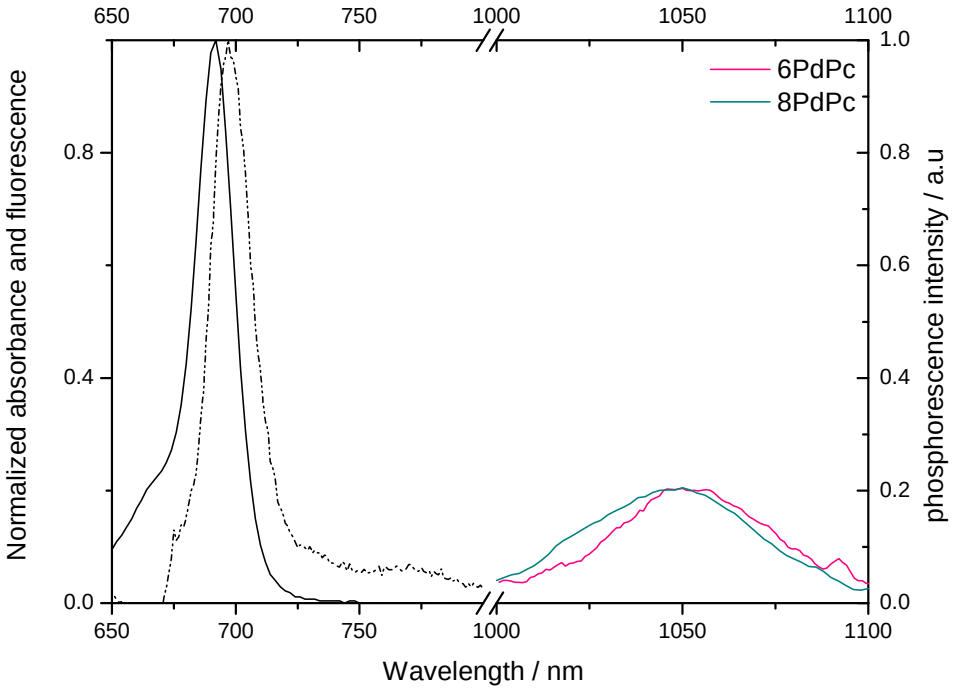

Figure 6. 3. Absorption (solid line), fluorescence (dash, dot, dot) and phosphorescence spectra of 6PdPc and 8PdPc measured at room temperature, in 1% v/v toluene/pyridine. The absorption and fluorescence are normalized to an arbitrary maximum of 1.0. The fluorescence was obtained in air-saturated solution. The phosphorescence spectra were obtained with freeze-pump-thaw degassed samples and λ_{ex} = 632 nm.

standard absorption spectra, indicating no change in symmetry upon substitution.

The emission and excitation spectra obtained for the 6PdPc and 8PdPc compounds are similar and an example can be seen in Figure 6.3. The weak emission has maximum at 694 nm and maximum absorption at 690 nm: a Stokes shift of 4 nm. This is similar to other substituted palladium phthalocyanines.

Besides fluorescence emission, the degassed solutions of 6PdPc and 8PdPc exhibit an additional emission in the near-infrared, Figure 6.3.

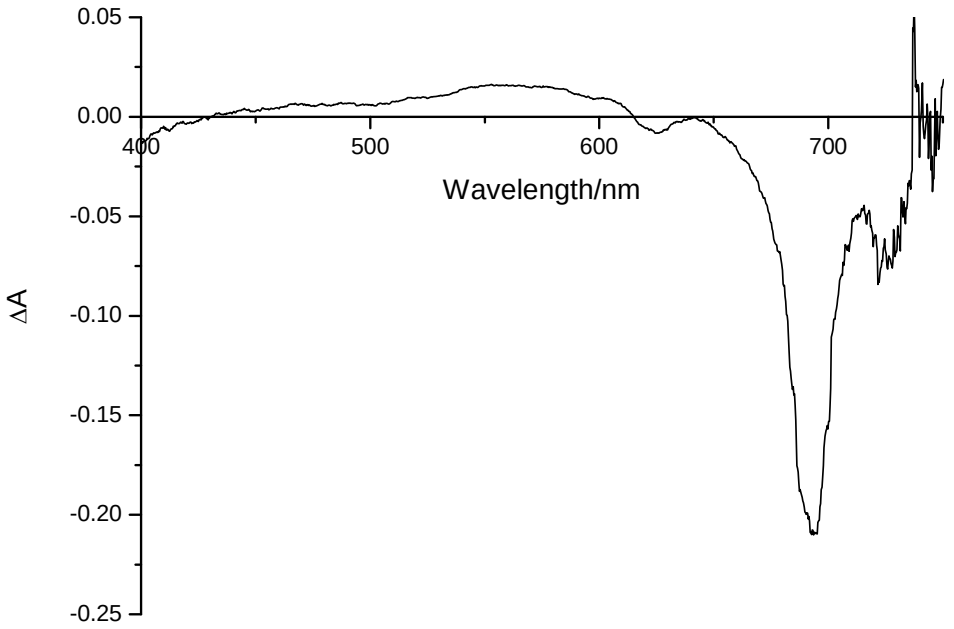

Figure 6. 4. Transient triplet-triplet absorption spectrum of 6PdPc in 1% v/v pyridine/toluene, λ_{ex} = 355 nm. The broad absorption with peak observed between 450 - 620 nm is due to T – T* absorption.

This peak vanishes upon reintroduction of oxygen to the system and is subsequently assigned to phosphorescence. In degassed toluene/pyridine the T1 (0,0) emission maxima are 1048 and 1052 nm for 6PdPc and 8PdPc compounds, respectively, at room temperature. These values compare well with previously published values of alpha octabutoxy PdPc which has a peak at 1107 nm.[9] Both compounds are red-shifted compared with the parent compound that exhibits T1(0,0) emission band at 1007 nm.[1]

Fluorescence lifetime decays could not be measured for these compounds due to the weak fluorescence and quantum yields determined were < 0.02. Such low fluorescence is a favourable property of photosensitizers used in PDT as it indicates that energy not lost via radiative pathways. The values are also typical of

palladium phthalocyanines studied to date as the heavy-atom effect promotes spin-forbidden intersystem crossing.

6.2.2 Photophysics

The transient absorption spectra of both substituted palladium phthalocyanines are similar in shape with a broad peak between 450 – 620 nm and maximum at 542 nm, Figure 6.4. Triplet decays were measured at this point by fitting an exponential. The triplet lifetimes were found to be 5 μs and 6 μs for 6PdPc and 8PdPc, respectively. These short lifetimes are typical of palladium phthalocyanines and are comparable to literature values of 25 μs for the unsubstituted parent compound, PdPc, and 3 μs for $(OBu)_8$PdPc, which is within the expected range for phthalocyanines.[1, 9] Triplet extinction coefficients were determined to be 1.0 and 1.2 x 10^4 M^{-1} cm^{-1} and using these values triplet quantum yields of 0.94 and 0.96 for 6PdPc and 8PdPc, respectively, were calculated. These values are close to unity and bode well for a potential photosensitizer, though the short triplet lifetimes are favourable, the high triplet quantum yields suggest minimal loss of energy through non-radiative pathways.

6.2.3 Photochemistry

Singlet delta oxygen, Φ_Δ, values are the final property required to quantify the potential of any given compound as a photosensitizer for photodynamic therapy. Using time-resolved singlet oxygen phosphorescence detection, Φ_Δ values of 0.92 and 0.93 for 6PdPc and 8PdPc, respectively, were obtained. These values are close to unity and very promising in the search for efficient chemical photosensitizers. Furthermore, these compounds also have high S_Δ values of 0.98 and 0.97 for 6PdPc and 8PdPc, respectively. This

coincides well with enhanced triplet state populations and the red-shift observed in the wavelength of phosphorescence.

6.3 Conclusion

To conclude, the substitution of long alkyl chains has a significant impact on the photophysical and photochemical properties of the palladium phthalocyanine molecule. This includes the 26 nm red-shift of the Q-band, facilitating deeper skin penetration, high triplet quantum yields, leading to the enhancement of the triplet state population, a red-shift of the triplet state, leading to high singlet oxygen quantum yields. Though there is no improvement in solubility within aqueous solvents and these molecules also have short triplet lifetimes, there is significant improvement of the photophysical and photochemical properties and the peripherally substituted compounds compare well with the analogous alpha-substituted palladium phthalocyanine compounds.

6.4 References

1. P. S. Vincett, E. M. Voigt and Rieckhof.Ke, *J. Chem. Phys.*, 1971, **55**, 4131.
2. T. B. Ogunbayo and T. Nyokong, *J. Mol. Struct.*, 2010, **973**, 96.
3. S. Ogura, K. Tabata, K. Fukushima, T. Kamachi and I. Okura, *J. Porph. Phthal.*, 2006, **10**, 1116.
4. T. Nyokong, *Coord. Chem. Rev.*, 2007, **251**, 1707.
5. T. B. Ogunbayo, A. Ogunsipe and T. Nyokong, *Dyes and Pigments*, 2009, **82**, 422.
6. T. B. Ogunbayo and T. Nyokong, *Polyhedron*, 2009, **28**, 2710.
7. T. C. Gunaratne, A. V. Gusev, X. Peng, A. Rosa, G. Ricciardi, E. J. Baerends, C. Rizzoli, M. E. Kenney and M. A. J. Rodgers, *J. Phys. Chem.*, 2005, **109**, 2078.
8. B. D. Rihter, M. E. Kenney, W. E. Ford and M. A. J. Rodgers, *J. Am. Chem. Soc.*, 1990, **112**, 8064.
9. A. V. Soldatova, J. Kim, C. Rizzoli, M. E. Kenney, M. A. J. Rodgers, A. Rosa and G. Ricciardi, *Inorg. Chem.*, 2011, **50**, 1135
10. G. Ricciardi, A. V. Soldatova and A. Rosa, *J. Inorg. Biochem.*, 2008, **102**, 406.
11. A. Auger, W. J. Blau, P. M. Burnham, I. Chambrier, M. J. Cook, B. Isare, F. Nekelson and S. M. O. O' Flaherty, *J. Mat. Chem.*, 2003, **13**, 1042

7. Discussion and Conclusion

7.1 Variation of Central Metal Ion

The aim of this work was to follow the effect of systematic changes to the phthalocyanine molecule on the photophysical and photochemical properties and evaluate these compounds as potential photosensitizers in photodynamic therapy. Three distinct families of phthalocyanines were studied containing either silicon hydroxide, zinc(II) or palladium(II) centres. Each has been reviewed relative to standards and parent compounds, where available, within their distinct group. However, the substitution of hexyl and octyl groups in the alpha position was applied in all three series and afforded a series of compounds identical in structure, but differing in metal ion centre. Tables 7.1 and 7.2 show the results collated across the groups.

Compound	λ_Q / nm	ε_s / $M^{-1}cm^{-1}$ x 10^5	λ_f / nm	τ_f / ns	Φ_F	k_f / $10^7 s^{-1}$
ZnPc[1]	671	2.8	676	3.1	0.34	11
1ZnPc	694	2.5	704	2.5	0.16	
6ZnPc	704	1.8	718	1.8	0.12	6.67
8ZnPc	704	1.8	718	1.8	0.12	6.67
6ZnTBTAP	698, 674		703			
$Si(OH)_2Pc$	692		702			
$6Si(OH)_2Pc$	710	2.3	724	3.8	0.27	6.32
$8Si(OH)_2Pc$	710	2.3	724	3.8	0.27	6.32
PdPc[3]	660		664			
6PdPc	688	0.67	-	-	-	-
8PdPc	688	0.67	-	-	-	-

Table 7. 1. Photophysical properties of the parent and alpha substituted phthalocyanine derivatives.

Compound	τ_T / μs	T-T_{max} / nm	$\Delta\varepsilon$ / 10^4 $M^{-1}cm^{-1}$	Φ_T	Φ_Δ	S_Δ	E_T / nm
ZnPc	330	480	3.4	0.65	0.58	0.89	1092 (77K)
1ZnPc	113		3.0	0.73	0.54	0.74	
6ZnPc	51	534	2.8	0.84	0.73	0.87	
8ZnPc	50	534	2.6	0.81	0.71	0.88	
6ZnTBTAP	380	520					
$Si(OH)_2Pc$	103						
$6Si(OH)_2Pc$	161	552	2.5	0.65	0.52	0.80	
$8Si(OH)_2Pc$	196		4.6	0.72	0.50	0.70	
PdPc	25						1007 (300K)
6PdPc	5			0.94	0.92	0.98	1048 (300K)
8PdPc	6	542	0.4	0.96	0.93	0.97	1052 (300K)

Table 7. 2. Triplet and photochemical properties of parent and alpha substituted phthalocyanines derivative.

As has been previously discussed, there are a number of key points that must be taken into consideration upon optimisation of any compound as a photosensitizer. With the modifications applied to the basic phthalocyanine molecule it is possible to assess the advantages gained in each case.

7.2 Amphiphilicity

Hydrophobicity and hydrophilicity is key in the administration of photosensitisers due to the complex nature of cells and cell membranes.[2] In all cases, it was observed that solubility in the pyridine-toluene mixture improved upon alkyl substitution. However, in the phthalocyanine derivatives studied the silicon series showed the greatest potential. This is due to the axial component of the molecule, which inhibits π-π stacking, the main source of aggregation.

Aggregation needs to be prevented as it leads to quenching, which significantly reduces the yield of the triplet state and therefore the efficiency of the compound as a photosensitiser.[4] Furthermore, substitution of alkyl chains on the silicon phthalocyanines significantly improved solubility in aqueous media, and most importantly water. Though there are methods for combating a lack of solubility, including the introduction of phthalocyanines into liposomes and cyclodextrins, the administration of a single compound is considered to be important in the identification of a biological target.

7.3 Red Absorption

The importance of high molar extinction coefficients in the red, in particular the optical window of 600 – 850 nm, has been mentioned repeatedly as one of the keys to the success of PDT.[5] One of the principal disadvantages associated with Photofrin® is low molar extinction coeffients, ε_s = 3000 $cm^{-1} M^{-1}$ at 630 nm.[6, 7] The low extinction coefficient and therapeutic wavelength limit the available treatment depth to millimetres and therefore restricts the overall benefit of this treatment over current methods. The Q-band maxima of all phthalocyanines studied have high extinction coefficients that fall well within the optical window, see Figure 7.1.[8] It is clear to see that phthalocyanines exhibit a blue-shift upon increase in atomic number of the central metal ion, which is due to the stabilisation of the HOMO. However, a significant decrease in molar extinction coefficient with increase in atomic number of the central metal ion must also be noted. Addition of alpha-alkyl substituents, independent of chain length, induces a red-shift of the Q-band of approximately 20 – 30 nm in all cases. Consequently, such modifications show a significant

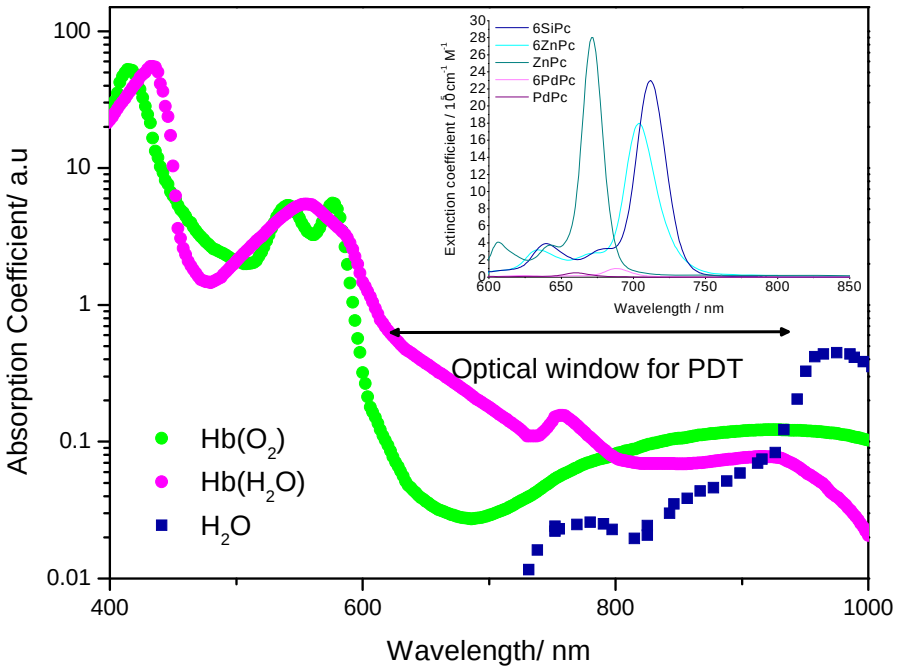

Figure 7. 1. Illustration of the optical window as defined by a logarithmic plot of the absorption of key chromophores within a cell. Top right inset shows the relative absorption of hexyl-substituted silicon, zinc and palladium phthalocyanine derivatives and the parent compounds ZnPc and PdPc.

improvement in the potential penetration depth of PDT in comparison to current photosensitizers.[9]

7.4 Fluorescence

In an attempt to produce the most energetically efficient photosensitiser, low fluorescence is a desirable property. High fluorescence leads to energy loss directly from the singlet states rather than the excited molecule undergoing intersystem crossing to produce the triplet state. In the case of the phthalocyanines studied, fluorescence decreased significantly with increase in atomic number of the central metal ion and also upon alkyl-substitution, a clear indication of enhancement of spin-forbidden intersystem-crossing

from the excited singlet state to the triplet state. However, there must also be some acknowledgement of the benefit of fluorescence such that, in the case of the substituted silicon phthalocyanines, with $\Phi_f = 0.27$, the fluorescence can be utilised either as a diagnostic tool or as a means of determining optimum tumour saturation and so identify an optimum treatment time. Fluorescence of the photosensitiser also provides a means for measuring the rate of clearance of the drug from the system. Though, this is dependent on the metabolism of the compounds after administration and where the metabolites localise.

7.5 Triplet Yields

It is widely believed that the success of photodynamic therapy is due to the efficiency of triplet state formation by the photosensitisers and the lifetime of this state.[10] With the phthalocyanines, the palladium analogues have high triplet quantum yields and favourable triplet energy, but very short triplet lifetimes and low triplet extinction coefficients. The success of photodynamic therapy depends on photosensitisers having triplet states with long lifetimes in order to form singlet delta oxygen from the molecular oxygen present in the cells. The drawbacks of such short-lived states are a loss of energy typically through triplet-triplet annihilation. Zinc and silicon phthalocyanines on the other hand exhibit lower triplet quantum than the palladium analogues as one might expect from a reduced heavy-atom effect and therefore reduced spin-forbidden intersystem-crossing. In the case of the silicon phthalocyanines alpha-alkyl substitution also leads to an increase in triplet lifetimes.

7.6 Singlet Oxygen Quantum Yields

Singlet oxygen quantum yields are the quantitative measure of the potential of any compound as a photosensitiser in *in vitro* conditions. It describes the efficiency of any given compound in the production of singlet delta oxygen, which is thought to be the destructive component of photodynamic therapy. The data indicates that singlet delta oxygen quantum yields increase with increasing heavy-atom effect and also with alpha-substitution of electron-donating groups. In fact, the pattern closely reflects the pattern of triplet state formation. If we look at the fraction of triplet states formed that lead to singlet delta oxygen states, S_{Δ}, it can be seen that silicon and palladium phthalocyanines are the most efficient *in vitro*.

7.7 Stability, Toxicity and Tumour Selectivity

All of the parameters that have been evaluated for these phthalocyanines are a measure of the photochemistry and photophysics of the compounds. The following step in the determination of the validity of any one of these molecules as a future photosensitiser is to identify their stability in biological matter and whether any of these compounds exhibit tumour selectivity, before following up with clinical trials. Provisional cell kill data has previously been measured for the silicon and zinc phthalocyanine derivatives, which may suggest that the silicon derivatives are the more efficient photosensitisers.[11]

7.8 Conclusion

The phthalocyanine molecule has proved to be a compound with the potential for countless modifications.[12] This study focused on the capacity to fine-tune the properties of phthalocyanines towards that of

an ideal photosensitiser. These included properties such as amphiphilicity, red absorption, low fluorescence, high triplet quantum yields and high singlet delta oxygen quantum yields. The benefits and drawbacks of each of the modifications have been discussed. In terms of the suitability of any one of the compounds studied and their potential as photosensitisers in photodynamic therapy a great emphasis has been put on the singlet delta oxygen quantum yields. It is observed that all phthalocyanine derivatives considered in this study have good Φ_{Δ}, values typically greater than 0.5. However, there is a limit to the degree that this property can be improved.

Foscan is a good example of a highly potent photosensitiser that has moderate quantum yields, $\Phi_{\Delta} = 0.4$, absorbs at 660 nm and only requires low doses to achieve the same results as Photofrin®.[13] The success of the photosensitiser is considered to be, in part, due enhanced penetration through tissue, increasing the available depth of treatment. With this in mind, it can be concluded that the alkyl-substituted silicon phthalocyanine derivatives have the greatest potential as photosensitisers. These compounds, above all other phthalocyanine compounds considered in the study, exhibit the greatest red-shift in the Q-band maximum and have the highest molar extinction coefficients, with the exception of zinc phthalocyanine. The benefits of this include deeper penetration into tissue; hence lower light and photosensitiser doses. Coordination of the hydroxide ligands in the axial position affords greater solubility, due to a decrease in aggregation. Aggregation is largely brought about by $\pi - \pi$ stacking in these systems.[4] Solubility and amphiphilicity is a much sought after property in the field of photodynamic therapy as it aids the administration of the photosensitiser to the desired site through a

variety of aqueous and lipid cellular environments. Furthermore, solubility is further enhanced by the addition of alkyl substituents in the alpha position. In comparison with Photofrin® the photophysical and photochemical properties compare well and, as has previously been mentioned, cell kill data available in literature suggests that these silicon phthalocyanine derivatives are efficient photosensitisers.

7.9 Future Work

From the conclusions presented in this work it is clear that the silicon phthalocyanine derivatives make promising candidates for photosensitisers in photodynamic therapy and further work should be carried out to investigate how these compound function in biological environments. Two key properties to consider are selectivity and toxicity. It is essential to determine whether there is preferential absorption of these compounds by tumour cells over healthy cells and to ensure that the metabolism of the silicon phthalocyanines does not lead to harmful metabolites before moving forward with clinical trials.

The work presented in this thesis has not only considered the phthalocyanine derivatives studied in this work, but also tried to put the data into context with previous studies conducted on phthalocyanines. It is believed that the data collected can be used to conduct theoretical studies on the implications of structural modifications on a molecular orbital level. Previous density functional theory studies have been conducted on zinc phthalocyanine,[14, 15] and it is believed that such studies would enable one to be able to calculate the optimal modifications for the phthalocyanine molecule according to the desired properties. For example, it is known that one could enhance solubility using electron donating substituents or optimise

triplet properties with the insertion of heavy metal atoms, but a model may be able to give an indication of the extent of such actions. A concise model and associated database would also enhance the understanding of these molecules and their unique optical properties.

7.10 References

1. S. M. Bishop, A. Beeby, A. W. Parker, M. S. C. Foley and D. Phillips, *J. Photochem. Photobiol. A. Chem.*, 1995, **90**, 39.
2. R. D. Gould, *Coord. Chem. Rev.*, 1996, **156**, 237.
3. P. S. Vincett, E. M. Voigt and Rieckhof.Ke, *J. Chem. Phys.*, 1971, **55**, 4131.
4. C. C. Leznoff, L. S. Black, A. Hiebert, P. W. Causey, D. Christendat and A. B. P. Lever, *Inorg.Chim. Acta*, 2006, **359**, 2690
5. A. Juzeniene, K. P. Nielsen and J. Moan, *J. Environ. Pathol. Toxicol. Oncol.*, 2006, **25**, 7
6. J. Moan, Q. Peng, J. F. Evensen, F. Berg, A. Western and C. Rimington, *Photochem. Photobiol.*, 1987, **46**, 713
7. D. V. Ash and S. B. Brown, *Eur. J. Cancer*, 1993, **29A**, 1781
8. K. Plaetzer, B. Krammer, J. Berlanda, F. Berr and T. Kiesslich, *Lasers Med. Sci.*, 2009, **24**, 259
9. M. C. DeRosa and R. J. Crutchley, *Coord. Chem. Rev.*, 2002, **233**, 351.
10. R. Bonnett, *Chem. Soc. Rev.*, 1995, **24**, 19.
11. F. M. Cotterill, Ph.D. Thesis, University of East Anglia, Norwich, UK, 2004.
12. T. Nyokong, *Coord. Chem. Rev.*, 2007, **251**, 1707.
13. R. Bonnett, R. D. White and U. J. Winfield, *Biochem. J*, 1989, **261**, 277
14. G. Ricciardi, A. Rosa and E. J. Baerends, *J. Phys. Chem. A*, 2001, **105**, 5242.

15. G. Cheng, X. Z. Peng, G. L. Hao, V. O. Kennedy, I. N. Ivanov, K. Knappenberger, T. J. Hill, M. A. J. Rodgers and M. E. Kenney, *J. Phys. Chem. A*, 2003, **107**, 3503.